

A photograph of a person wearing dark waders and a blue tank top, standing in a shallow, rocky stream. The person is holding a small object, possibly a sample, and looking down at it. The stream is surrounded by dense green vegetation, including tall grasses and shrubs. The water is clear, reflecting the sky and the surrounding greenery. The scene is set in a natural, wooded area.

Bulletin 115 • 2021

Potential effects of climate change on stream temperature in the Marengo River headwaters

Anna C. Fehling

David J. Hart



Wisconsin Geological
and Natural History Survey

DIVISION OF EXTENSION

UNIVERSITY OF WISCONSIN-MADISON





Wisconsin Geological
and Natural History Survey
DIVISION OF EXTENSION
UNIVERSITY OF WISCONSIN-MADISON

Bulletin 115 • 2021

Potential effects of climate change on stream temperature in the Marengo River headwaters



Anna C. Fehling

David J. Hart

Suggested citation:

Fehling, A.C., and Hart, D.J., 2021, Potential effects of climate change on stream temperature in the Marengo River headwaters: Wisconsin Geological and Natural History Survey Bulletin 115, 74 p., 3 pl., 3 datasets, <https://wgnhs.wisc.edu/pubs/000976>.

Research for this project was supported by the USDA Forest Service under contract 16-CS-11091300-074.



Published by and available from:

Wisconsin Geological and Natural History Survey

3817 Mineral Point Road • Madison, Wisconsin 53705-5100
608.263.7389 • www.WisconsinGeologicalSurvey.org
Kenneth R. Bradbury, Director and State Geologist

ISSN: 0375-8265

ISBN: 978-0-88169-975-3

Photo credits

Front cover: Measuring temperature in the Marengo River, © Pete Chase

Back cover: Marengo River, © Anna Fehling

Contents

Abstract	viii
---------------------------	------

Chapter 1: Introduction	1
Background	1
Purpose and scope	1
Approach	4
Acknowledgments	4

Chapter 2: Setting	5
Overview	5
Geology	5
Geologic history	5
Bedrock geology	5
Glacial geology	8
Hydrology	8

Chapter 3: Field characterization	12
Data collection methods	12
Previous work	12
Temperature, stage, and precipitation	12
Streamflow measurements	12
Water chemistry	12
Groundwater investigation	16
Shade	16
Trout habitat	16
Results	16
Air temperature and precipitation	16
Stream temperature	18
Groundwater temperature	24
Stage	24
Streamflow	26
Water chemistry	26
Groundwater interactions at Blaser Creek	29
Discussion	30

Chapter 4: Groundwater-flow model	31
Description of GFLOW model code	31
Conceptual model of Marengo River study area	31
Overview of parent model	34
Targets	34
Model refinement and calibration	37
Model extent	37
Streams	37
Recharge	37
Transmissivity	39
Model performance	41
Discussion	43
Climate change scenarios for baseflow	44
Climate-change scenarios	44
Results	45
Discussion	45

Chapter 5: Stream-temperature modeling	46
Description of model code	46
Model construction	47
Stream geometry	47
Shade	47
Hydrology	49

Calibration	49
Model performance	50
Scenarios for stream temperature	52
Climate-change scenarios	52
Management scenarios	54
Flooding	54
Evaluating potential impact to trout	54
Results	55
Discussion	57

Chapter 6: Conclusions	63
Implications for management	64
Research implications and suggestions for future work	64

Appendices	
1. Chemistry	65
2. Groundwater-flow model performance	68
3. Stream-temperature model performance	70

References	71
-----------------------------	----



Figures

1. Study area location in Wisconsin 2
2. Marengo River study area . . . 3
3. Bedrock geology. 6
4. Geology of the Marquette Range Supergroup. 7
5. Surficial geology. 9
6. Hydrology 10
7. Topography 11
8. Locations of previous U.S. Forest Service stream temperature and discharge measurements. 13
9. Locations of thermographs in 2018 14
10. Daily mean air temperature at three measurement locations for mid-May through late September of 2018. 17
11. Monthly average air temperature in 2018 compared to the long-term (2008–2017) average at Clam Lake weather station 17
12. Monthly average precipitation in 2018 compared to the long-term (2008–2017) average at Clam Lake weather station . . 18
13. Maximum 7-day mean water temperature at stream thermograph locations in 2018 19
14. Stream temperatures from the headwaters to the waterfall in the study area 20
15. Stream temperatures from the waterfall downstream to FR198 in the study area. . . . 21
16. Stream temperatures from FR198 to FR384 in the study area 22
17. Warmest and coldest temperature records for the main channel of the Marengo River in 2018 compared to precipitation and river depth . 23
18. Groundwater temperature in 2018. 24
19. Depth to groundwater in the Blaser monitoring well in 2018 25
20. Marengo River depth and temperature in 2018 25
21. Electrical conductivity measurements. 28
22. Results of stable isotope sampling in spring and fall of 2018 29
23. Transmissivity zones in the groundwater-flow model and surficial geologic units 32
24. Detail of high- and low-transmissivity zones in the groundwater-flow model, showing bedrock geologic units 33
25. Locations of the groundwater-flow model targets 35
26. Simulated groundwater drainage area for two baseflow targets compared to the surface watershed 38
27. Simulated average annual recharge in the groundwater-flow model 40
28. Map showing groundwater-flow-model results 42
29. Comparison of simulated and observed heads 43
30. Comparison of simulated and observed baseflows 43
31. Simulated annual recharge from 10 general circulation models (GCMs) over one past and two future periods. . . . 45
32. Heat fluxes simulated in the stream-temperature model. . 46
33. Layout of the stream-temperature model 48
34. Topographic, hydrographic, and vegetative features used for the shading parameters in the stream-temperature model 49
35. Modeled daily discharge, measured daily stage, and measured flow in 2018 downstream of Tributary 7 . . 50
36. Map showing the results of the stream-temperature model 51
37. Simulated and measured daily mean water temperatures at FR198 and upstream of Tributary 6 during calibration period 52
38. Air temperatures for the low-, medium-, and high-air-temperature scenarios developed from three general circulation models and measured during calibration period 53
39. Simulated mean temperature during calibration period and for six climate-change scenarios at FR198 and upstream of Tributary 6. . . . 55
40. Simulated and measured temperatures at FR198 compared to trout thermal tolerance limits 57
41. Simulated and measured temperatures upstream of Tributary 6 compared to trout thermal tolerance limits . . . 58
42. Modeled locations where trout thermal tolerance limits were exceeded for the low- and medium-air-temperature scenarios 59
43. Modeled locations where trout thermal tolerance limits were exceeded for the high-air-temperature scenario . . . 60
44. Simulated and measured temperatures at FR198 during low flow and during flooding compared to trout thermal tolerance limits 61

Tables

1. Thermograph locations . . . 15
2. Average daily air and water temperatures during high and low flows of the Marengo River at FR198 . . . 23
3. Water temperatures of the Marengo River at FR198 . . . 23
4. Streamflow measurements . . 27
5. Baseflow targets 36
6. Model transmissivity zones . . 41
7. Shade parameters for each vegetation type 47
8. Average projected air temperatures compared to the 2018 calibration period for low-, medium-, and high-air-temperature general circulation models 53
9. Mean simulated daily mean stream temperatures for climate-change scenarios.
10. Change in average simulated stream temperatures for management scenarios . . . 56

Appendix tables

- 1.1 Field chemistry measurements. 66
- 1.2. Chemistry laboratory results . 68
- 2.1. Model performance—Baseflow targets 69
- 2.2. Model performance—Head target elevations in watershed 69
- 2.3. Simulated baseflow for climate-change scenarios . . 70
- 3.1. Error in simulated mean daily temperature by location . . . 71

Plates

Available separately at <https://wgnhs.wisc.edu/pubs/000976>.

1. Simulated baseflow at current long-term average conditions
2. Simulated baseflow with 21% increase in recharge
3. Simulated baseflow with 12% decrease in recharge

Supplementary datasets

Available separately at <https://wgnhs.wisc.edu/pubs/000976>.

1. GFLOW groundwater flow model
2. Geodatabase files representing baseflow during current conditions, increased recharge, and decreased recharge
3. Measurements of water chemistry, streamflow, and stream temperature (spreadsheets)



Marengo River waterfall | Pete Chase

Abstract

Cool-water trout habitat in Wisconsin is projected to substantially decrease as a result of climate change. The extent of habitat loss depends, in part, on groundwater discharge to streams, which can provide cool-water refuges for trout. Field measurements and models of groundwater flow and stream temperature were used to evaluate how climatic changes are likely to affect groundwater discharge and stream temperatures during summer low-flow conditions in the Marengo River headwaters in the Chequamegon-Nicolet National Forest in northern Wisconsin.

Variations in groundwater discharge and stream temperature in the watershed correlate with the highly varied geology. Two cool-water tributaries receive groundwater from distinct areas: (1) Shallow groundwater in glacial sand deposits discharges to a wetland tributary with temperatures near 10°C to 16°C. (2) Deeper groundwater flows on a longer path through fractured and faulted bedrock and

discharges to a different tributary (less than 12°C) and the main stem, increasing flow in the main stem by about 6 cubic feet per second (cfs) (roughly a 50% increase) over 0.5 mile. Trout are commonly observed downstream of this second discharge area. In contrast, the warm stream segments in flat wetland areas with shallow crystalline bedrock reach temperatures higher than 30°C, well above the lethal threshold for trout.

A groundwater-flow model was developed to simulate possible changes to the groundwater system. Climate change may affect the long-term average baseflow through changes in groundwater recharge. Previously published results from a soil-water balance model run using a suite of general circulation models suggest recharge in this watershed could change from -12% to +21% by the end of the century. Based on these changes in recharge, the main stem baseflow is simulated to change up to 30% from current long-term average conditions, whereas flow in the

groundwater-dominated tributaries is simulated to remain fairly constant relative to current conditions.

Potential thermal impacts from climate change were simulated by modifying groundwater discharge, air temperature, and groundwater temperature in a mechanistic stream-temperature model. Air temperature from 2018 was scaled to low, medium, and high possible future time series using probabilistic downscaling data for three general circulation models that represent a range of increases in temperature. The groundwater temperature thermal sensitivity (a measurement of how much the groundwater temperature increases relative to air temperature), was varied from 0 to 1. Results were compared to trout thermal tolerance limits over several time periods ranging from 1 to 42 days to evaluate habitat impacts. The mean daily average stream temperature downstream of the focused groundwater-discharge area was simulated to increase between 0.8°C and 4.6°C in 30 to 70 years, depending on the climate-change scenario. This area remains below the trout thermal tolerance threshold under the low- and medium-air-temperature scenarios but exceeds the threshold for the high-air-temperature scenario. An increase in the frequency and magnitude of extreme rain events may also increase stream temperatures in groundwater-dominated areas. Trout may most likely be adversely affected by longer sustained increases in stream temperatures over weeks or months, rather than by more rapid increases in daily mean temperature, for both flooding and low-flow conditions. This improved understanding of system dynamics may help the U.S. Forest Service manage the watershed for trout survival.



Stream gaging a tributary of the Marengo River | Anna Fehling

Chapter 1: Introduction

Background

Stream temperature is critical for determining a habitat's suitability for cold-water species such as trout (Wehrly and others, 2007; Lyons and others, 2009; Diebel and others, 2015). Trout prefer cool waters around 12°C to 18°C and suffer thermal stress above these temperatures (Bell, 2006). The thermal tolerance limits devel-

oped by Wehrly and others (2007) suggest a maximum 7-day mean temperature of 23.3°C and a daily maximum of 27.6°C, above which trout cannot survive. Summer maximum temperatures are therefore often considered a critical threshold for trout (for example, Lyons and others, 1996, 2009).

Groundwater input to streams is a key factor influencing temperature in many headwater streams, providing cool-water refuges for trout (Snyder and others, 2015). Physical characteristics such as shade, gradient, and channel geometry also influence stream temperature.

Trout populations in Wisconsin are at risk from increasing temperatures due to climate change (Wisconsin Initiative on Climate Change Impacts (WICCI), 2011; Stewart and others, 2015; Mitro and others, 2019). The average annual temperature in Wisconsin has increased by about 1.1°C since the beginning of the 20th century and is predicted to increase

another 2.8°C or more by the end of this century (Frankson and others, 2017; Reidmiller and others, 2018). Lyons and others (2010) projected that species distribution could change dramatically in cool-water streams in northern Wisconsin. More recently, Mitro and others (2019) projected a 68% decline in Wisconsin stream habitat for brook trout (*Salvelinus*

fontinalis) and 32% decline for brown trout (*Salmo trutta*) between the late 20th century and mid-21st century. Climate change is also altering precipitation, which affects groundwater recharge and baseflow (the groundwater component of streamflow). However, the direction of change is uncertain. In

Wisconsin, changes in temperatures and precipitation could lead to either an increase or decrease in groundwater recharge (WICCI, 2011). The resulting changes to baseflow will affect both low-flow conditions and stream temperatures.

The U.S. Forest Service (USFS) is engaged in the stewardship of water resources on National Forest System lands. Site-specific information is needed to successfully manage these resources. Previous statewide studies can provide general trends but rarely account for variations in local conditions that can be important for fish habitat (for example, Deitchman and Loheide, 2012). This study focuses

on the Marengo River headwaters in the Chequamegon-Nicolet National Forest in northern Wisconsin. The watershed has historically supported populations of brook trout and brown trout. The USFS requested that the Wisconsin Geological and Natural History Survey (WGNHS) evaluate the potential impacts to stream temperature and baseflow from climate change and the implications for trout viability to guide future resource management.

Purpose and scope

The purpose of this report is to present findings from a study of groundwater flow and stream temperature as they relate to trout habitat in the Marengo River headwaters. The study area includes the portion of the 12-digit hydrologic unit located within the Great Divide Ranger District of the Chequamegon-Nicolet National Forest in Bayfield and Ashland Counties (figs. 1–2) (Natural Resources Conservation Service, 2018). The overall goal of this project is to work with the USFS to advance the understanding, protection, and enhancement of groundwater resources within the Chequamegon-Nicolet National Forest. An interim report was provided to USFS in December 2018. This report includes results from the entire 2-year study.

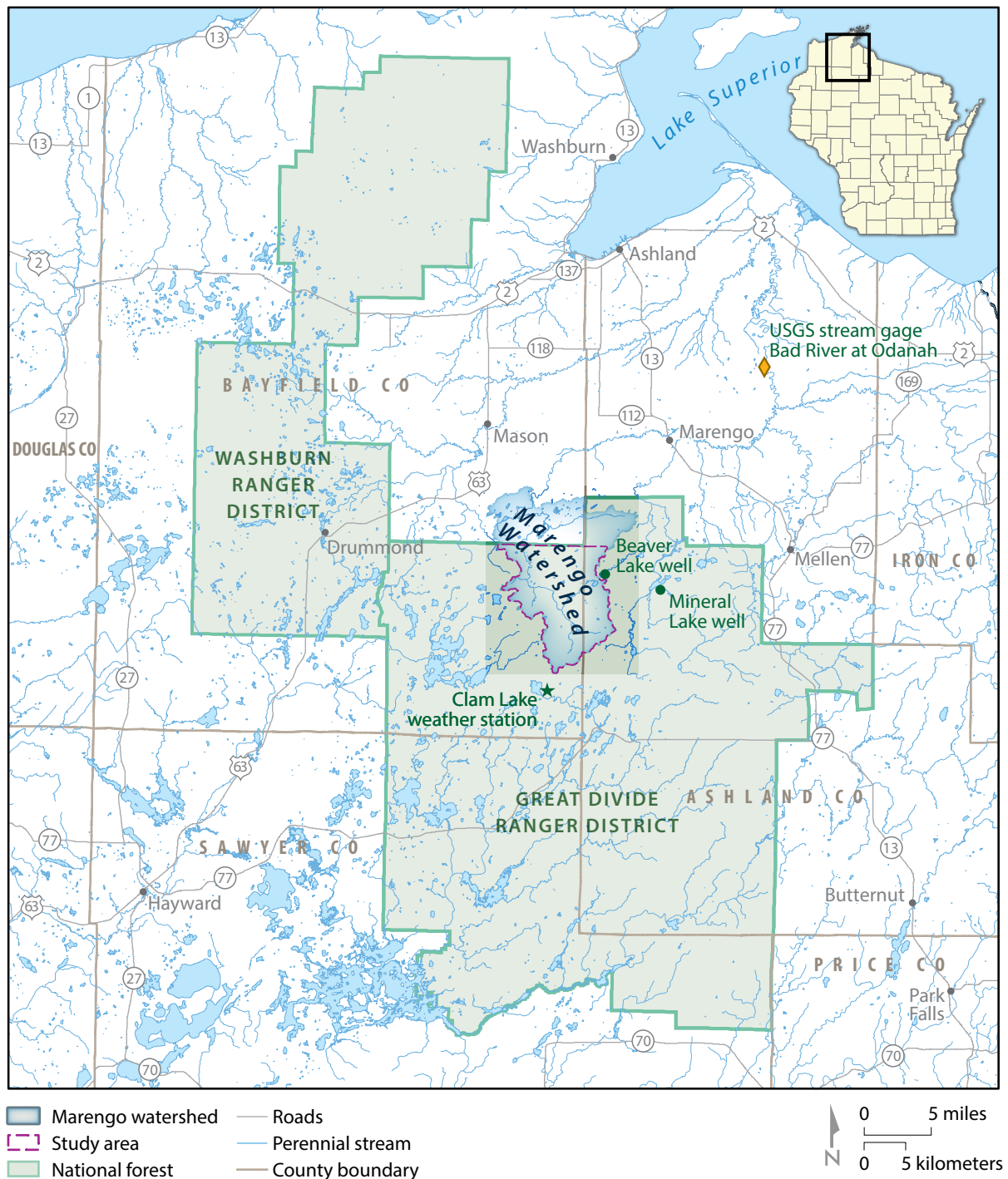
The objectives of the study were to evaluate the following:

- Potential impacts to baseflow from climate change
- Potential impacts to stream temperature from climate change
- Implications for trout viability
- Effect of different management strategies



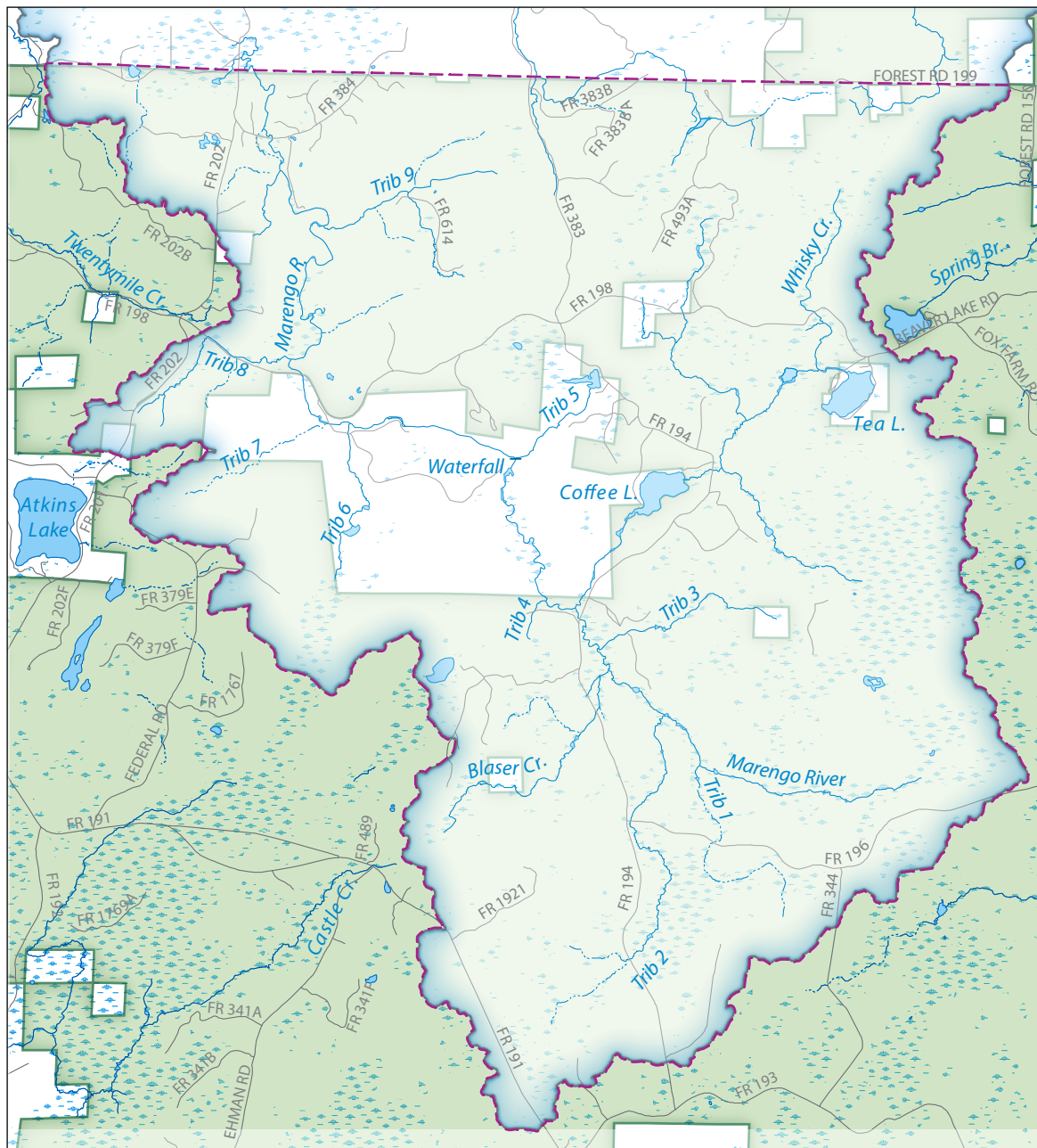
Marsh marigold | Catherine Christenson

Figure 1. Study area location in northern Wisconsin showing key regional features, counties, and national forest units.

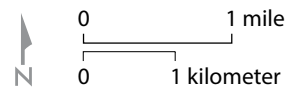


Political boundaries from Wisconsin Department of Natural Resources, 2011. National Forest boundaries from the USDA Forest Service, 2011. Roads from U.S. Census Bureau, 2015. Hydrography from National Hydrography Dataset (U.S. Geological Survey, 2016).

Figure 2. Marengo River study area and its hydrographic features. Abbreviation: FR, Forest Road; Trib, Tributary.



- Marengo River watershed
- Study area
- National forest
- Wetland
- Roads
- Perennial stream
- Intermittent stream



National Forest boundaries from the USDA Forest Service, 2011. Hydrography from National Hydrography Dataset (U.S. Geological Survey, 2016).

Approach

Data collection and computer simulations (modeling) were used together to evaluate potential climate change impacts. The approach was divided into three parts: (1) data collection about stream temperature, flow, chemistry, and physical characteristics; (2) refinement of a groundwater-flow model in the study area to better evaluate changes to the groundwater system; and (3) development of a stream-temperature model to examine which factors influence temperature the most, infer what might be expected from changes in air temperature and groundwater recharge, and test different management strategies.

Acknowledgments

We thank the USFS for their invaluable knowledge and interest in the site, collaboration during field work, and providing project funding. Jean Bahr and Steve Loheide (University of Wisconsin (UW)–Madison) provided valuable project guidance and reviews of the initial manuscript. The published version of the manuscript benefitted from peer reviews by Andrew Leaf (U.S. Geological Survey (USGS)), Matthew Mitro (Wisconsin Department of Natural Resources), and Maureen Muldoon (WGNHS). We also thank Pete Chase (WGNHS) and Catherine Christenson (UW–Madison) for substantial fieldwork support, Bill Selbig (USGS) for guidance on the

Stream Network Temperature Model (SNTEMP) model, Daniel Vimont of UW-Madison for providing climate data, Steve Westenbroek (USGS) for sharing modeled recharge results, Caroline Rose (WGNHS) for help developing the figures, Alicia Iverson and Tanya Anderson (UW-Madison Cartography Laboratory) for cartography support, and Elizabeth Koozmin (Catoctin Editorial Services) and Linda Deith (WGNHS) for editing.



Marengo River | Pete Chase

Chapter 2: Setting

Overview

The study area covers the portion of the Marengo River headwaters' watershed predominantly within the Chequamegon-Nicolet National Forest in Bayfield and Ashland Counties (figs. 1–2). The study area occupies 36 square miles (mi²) (about 60%) of the watershed, of which 31 mi² are National Forest property. The private land in the study area is generally undeveloped. Much of the study area is forested but includes about 7 mi² of wetland (Wisconsin Department of Natural Resources, 2011). The climate is humid and temperate. The average annual precipitation from 1971 through 2000 was 32.0 and 32.4 inches (in.) for the northwest and north-central regions of Wisconsin, respectively (Wisconsin State Climatology Office, 2018). Local weather records for this project were obtained online from a Remote Automatic Weather Station at Clam Lake, about 1 mile (mi) south of the watershed boundary (fig. 1) (Western Regional Climate Center, 2018). The Clam Lake station reported an average annual precipitation of 32 in. from 2007 through 2018. Although Clam Lake is near the watershed, it may not always reflect actual precipitation in the watershed as there can be substantial spatial variation in precipitation patterns in this region (for example, Leaf and others, 2015).

Geology

Geologic history

Precambrian bedrock and unlithified Pleistocene to Holocene deposits in the study area document a long and complex history of deposition

Marenisco fault; fig. 3) was activated in the study area and thrust younger igneous rocks an estimated 9 mi over older rocks to the south (Bjornerud and Cannon, 2011). Following a long gap in the geologic record, several glaciations between about 16,000



Measuring surface-water temperature | Anna Fehling

and deformation. The structure and composition of bedrock was perhaps most substantially influenced by mid-continental rifting about 1.1 billion years ago (giga-annum, or Ga). During this period, extension of the Earth's crust created a valley that was then filled with thick sequences of igneous and sedimentary rock. Today, rift-associated rocks form a 1,200-mi-long southward-opening arc centered over Lake Superior (Ojakangas and others, 2001). The study area intersects the southern extent of the rift basin, where rifting tilted the bedrock 40° to 90° northward (Cannon and others, 2007) and exposed bedrock strata in an oblique cross section. Substantial contact metamorphism occurred in the study area from rift-related igneous intrusions. As the rift closed, a major thrust fault (the Atkins Lake–

and 9,500 years ago deposited till and outwash sediment on the underlying bedrock (Clayton, 1984). Postglacial deposits in the study area include stream sediment (sand and gravel) and peat.

Bedrock geology

The igneous rocks that filled in the Midcontinent Rift basin are located in the northern part of the study area, with increasingly older rocks to the south (fig. 3). In the north, Middle Proterozoic rocks associated with mid-continental rifting include volcanic rocks of the Keweenawan Supergroup and the gabbroic rocks of the Mineral Lake intrusion (part of the Mellen Complex). These units unconformably overlie Early Proterozoic metasedimentary rocks of the Marquette Range Supergroup to the south (shown in more detail on fig. 4), a

Figure 3. Bedrock geology of the Marengo River study area and vicinity.

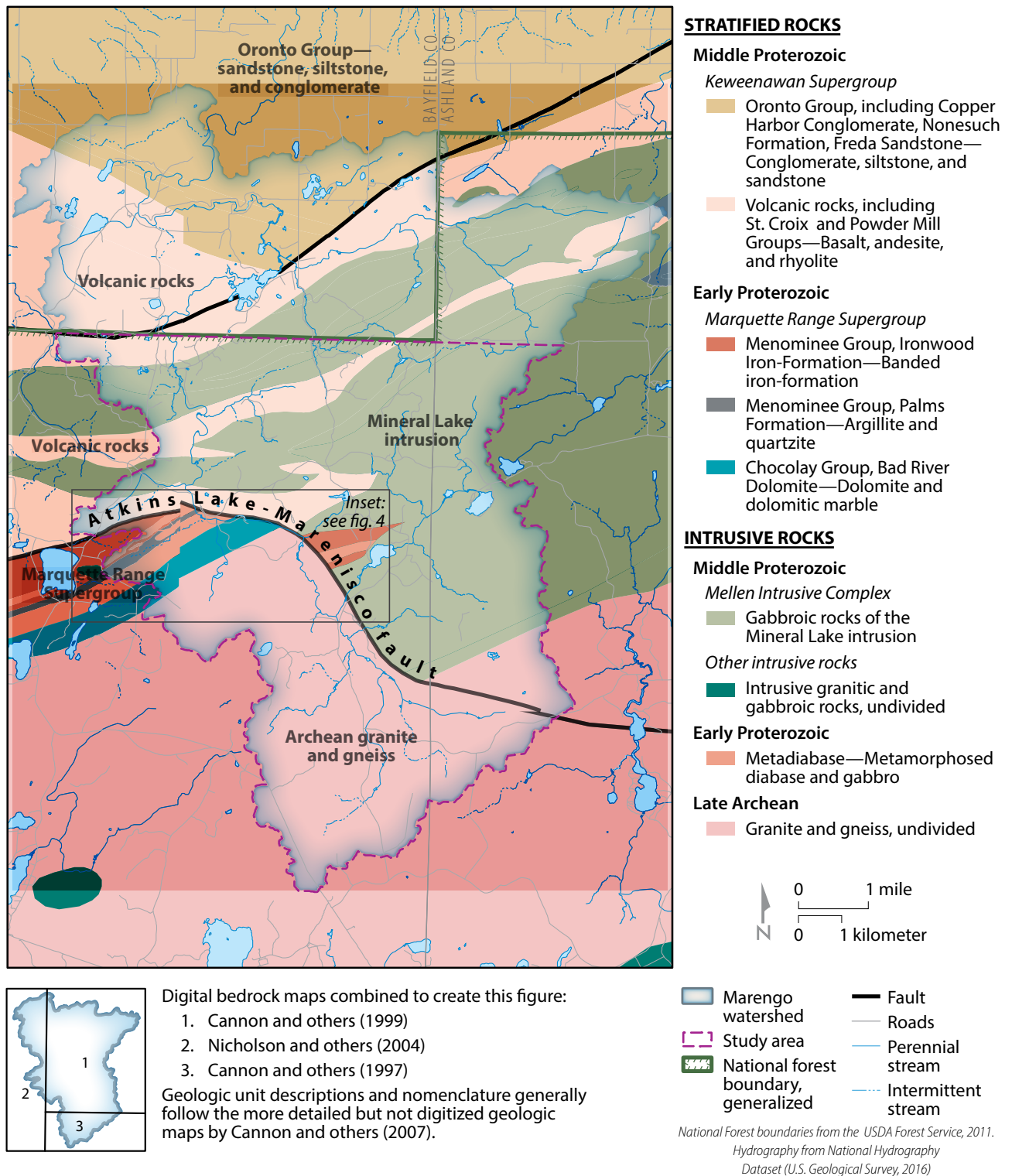
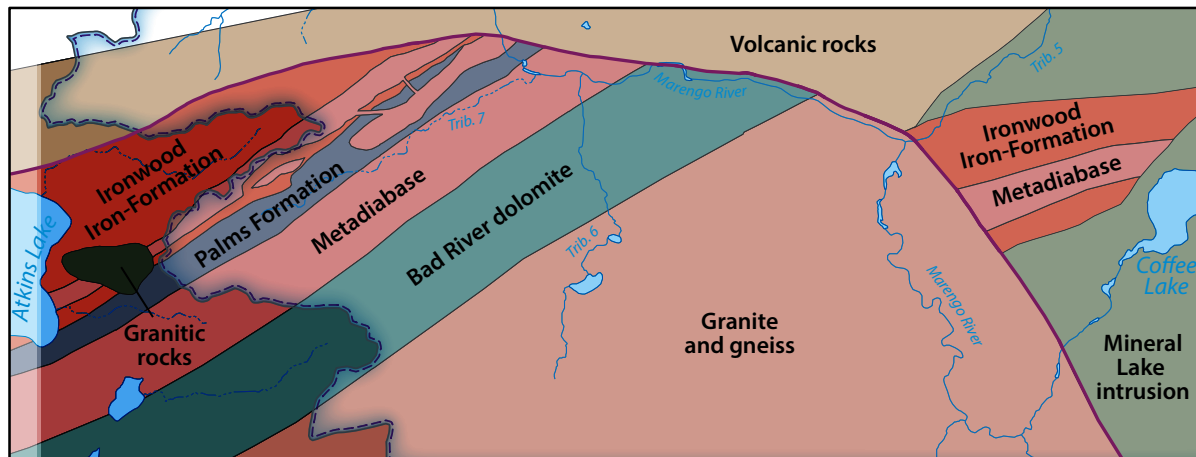


Figure 4. Geology of the Marquette Range Supergroup. Modified from Cannon and others (2007, plate 1).



STRATIFIED ROCKS

Middle Proterozoic

Keweenawan Supergroup

- Volcanic rocks, including St. Croix and Powder Mill Groups—Basalt, andesite, and rhyolite

Early Proterozoic

Marquette Range Supergroup

- Menominee Group, Ironwood Iron-Formation—Banded iron-formation
- Menominee Group, Palms Formation—Argillite and quartzite
- Chocoma Group, Bad River Dolomite—Dolomite and dolomitic marble

INTRUSIVE ROCKS

Middle Proterozoic

Mellen Intrusive Complex

- Gabbroic rocks of the Mineral Lake intrusion
- Intrusive granitic rocks, undivided

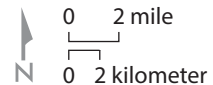
Early Proterozoic

- Metadiabase—Metamorphosed diabase and gabbro

Late Archean

- Granite and gneiss, undivided

- Marengo River watershed
- Study area
- Atkins Lake–Marenisco fault
- Perennial stream
- Intermittent stream



National Forest boundaries from the USDA Forest Service, 2011.
Hydrography from National Hydrography Dataset (U.S. Geological Survey, 2016).

package of steeply northward-dipping rocks that forms the southern extent of the rift basin. The rocks are exposed north and south of the Atkins Lake–Marenisco fault where it parallels the Marengo River. From oldest to youngest, the Marquette Range Supergroup in the study area includes the Bad River Dolomite of the Chocoyay Group, clastic rocks of the Palms Formation of the Menominee Group, and the Ironwood Iron-Formation of the Menominee Group. Diabase and gabbro sills and dikes are common, particularly in the Ironwood. The Ironwood Iron-Formation is the primary iron-bearing unit of the Gogebic iron range (locally called the Penoque range), an 80-mi-long ridge extending east-north-east of the study area (Cannon and others, 2007). Before rifting, the Paleoproterozoic rocks experienced compression and deformation during the Penoquean orogeny at about 1.85 Ga. The Marquette Range Supergroup overlies low-relief Archean intrusive granitic rocks in the southern part of the study area. At about 2.7 Ga, they are some of Wisconsin’s oldest rocks.

Glacial geology

Pleistocene glacial till and outwash deposits are present throughout the study area (fig. 5). In the southern headwaters, unlithified glacial deposits primarily consist of hummocky till (clayey sand and silty sand) of the Copper Falls Formation, with some sandy stream sediment along Blaser Creek (Clayton, 1984). Glacial deposits are about 100 feet (ft) thick at the southern boundary of the study area and thin northward (Fehling and others, 2018). Glacial deposits are thin to absent in the central part of the study area, but they transition to stream sediment near the northern boundary.

Hydrology

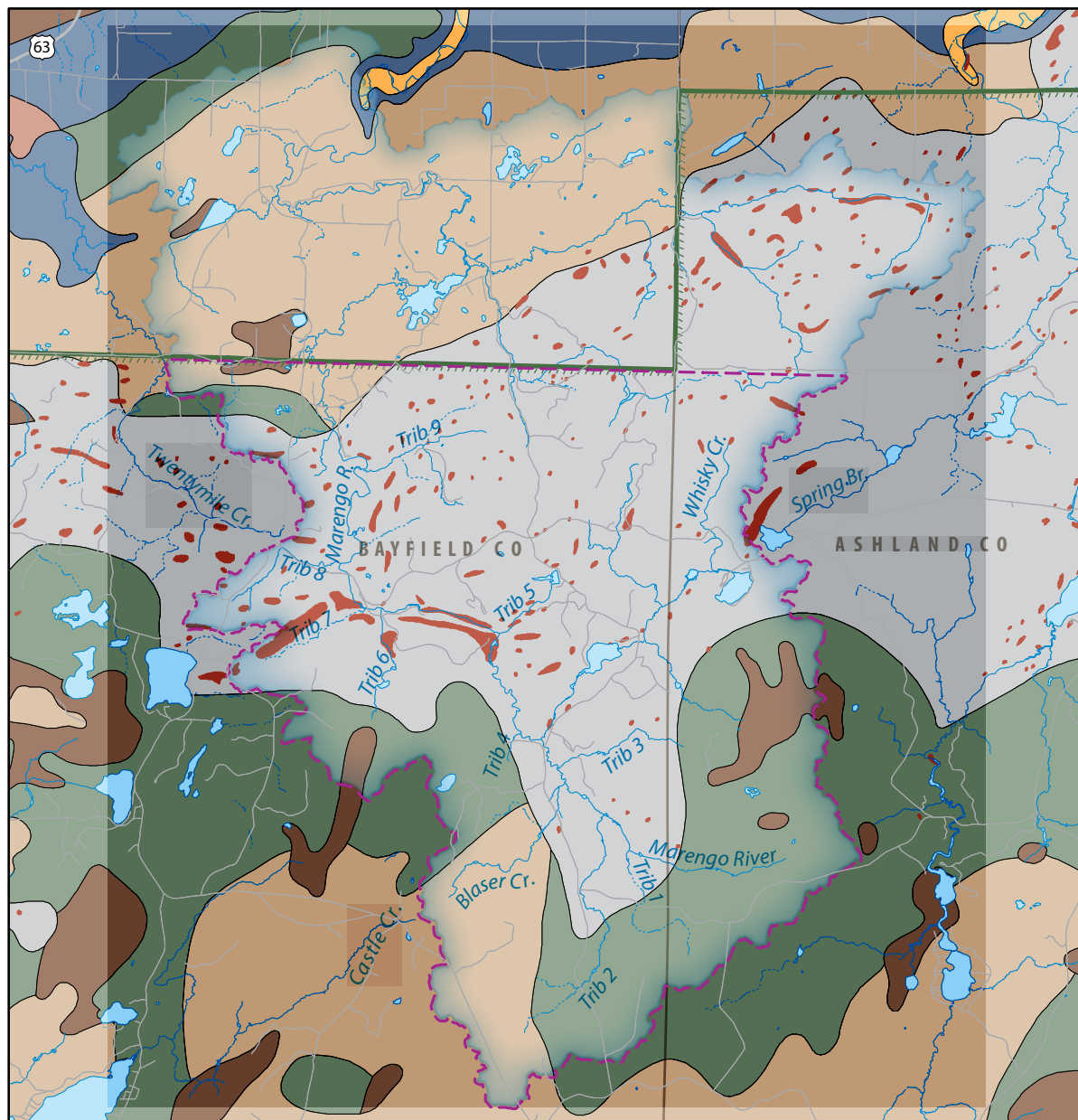
The Marengo River headwaters watershed is situated at the southern limit of the Lake Superior drainage basin. The Marengo River flows generally north and then east to the Bad River, where it ultimately drains into Chequamegon Bay. The nearest downstream U.S. Geological Survey (USGS) stream gage is located on the Bad River at Odanah (USGS #4027000, fig. 1).

Within the study area, the watershed can be divided into two hydrologic regions, split by a 50-ft-tall unnamed waterfall where the Marengo River intersects the Atkins Lake–Marenisco fault (fig. 6). Similar regions were described on a regional basis by Wheeler and Bodette (2011) and Leaf and others (2015). South and upstream of the waterfall, the study area is characterized by low-relief topography and relatively thin glacial soils overlying Archean crystalline bedrock. Glacial deposits are thickest at the southern extent of the watershed and thin northward. Land-surface elevation ranges from about 1,580 ft above sea level on till deposits in the southwest to 1,350 ft at the top of the waterfall (fig. 7). The Marengo River begins in the southeastern part of the watershed and flows west and northward with a low gradient. Wetlands are common (fig. 6), and drainage is poorly developed.

The intersection of the Marengo River with the Atkins Lake–Marenisco fault marks the boundary of the northern hydrologic zone. At this point, the river turns west-northwest to follow the fault for about 1.6 mi. This part of the watershed has high-relief topography and shallow bedrock; the topography generally follows the bedrock surface. The Marengo River has a higher gradient here than above the waterfall, as well as steeper and narrower valley walls. Land-surface elevation ranges from 1,600 ft on the informally named Penoque ridge on the western edge of watershed to 1,130 ft at Forest Road (FR) 384. Drainage patterns are often angular, following faults and fractures. The high-relief topography limits surface storage, and high-intensity rains can produce flash flooding. The flood that followed extreme rainfall in July 2016—when at least 7 inches in 24 hours was recorded at Clam Lake (Western Regional Climate Center, 2018)—caused substantial damage to roads and washed away a private bridge in the study area, transporting it several hundred feet downstream.

Groundwater flow in the study area is controlled primarily by the thickness and coarseness of glacial deposits and by the presence of hydraulically active bedrock fractures. Throughout most of the watershed where glacial deposits are thin, groundwater flow is limited to shallow fractures in the crystalline bedrock and flow paths are relatively short. In contrast, the aquifer has higher transmissivity in areas with coarse-grained glacial deposits, such as near Blaser Creek; in areas with thick glacial deposits, such as at the southern extent of the watershed; and in areas with hydraulically active fractures, such as the bedrock near Tributary 7 (see *Conceptual model of Marengo River study area* in chapter 4).

Figure 5. Surficial geology of the study area. Generalized surficial sediments from Clayton (1984); bedrock outcrops from Cannon and others (1989) and Nicholson and others (2004).



GENERALIZED SURFICIAL SEDIMENTS

Post-glacial

- Sand and gravel
- Peat

Copper Falls Formation

- Sand and gravel
- Clayey sand and silty sand

Miller Creek Formation

- Sand and gravel
- Silt and clay

Precambrian

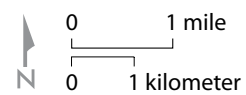
- Bedrock, overlain by thin layer of sediments

- Bedrock outcrop
- Contact

- Marquette River watershed

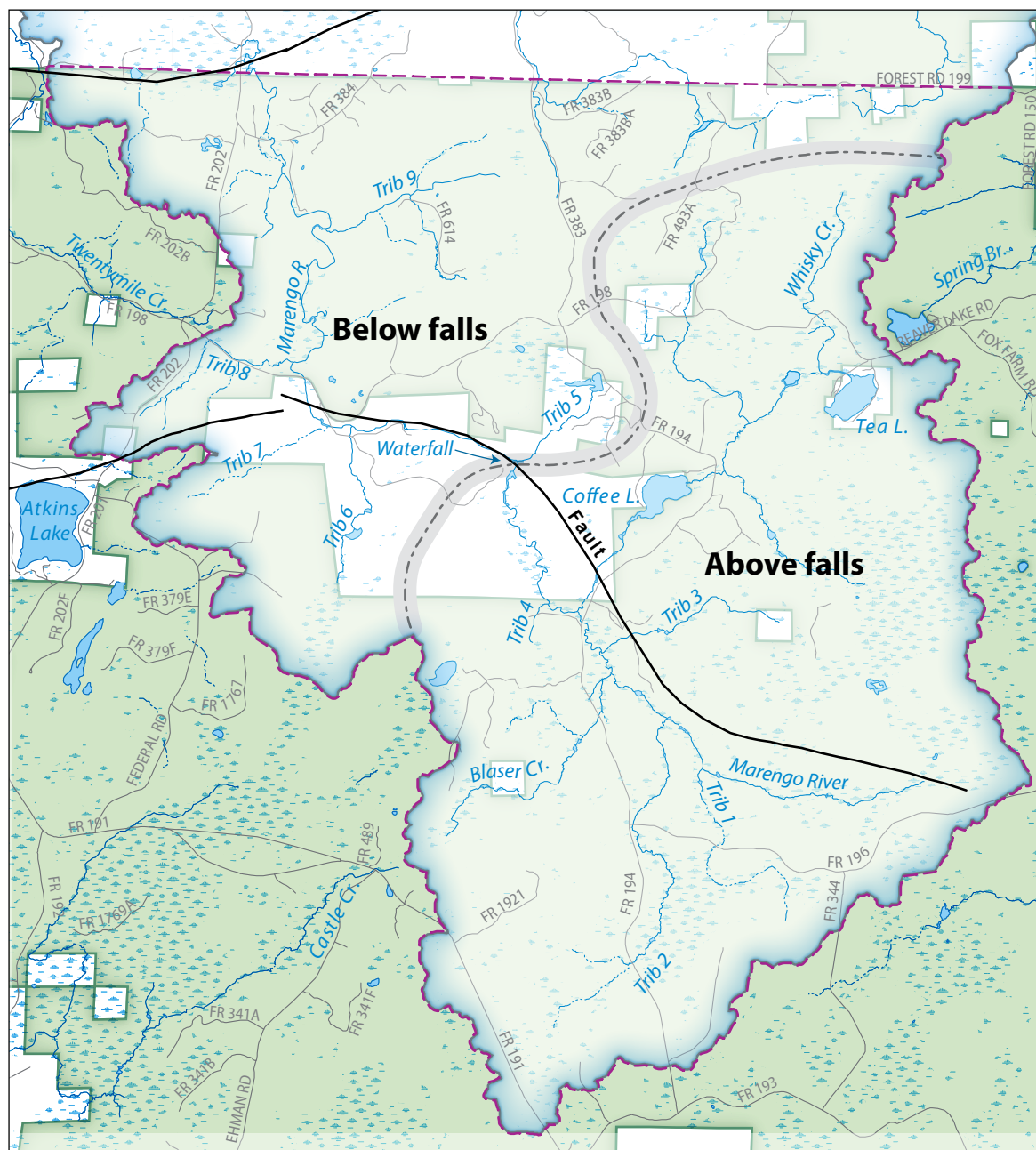
- Study area
- National forest boundary, generalized

- Roads
- Perennial stream
- Intermittent stream



Hydrography from National Hydrography Dataset (U.S. Geological Survey, 2016)

Figure 6. Hydrology of the Marengo River study area. Hydrologic regions represent conceptual divisions in hydrology developed for this project. The Marengo River follows the Atkins Lake–Marenisco fault west for several miles after the unnamed waterfall.



National Forest boundaries from the USDA Forest Service, 2011. Hydrography from National Hydrography Dataset (U.S. Geological Survey, 2016).

11



Chapter 3: Field characterization

The study area was characterized using an integrated analysis of various field observations to improve the understanding of the hydrologic system. Measured parameters included water temperature, streamflow, water chemistry, groundwater discharge, and physical characteristics of the stream.

Data collection methods

The methods used for collecting field data are presented in this section. With the exception of the data described in the *Previous work* section below, data were collected in calendar year 2018.

Previous work

The USFS has collected various data in the study area and the larger watershed for the past few decades. The locations of stream temperature and discharge measurements collected prior to this study are shown in figure 8. Low-flow stream discharge was measured during August and September of 2002 and 2003. Thermographs (sensors that measure stream temperature) have been installed periodically at various locations since 1998 to measure summer stream temperature; typically, between 0 and 4 thermographs are installed each year. The thermographs measure temperature at 30-minute intervals. Measurements of alkalinity and stream width have also been collected. The USFS has classified the Marengo River's headwater streams based on temperature, width, and alkalinity; the temperature classifications are shown in figure 8.

Temperature, stage, and precipitation

Stream, groundwater, and air temperature were monitored from June to September 2018 to capture peak stream temperatures, which are commonly observed in July. A total of 22 thermographs were installed: 18 in the stream, 2 in groundwater, and 2 hung from trees (fig. 9, table 1). Thermographs used included 10 HOBO Tidbit temperature loggers, 4 Solinst Leveloggers, and 8 HOBO Water Temp Pro v2 sensors deployed by the USFS. Thermographs recorded temperature at 15-minute intervals (USFS sensors used a 30-minute interval). The Leveloggers, which measure both temperature and pressure, served additional purposes: (1) Transducers in the Blaser monitoring well and adjacent Blaser Creek also recorded the gradient between the groundwater and the stream; (2) a transducer in the Marengo River downstream of the waterfall also recorded fluctuations in river stage; and (3) a transducer in the air also recorded barometric pressure. Groundwater temperature was monitored in the Blaser monitoring well and in a seep at the bottom of a hill slope (fig. 9). Instantaneous stream temperatures were measured using a handheld probe at multiple locations throughout the watershed, including at all the thermograph locations. Temperature variations within the stream's cross section at various thermograph locations were within 0.1°C. Air temperature and precipitation data were obtained from a Remote Automatic Weather Station at Clam Lake about 1 mi south of the watershed boundary (fig. 1) (Western Regional Climate Center, 2018).

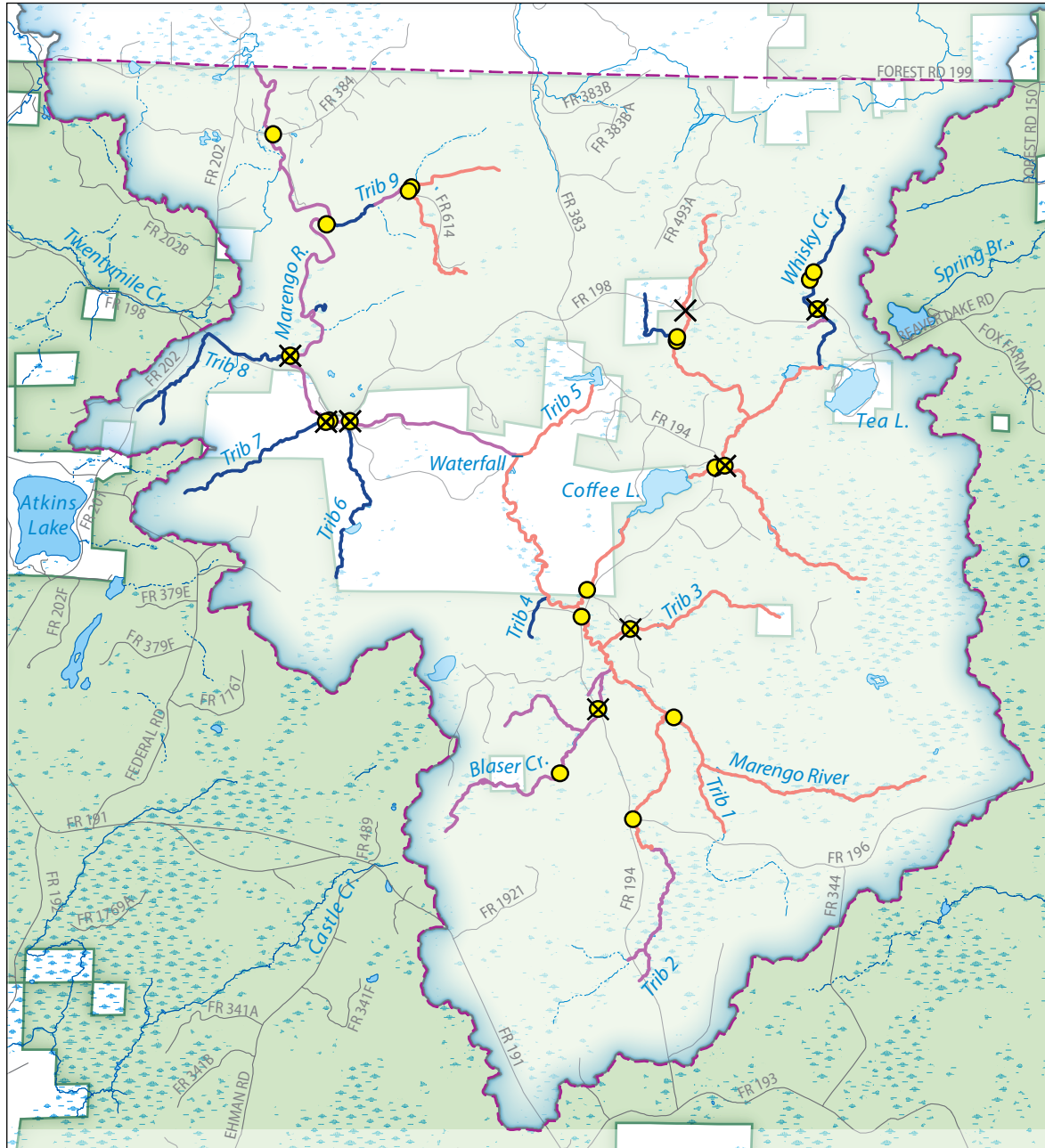
Streamflow measurements

Streamflow was measured at several locations in the watershed throughout the summer of 2018, during both low and moderate flows. Measurements were made using either an acoustic Doppler meter (SonTek/YSI FlowTracker) or a Marsh-McBirney flow meter. The USGS also made two measurements in the Marengo River watershed during the summer of 2018 that are reported in the National Water Information System (NWIS; <https://waterdata.usgs.gov/nwis>). Select streamflow measurements were used to estimate the average annual baseflow (see *Targets* in chapter 4).

Water chemistry

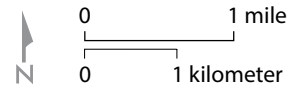
Field measurements and laboratory samples were used to evaluate baseline water chemistry and support the characterization of groundwater and surface water in the study area. Electrical conductivity, temperature, and pH were measured at thermograph locations throughout the summer using an Oakton Con 10 pH/conductivity meter. Dissolved oxygen was measured with an Oakton DO6+ dissolved oxygen meter at selected locations. Six locations were sampled twice each (spring and fall) for analysis of alkalinity, chloride, nitrogen, and metals by the University of Wisconsin-Stevens Point Water and Environmental Analysis Laboratory (<https://www.uwsp.edu/cnr-ap/weal/>).

Figure 8. Locations of previous U.S. Forest Service (USFS) stream temperature and discharge measurements, and the classification of streams by temperature based on previous USFS data collection. Temperatures were classified on the basis of the average annual maximum temperature. Temperature classification scheme and other USFS data is from Dale Higgins, U.S. Forest Service, personal communication. Abbreviation: °C, degrees Celsius.



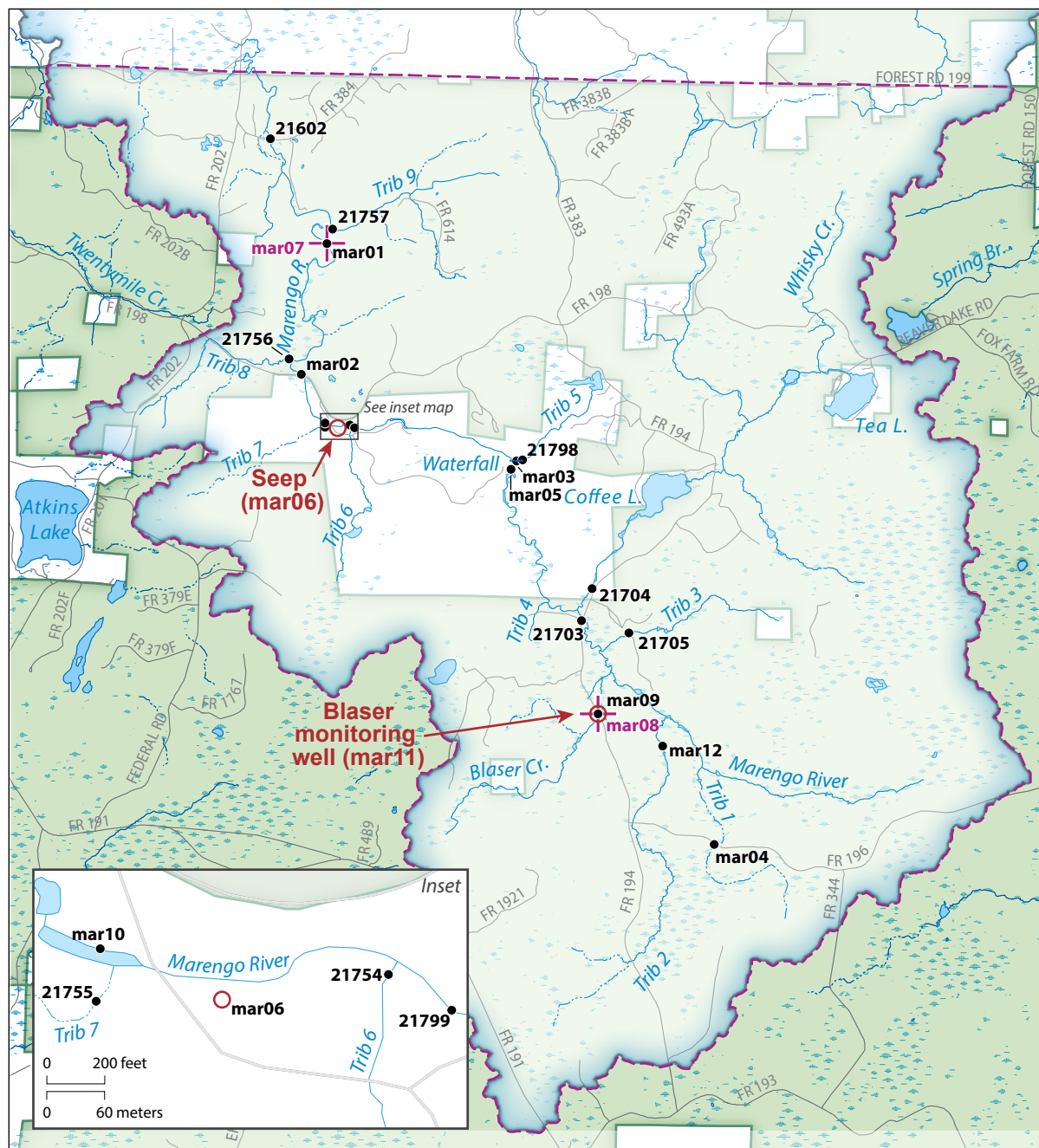
Temperature classification

- Cold (<23°C)
- Cool (23°C–26°C)
- Warm (>26°C)
- USFS thermograph location
- ✕ USFS discharge measurement location
- Marengo River watershed
- ▭ Study area
- National forest
- Wetland
- Roads
- Perennial stream
- Intermittent stream



National Forest boundaries from the USDA Forest Service, 2011.
Hydrography from National Hydrography Dataset (U.S. Geological Survey, 2016).

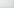






Figure 9. Locations of thermographs in 2018 and their identifiers.



Thermograph locations in 2018

Label shows station identification

- ✚ Air
- Groundwater
- Stream

-  Marengo River watershed
-  Study area
-  National forest
-  Wetland
-  Roads
-  Perennial stream
-  Intermittent stream

National Forest boundaries from the USDA Forest Service, 2011. Hydrography from National Hydrography Dataset (U.S. Geological Survey, 2016).

Table 1. Thermograph locations, listed in order from downstream to upstream.

Station ID	Location	Type	Source	Latitude (decimal degrees)	Longitude (decimal degrees)
21602	Marengo River at FR384 bridge	Stream	WGNHS	46.3202782	−91.0022354
21757	Tributary 9	Stream	USFS	46.3104668	−90.9922943
mar01	Marengo River at North Country trail	Stream	WGNHS	46.3089905	−90.9932556
mar07	Marengo River at North Country Trail, hung from tree	Air	WGNHS	46.3089905	−90.9932556
21756	Tributary 8	Stream	USFS	46.2961998	−90.9989014
mar02	Marengo River at FR198/ Wisco Road	Stream	WGNHS	46.2946014	−90.9969559
mar10	Marengo River down-stream of Tributary 7	Stream	WGNHS	46.2892914	−90.9931335
21755	Tributary 7	Stream	USFS	46.2888298	−90.9931183
mar06	Seep	Groundwater	WGNHS	46.2888145	−90.9913864
21754	Tributary 6	Stream	USFS	46.2891045	−90.9891815
21799	Marengo River upstream of Tributary 6	Stream	USFS	46.2887878	−90.9884338
21798	Tributary 5	Stream	USFS	46.2855568	−90.9627762
mar03	Marengo River at water-fall	Stream	WGNHS	46.2853966	−90.962883
mar05	Marengo River above waterfall	Stream	WGNHS	46.2844849	−90.9637146
21704	Whisky Creek	Stream	WGNHS	46.2715416	−90.9506378
21703	Marengo River at FR194	Stream	USFS	46.2680206	−90.9522934
21705	Tributary 3	Stream	WGNHS	46.2667313	−90.9447632
mar08	Blaser Creek, hung from tree	Air	WGNHS	46.2579575	−90.9496689
mar09	Blaser Creek at FR194	Stream	WGNHS	46.2579613	−90.9496078
mar11	Blaser monitoring well	Groundwater	WGNHS	46.2579842	−90.9496536
mar12	Tributary 2	Stream	USFS	46.254425	−90.9393234
mar04	Tributary 1	Stream	WGNHS	46.2437172	−90.9309235

Abbreviations: FR, Forest Road; ID, identification number; USFS, U.S. Forest Service; WGNHS, Wisconsin Geological and Natural History Survey.

Ratios of stable isotopes in water are commonly used in hydrologic studies to evaluate source areas and the relative mixing of groundwater and surface water (for example, Krabbenhoft and others, 1990; Hunt and others, 2006; Leaf and others, 2015). This study reports ratios of the naturally occurring stable isotopes of both hydrogen (^2H and ^1H) and oxygen (^{18}O and ^{16}O) in water samples. For both elements, water molecules containing the lighter isotope (^1H and ^{16}O) evaporate preferentially and the resulting “fingerprint” of evaporation is a conservative tracer (Gat, 1996) because the remaining groundwater has a higher proportion of the heavier isotopes. Evaporation can be inferred in surface water and groundwater when stable isotope ratios systematically differ from local meteoric water. Here, isotopic ratios are reported in standard delta (δ) notation as units per mil or parts per thousand notation (‰) relative to the Vienna Standard Mean Ocean Water (VSMOW). The water samples collected in spring and fall as described above (six locations, twice each) were analyzed for $\delta^{18}\text{O}$ and $\delta^2\text{H}$ by the Iowa State University Stable Isotope Lab (<https://siperg.las.iastate.edu/stable-isotope-lab-sil/>).

Groundwater investigation

A groundwater investigation was conducted in the vicinity of Blaser Creek at FR194 (Blaser monitoring well, station mar11 in fig. 9 and table 1). This location was selected because it was a likely area of groundwater upwelling and because it was one of the few places where instrumentation was not limited by cobbles or bedrock. A shallow monitoring well was installed 10 ft from Blaser Creek and a mini-piezometer was installed in the creek itself. The well was installed 5.4 ft below ground surface with a 5-ft long screen; the subsurface materials consisted primarily

of organic matter over about 1 ft of fine sand. The mini-piezometer, a type of monitoring well with a small screen opening for groundwater that is used to compare the stream stage with the groundwater head (see U.S. Geological Survey, 2000), was installed 3 ft below the streambed. The mini-piezometer was constructed using rigid tubing with mesh secured to the bottom to prevent soil from clogging the tube. A seepage meter was used to evaluate the groundwater exchange with the stream (see Rosenberry and LaBaugh, 2008). This instrument was constructed by WGNHS staff from a 5-gallon bucket that was inserted open-side down into the streambed. A small opening in the bucket was attached to a plastic bag, which filled with water if the groundwater was flowing upward into the stream. Because the area of the bucket was small and groundwater inflow is rarely uniform, the results were expected to vary substantially depending on where the instrument was installed; multiple tests were performed to allow for reasonable certainty in the direction (if not magnitude) of groundwater flow. One seepage meter test was completed on May 31, 2018, and three were completed on September 26, 2018.

Shade

Shade can be an important factor for keeping streams cool (Gaffield and others, 2005; Cross and others, 2013). However, it is difficult to quantify shade as a numeric parameter. Tree canopy height, tree crown width, distance from stream, and vegetation density were measured or estimated. These measurements can be used to estimate the percent of the stream surface that was shaded, which was used as an input for the stream temperature model (see *Shade* in chapter 5).

Trout habitat

The presence of trout and the quality of the potential habitat in the study area were subjectively evaluated by observing conditions, discussing these issues with USFS fisheries biologist Sue Reineke, and talking to anglers in the field. Small trout have been observed in parts of the headwaters, but most tributaries are either too warm to support a trout population or are too steep and rocky to provide passage for them. For example, the cold headwaters of Whisky Creek support trout, but the stream warms substantially by the time it reaches the Marengo River's main channel. The majority of the trout (and trout anglers) were observed in the main channel of the Marengo River, downstream of Tributary 7 (fig. 2).

Results

Air temperature and precipitation

In the study area, the daily mean air temperatures ranged from 7.5°C to 26.6°C (fig. 10). Records were similar between the Clam Lake weather station and the two local measurement locations at the North Country Trail (station mar07) and Blaser Creek (station mar08). The monthly average air temperature was similar to that of previous years measured at Clam Lake (fig. 11). The 2018 average annual air temperature of 4.5°C was slightly lower than the long-term average for 2008–2017 of 4.9°C. For the summer months, May and June 2018 were warmer than average.

The total precipitation in 2018 at Clam Lake was 32.2 in., which is equal to the average annual precipitation from 2008–2017. A drier than average spring was followed by a wetter than average fall (fig. 12). A regionally important rain event occurred from June 15–18, 2018. Clam Lake station recorded 3.8 in. over these 4 days. Drummond, about 15 mi to the west,

Figure 10. Daily mean air temperature at three measurement locations for mid-May through late September of 2018. Daily precipitation is shown for reference. See table 1 and figure 9 for location information. Abbreviations: °C, degrees Celsius; in., inches.

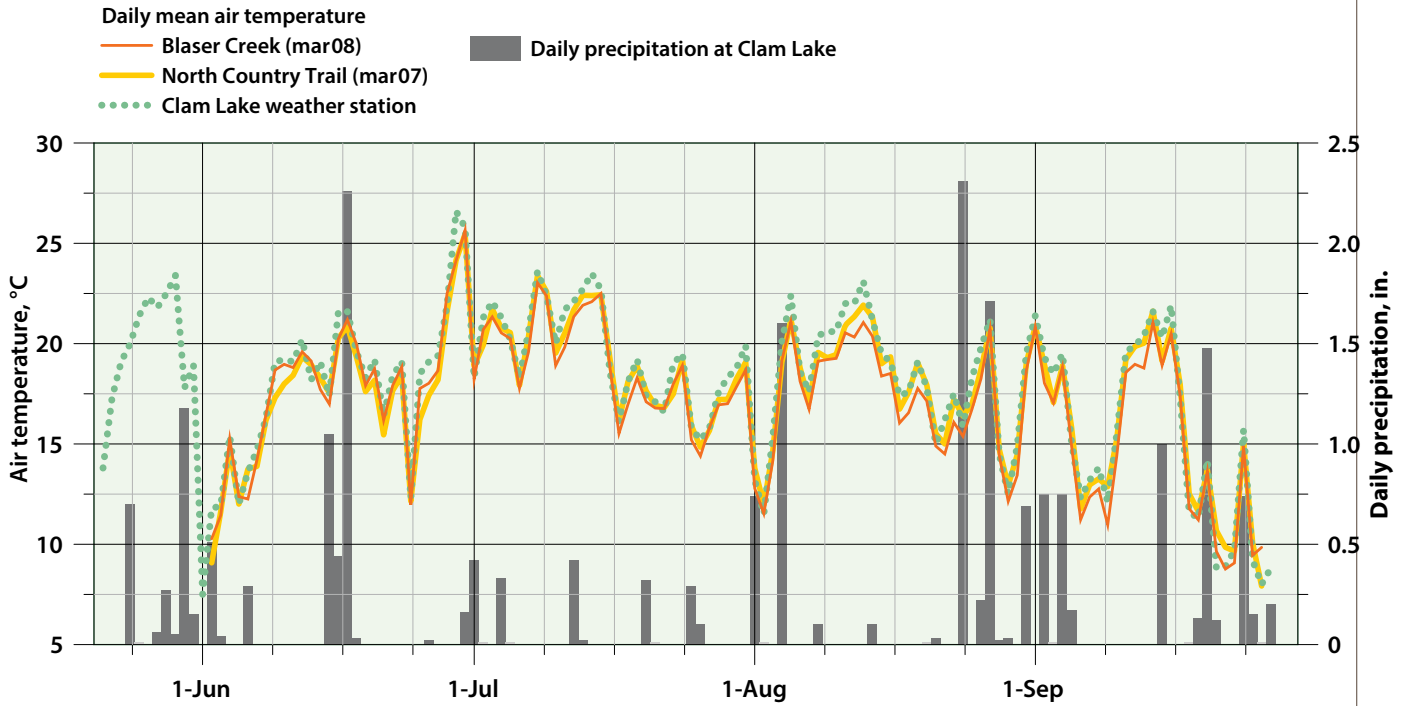
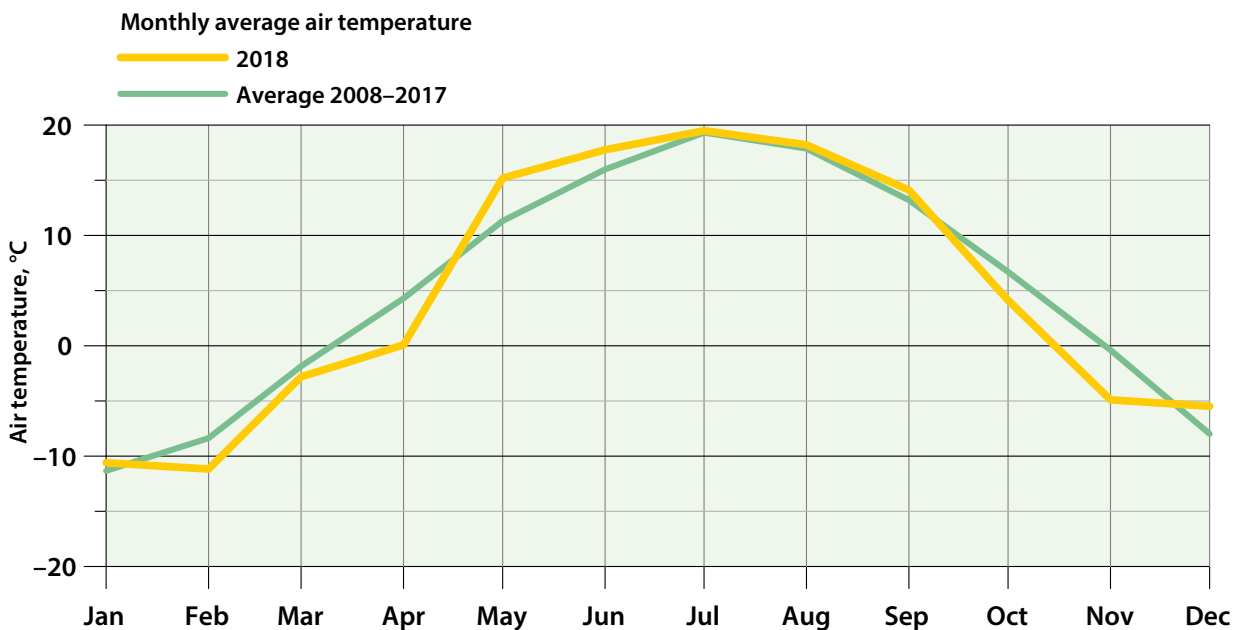


Figure 11. Monthly average air temperature in 2018 compared to the long-term (2008–2017) average at Clam Lake weather station. Abbreviation: °C, degrees Celsius.



received roughly 15 in. from this same event (https://www.weather.gov/dlh/June15-17_2018flooding). Gridded precipitation records from the National Weather Service suggest the study area may have received between 4.1 to 6.3 in. (<https://water.weather.gov/precip/>).

Stream temperature

The measured stream temperatures in the study area varied spatially (figs. 13–16, supplementary datasets). The maximum 7-day mean temperature ranged from 11.8°C at Tributary 7 (station 21755) to 25.0°C at Whisky Creek (station 21704; fig. 13). Figures 14–16 show the 7-day mean temperature time series in the Marengo River and selected tributaries, from upstream (fig. 14) to downstream (fig. 16). The water temperature in the main channel was moderately warm in the headwaters and increased downstream until the highest main channel record at the waterfall (station mar05; fig. 14). Below the waterfall (fig. 15), main channel temperatures dropped until the coolest main channel record at the

FR198 bridge (station mar02), about 0.5 mi downstream of the coldest surface-water record at Tributary 7 (station 21755). The temperature in the main channel continued to decrease downstream of Tributary 7 (station mar10) to FR198, suggesting the presence of an additional focused groundwater discharge to the main channel downstream of Tributary 7. The Marengo River warmed again slightly going downstream to FR384 (station 21602; fig. 16). Gaps in stream temperature data indicate periods when the stream stage dropped below the thermograph and the record likely represents the air temperature instead.

Figure 17 indicates that the warmest daily maximum water temperatures occurred in May and June and compares the warmest and coldest main channel records at the waterfall (stations mar03 and mar05) and FR198 (station mar02), respectively. The highest water temperature at the waterfall, 27.5°C, was measured on June 30. The air temperature measured at the North Country Trail

(station mar07) reached the highest of the season, 33.4°C, on the previous day. At FR198, the highest water temperature was measured early in the season on May 29 at 21.2°C. The nearest weather station (Clam Lake) reported a seasonally warm maximum air temperature of 32.8°C that day. (Local air-temperature sensors, as well as some stream-temperature and stream-depth sensors, were not deployed until 2 days later.) Warmer air temperatures were recorded later in the season, but they were not accompanied by equivalent increases in stream temperature at FR198. The differences could be attributed to the lack of vegetative shade or to the different sun angle during the early spring. The minimum recorded stream temperature was similar at both locations: 9.7°C at the waterfall and 9.6°C at FR198 on May 20, only 9 days before the first temperature peak. Daily temperature fluctuations were muted at FR198, where cool groundwater discharge buffers the daily extremes (also see Loheide and Gorelick, 2006).

Figure 12. Monthly average precipitation in 2018 compared to the long-term (2008–2017) average at Clam Lake weather station. Abbreviation: in., inches.

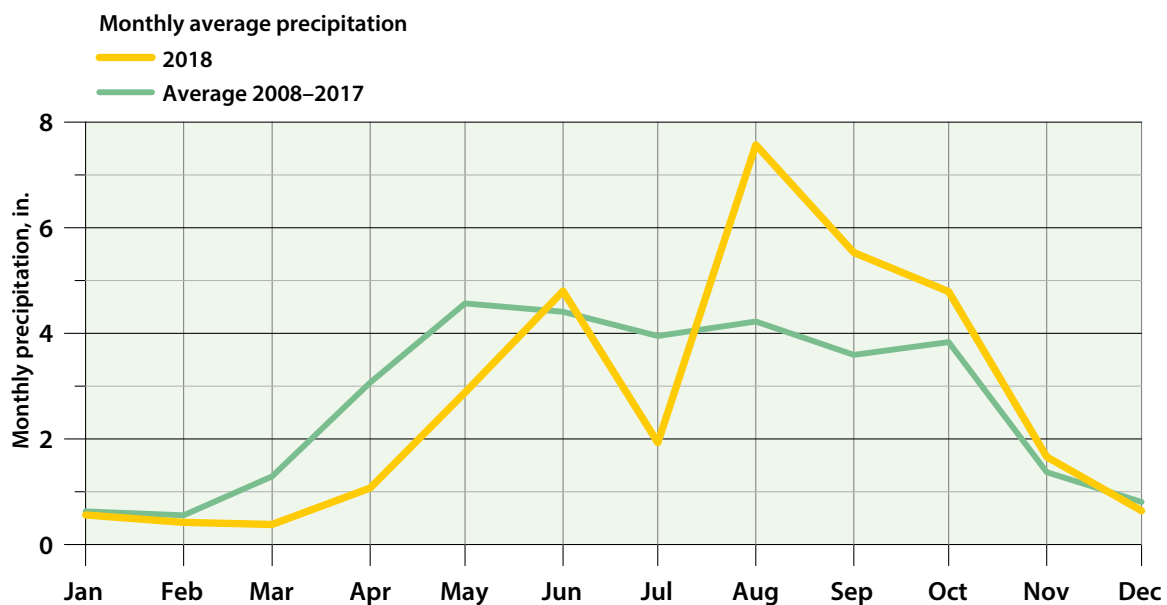
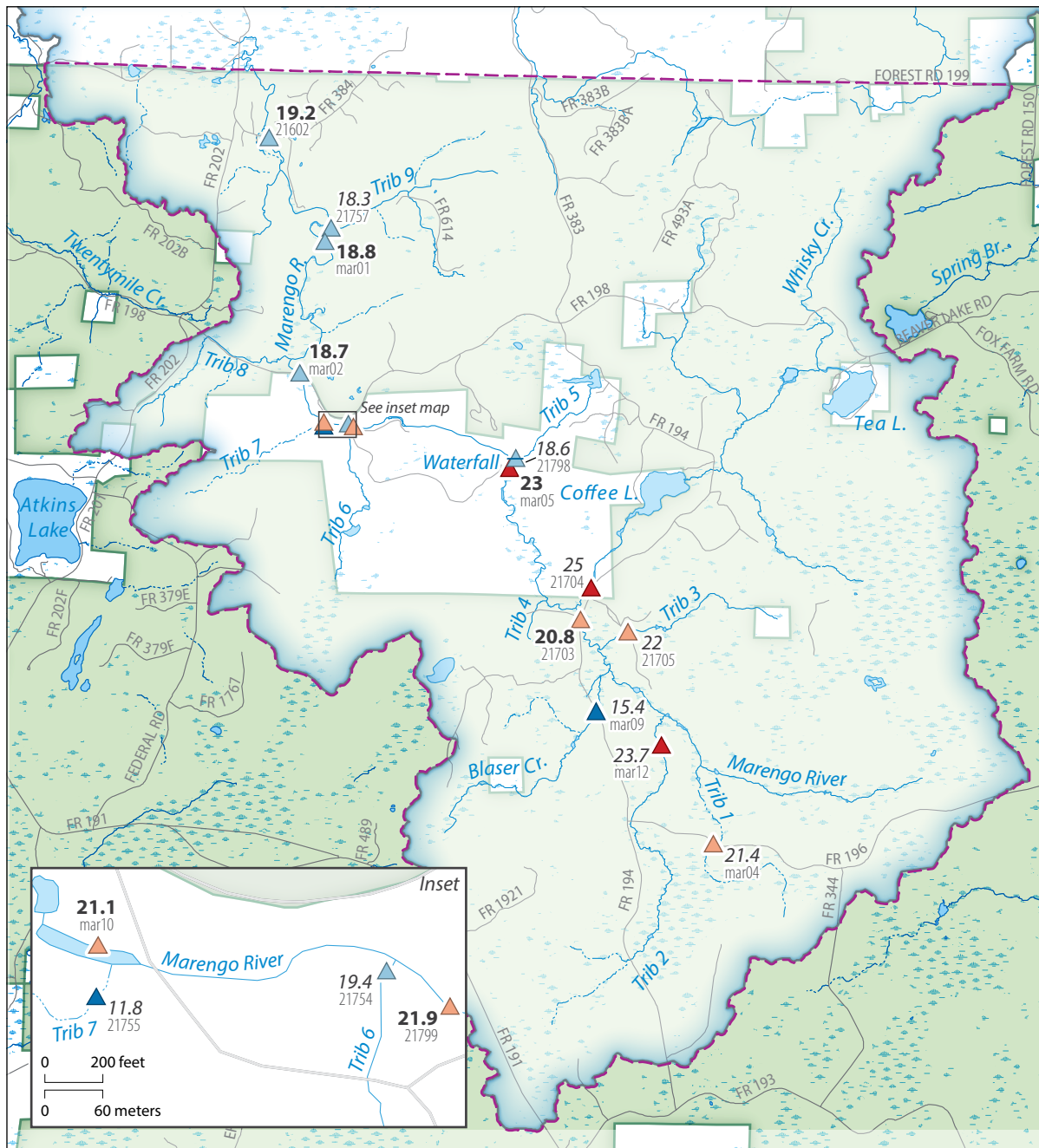


Figure 13. Maximum 7-day mean water temperature at stream thermograph locations in 2018.
Abbreviation: °C, degrees Celsius.



National Forest boundaries from the USDA Forest Service, 2011. Hydrography from National Hydrography Dataset (U.S. Geological Survey, 2016).

Figure 14. Stream temperatures from the headwaters to the waterfall in the Marengo River study area, with air temperature and precipitation at Clam Lake for comparison. A, Graph showing measured 7-day mean water temperature in 2018. B, Map showing locations of stream thermographs (also see table 1). Abbreviations: °C, degrees Celsius; FR, Forest Road; in., inches.

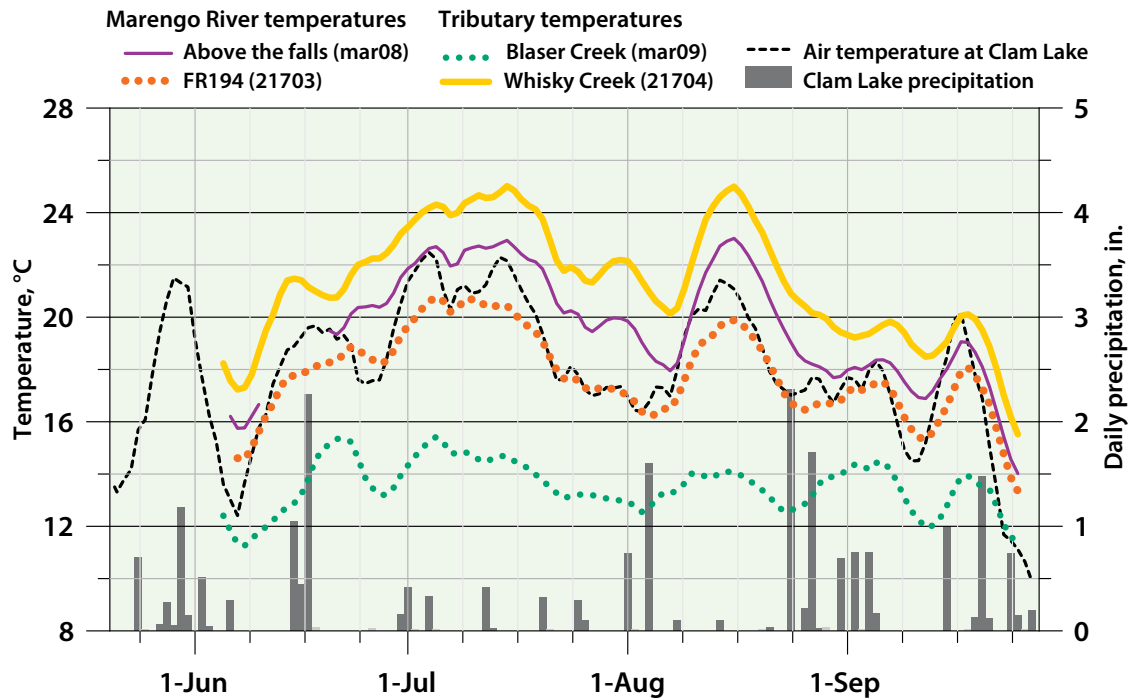


Figure 15. Stream temperatures from the waterfall downstream to FR198 in the Marengo River study area, with air temperature and precipitation at Clam Lake for comparison. A, Graph showing measured 7-day mean water temperature in 2018. B, Map showing locations of thermographs (also see table 1). Abbreviations: °C, degrees Celsius; FR, Forest Road; in., inches.

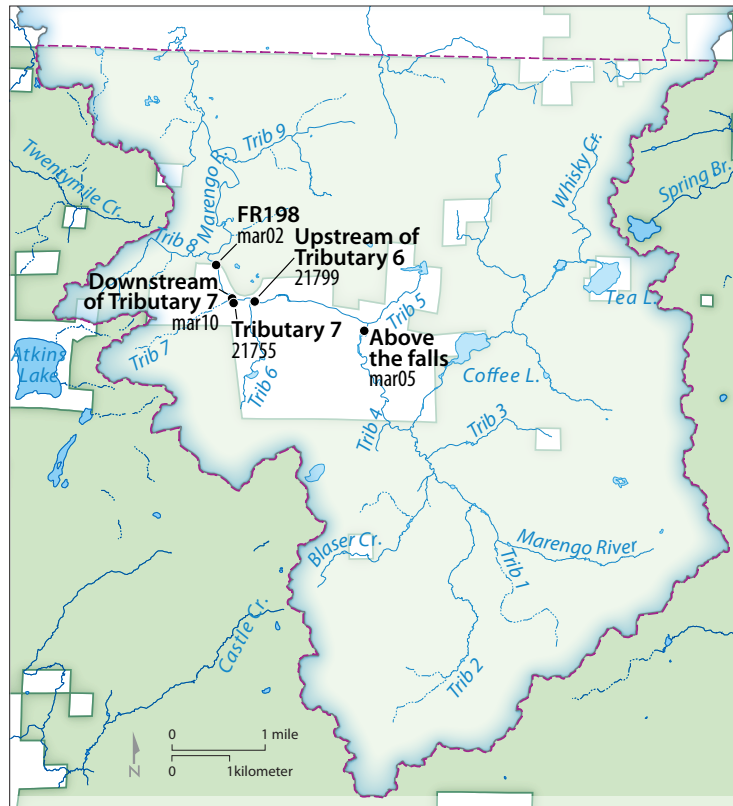
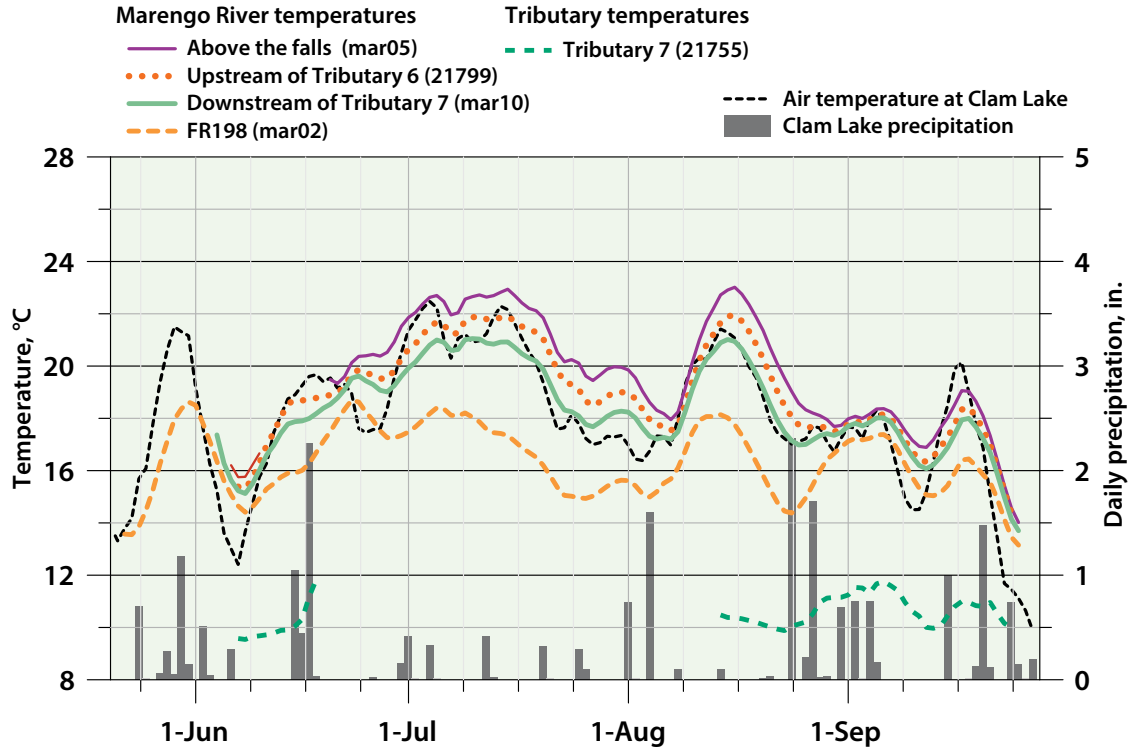
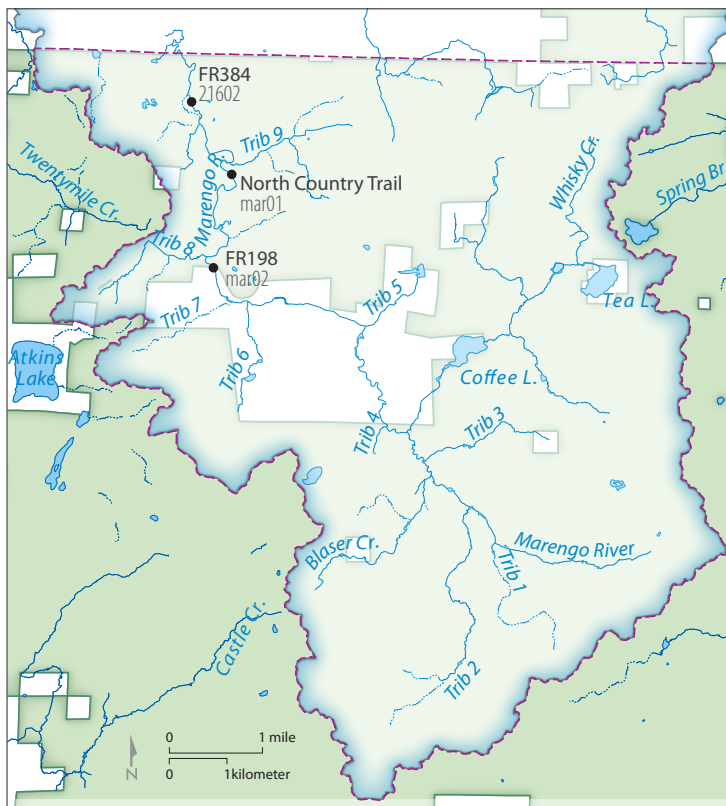
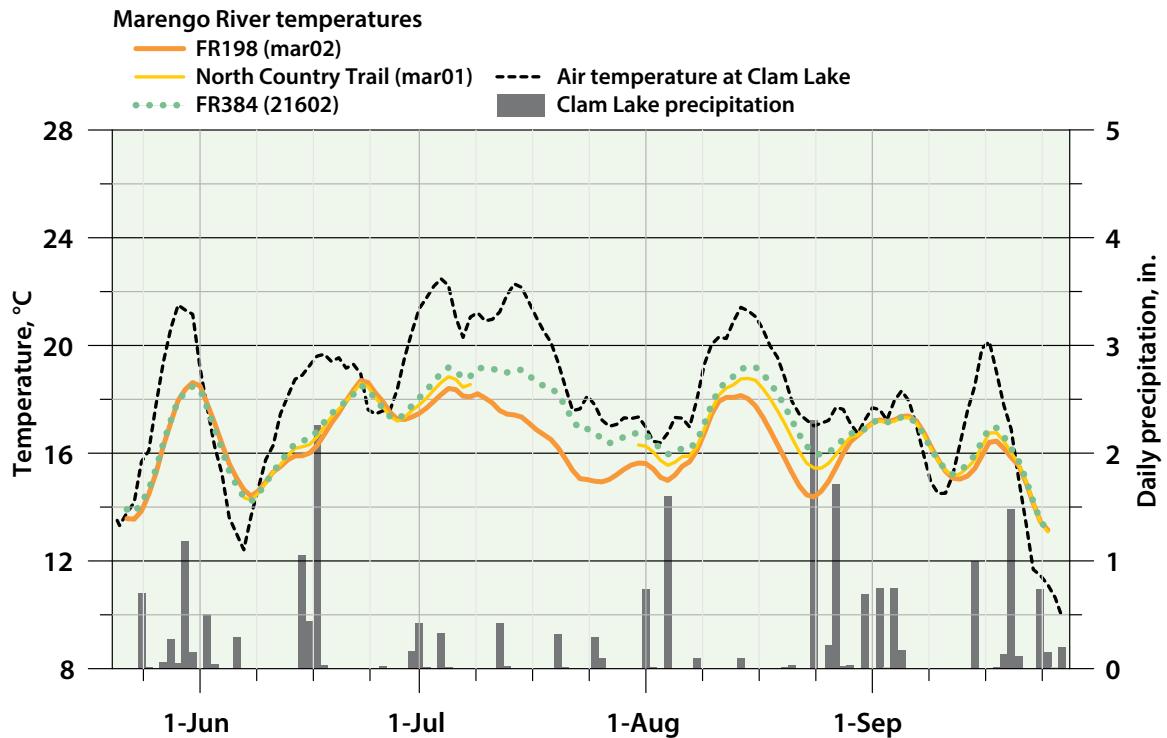


Figure 16. Stream temperatures from FR198 to FR384 in the Marengo River study area, with air temperature and precipitation at Clam Lake for comparison. A, Graph showing measured 7-day mean water temperature in 2018. B, Map showing locations of thermographs (also see table 1). Abbreviations: °C, degrees Celsius; FR, Forest Road; in., inches.



Both rainfall and air temperature were factors in warming some cool areas, including the Marengo River at FR198 (station mar02), Tributary 7 (station 21755), and Blaser Creek (station mar09). High streamflow may have limited the buffering ability of the groundwater discharge, as those places were overwhelmed by warmer runoff. Because the air temperature tended to be cooler during rain events, however, the average stream temperature at FR198 during high and low flows was approximately the same (table 2).

The stream temperature of the Marengo River at FR198 was 4°C to 6°C below the maximum thermal tolerance limits for trout during different measurement periods in 2018 (table 3) (Wehrly and others, 2007). Some warmer locations, such as the Marengo River above the waterfall (station mar05), already exceeded the

Figure 17. Warmest and coldest temperature records for the main channel of the Marengo River in 2018 compared to precipitation and river depth. The warmest record is based on nearly identical data from two stations spaced close to each other in the Marengo River (mar05 and mar03, above the waterfall and at the waterfall, respectively); these stations were chosen to avoid gaps in data. The river depth was measured at station mar10 below Tributary 7; the air temperature was measured at station mar01 at the North Country Trail (also see table 1 and fig. 9 for location information). Abbreviations: °C, degrees Celsius; FR, Forest Road; ft, feet; in., inches.

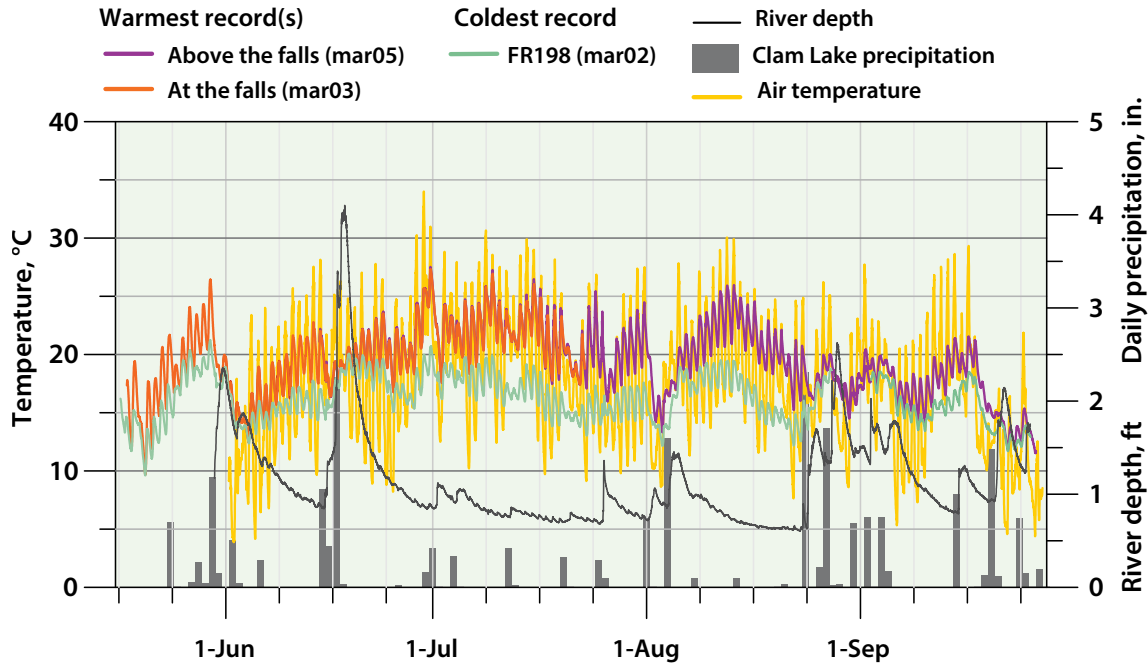


Table 2. Average daily air and water temperatures during high and low flows of the Marengo River at FR198 (station mar02), June 8–September 25, 2018.

Flow	Air temperature, °C	Water temperature, °C	Number of days
Low flow	18.3	16.2	82
High flow ^a	15.7	16.3	34

Abbreviation: °C, degrees Celsius.

^aHigh flow is defined as river depth above 1.25 feet.

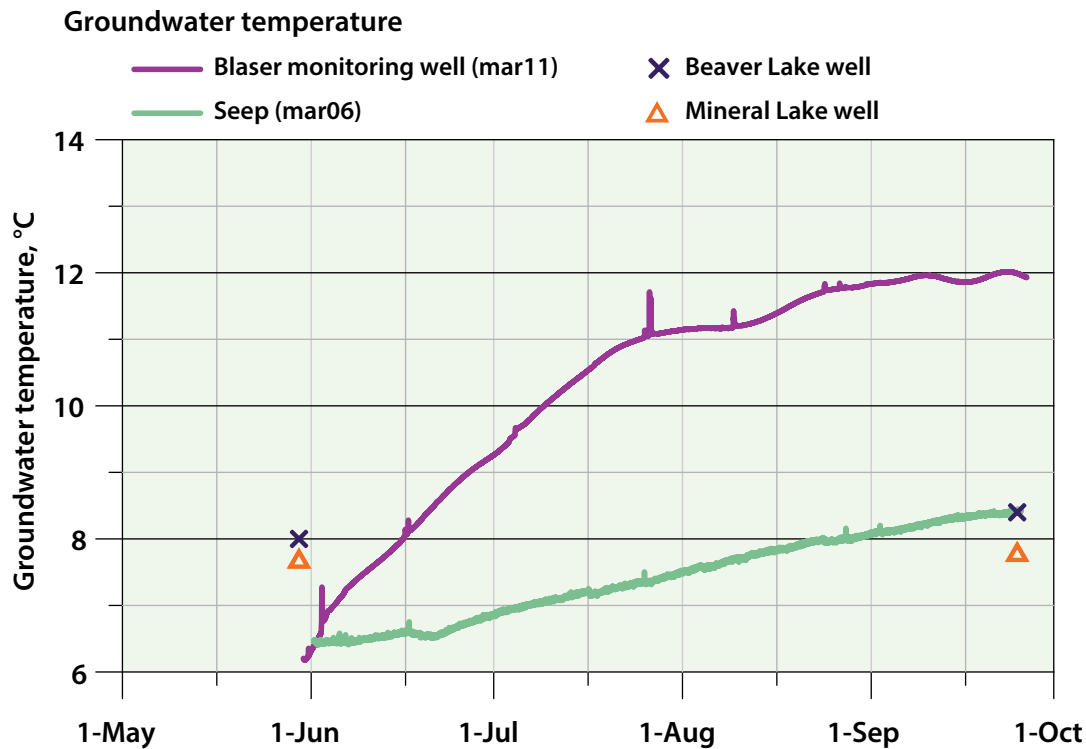
Table 3. Water temperatures of the Marengo River at FR198 (station mar02) measured during the summer of 2018 compared to the maximum thermal tolerance limit of trout.

Measure of thermal tolerance	Temperature, °C	
	FR198	Thermal tolerance limit ^a
Maximum daily mean	19.9	25.3
Maximum 7-day mean	18.7	23.3
Maximum 14-day mean	18.1	22.5
Maximum daily maximum	21.2	27.6
Maximum 7-day maximum	19.9	25.4
Maximum 14-day maximum	19.4	24.6

Abbreviations: °C, degrees, Celsius; FR, Forest Road.

^aThermal tolerance limits from Wehrly and others (2007)

Figure 18. Groundwater temperature in 2018. See table 1 and figures 2 and 9 for location information. Abbreviation: °C, degrees Celsius.



thermal tolerance limits. See *Evaluating potential impact to trout* in chapter 5 for further discussion.

Groundwater temperature

The shallow groundwater temperature in the Blaser monitoring well (station mar11) increased from 6.3°C in early June to 12°C by late September (fig. 18). Groundwater temperature in the seep (station mar06) did not increase as much, ranging from about 6.5°C to 8.4°C over the same period. These temperatures suggest that the groundwater feeding the seep follows longer, deeper flow paths than the groundwater feeding Blaser Creek and the surrounding wetlands. Deeper wells at the nearby Beaver Lake (FF650) and Mineral Lake (JB982) campgrounds (fig. 1) yielded an even narrower range of temperatures, from 7.8°C to 8.4°C. These wells are 44 and 77 ft

deep, respectively, and are screened in sand or sand and gravel. The groundwater temperatures in the campground wells were substantially warmer than the average annual air temperature of 4.8°C (Clam Lake from 2008–2017), which is sometimes used to estimate the regional groundwater temperature.

Stage

The approximate depth to groundwater at the Blaser Creek monitoring well (station mar 11 in fig. 9) is shown in figure 19. The water table is shallow (within 2 ft of the ground surface) and occasionally rises above the land surface during large rain events. Unfortunately, continuous measurements of the adjacent Blaser Creek stage (station mar09 in fig. 9) and its relation to the groundwater levels were unreliable and are not included in this report. However, single mea-

surements comparing water levels in the stream to those in the nearby monitoring well are consistent with a gaining stream in this location.

Figure 20 shows the stream depth and water temperature measured in the Marengo River downstream of Tributary 7 (station mar10 in fig. 9). The rain event from June 15–18, 2018, totaled between about 4 and 6 in. (see *Air temperature and precipitation* in chapter 3) and caused the stage to increase by 3 ft.

Figure 19. Depth to groundwater in the Blaser monitoring well (station mar11; see table 1 and fig. 9 for location) in 2018. Abbreviations: ft, feet; in., inches.

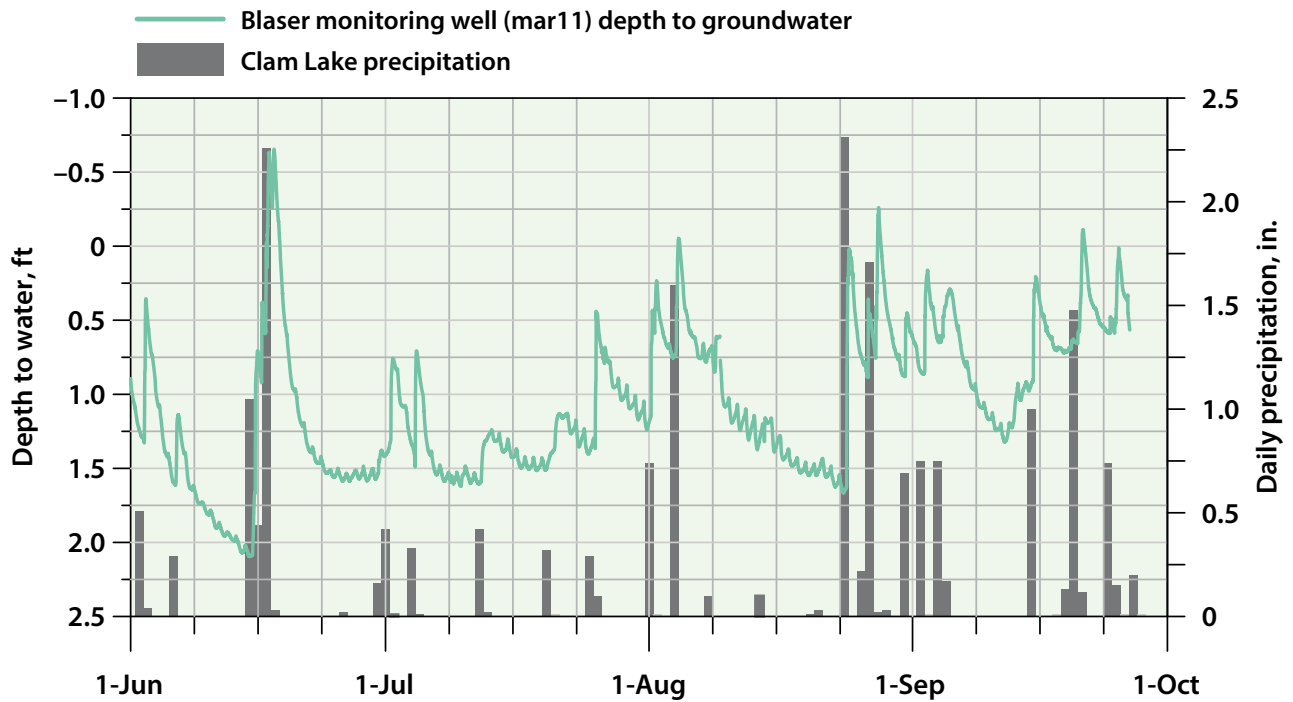
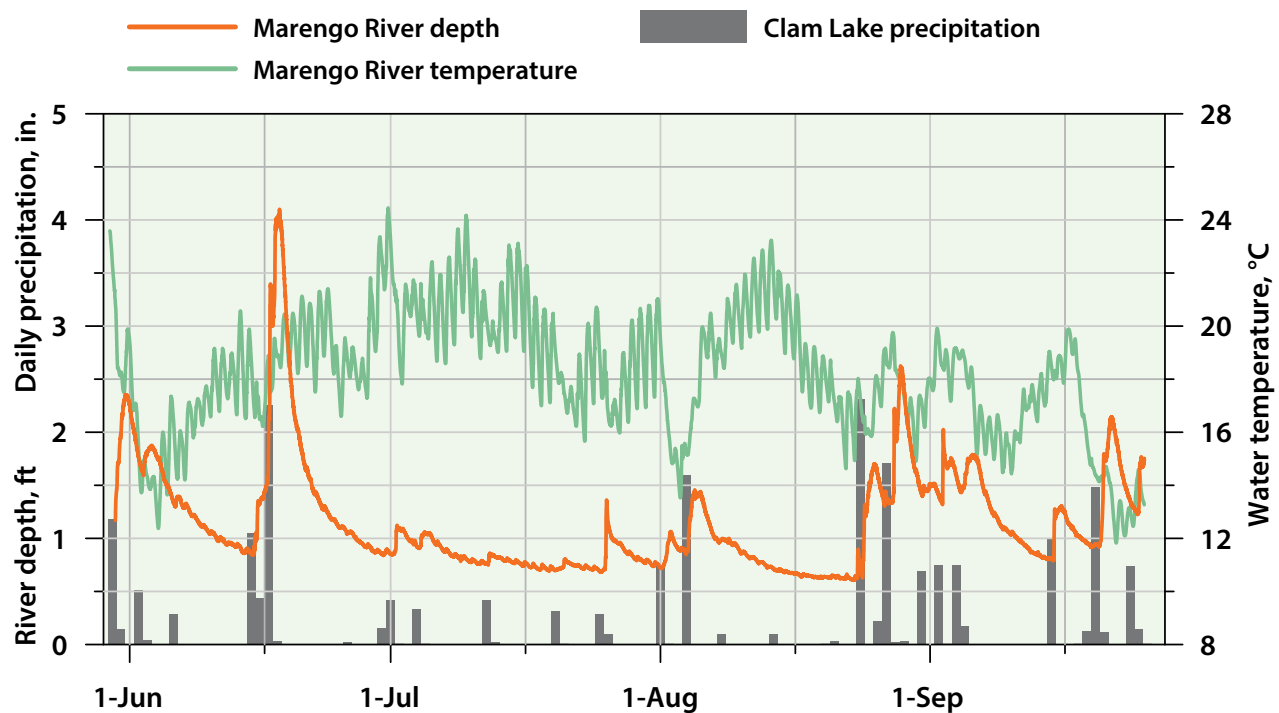


Figure 20. Marengo River depth and temperature in 2018. Readings taken in the Marengo River downstream of Tributary 7 (station mar10 on fig. 9; also see table 1). Precipitation measured at Clam Lake provided for comparison. Abbreviations: °C, degrees Celsius; ft, feet; in., inches.



Streamflow

The measured streamflow near the downstream end of the study area (stations 21602 and USGS #04026590) ranged from 14.5 to 129.6 cubic feet per second (cfs) in 2018 (table 4). The largest measured streamflow was at FR384 (station 21602 in fig. 9) after a rain event of 1.3 in. on May 30–31, 2018. Streamflows in tributaries were typically less than a few cubic feet per second, with the exception of Tributary 7 and the larger Whisky Creek. The Tributary 7 streamflows (3.1–4.4 cfs at station 21755; fig. 9) were notably high compared to Tributary 6 (0.1–0.7 cfs at station 21754; fig. 9), despite their similar drainage areas. See *Targets* in chapter 4 for further discussion. Some areas, such as Whisky Creek (station 21704 in fig. 9) and the Marengo River at FR194 (station 21703 in fig. 9), had relatively higher streamflows even several days after a rain event and may have included a higher percentage of surface-water runoff. These areas also tended to correlate with higher stream temperatures.

During the time period when the streamflow was measured, new beaver dams were observed in several parts of the headwaters, including downstream of measurement locations in the Marengo River at FR194 (station 21703) and in Blaser Creek (station mar09). Existing beaver dams were observed in spring of 2018 in several headwater tributaries, including Tributary 1 upstream of FR196, and in the Marengo River above Tributary 2.

Water chemistry

Field chemistry measurements including pH and conductivity were obtained during both wet and dry periods throughout the summer (appendix table 1.1). Two rounds of laboratory samples (appendix table 1.2) were collected in the spring and fall of 2018, both affected by rainfall. Spring samples were collected May 29–June 1 following a rain event May 24–31 that totaled 2.3 in., and fall samples from were collected September 25–27 following a rain event September 24–25 that totaled 0.9 in. Chemistry measurements are available for download from the supplementary datasets.

ION CHEMISTRY

The surface-water samples in the Marengo River were a calcium bicarbonate type with a near-neutral pH similar to the regional values reported in Fehling and others (2018). Compared to surface water, the groundwater samples in the study area were characterized by higher conductivity, alkalinity, and concentrations of ions, but they contained a similar relative quantity of ions. Chloride, nitrate, and phosphorus—commonly elevated in populated areas due to road salt and fertilizer use—were low in this watershed.

As with the stream-temperature measurements, electrical conductivity measurements were taken to identify possible areas of groundwater influence. The results indicate a substantial spatial variation in conductivity across the study area. The spatial patterns are illustrated in figure 21, which shows conductivity measured in mid-May and early August, both relatively dry periods. The highest electrical conductivity, 205 microsiemens per centimeter ($\mu\text{S}/\text{cm}$), was observed at the seep (station mar06; also see appendix table 1.1). Samples from Tributary 7 (station 21755), Tributary 8 (station 21756),

and Blaser Creek (station mar09) also had high conductivity; the lowest values were observed at Whisky Creek (station 21704) and Marengo River at the waterfall (station mar03). Conductivity was lower overall during wet sampling periods on May 30 and September 25, when water quality was heavily influenced by rainfall runoff. Compared with other samples, those from the seep had high electrical conductivity and alkalinity, higher concentrations of manganese and calcium, and lower concentrations of iron (fig. 21, appendix tables 1.1 and 1.2). These values are within the range of other groundwater samples from the area (Fehling and others, 2018).

ISOTOPES

The results from stable isotope sampling of groundwater and surface water in the study area are shown on figure 22 (also see supplementary datasets). The graph also shows the local meteoric water line (LMWL), which is the linear relation between $\delta^2\text{H}$ and $\delta^{18}\text{O}$ in precipitation. The LMWL is based on precipitation samples from Minnesota (Magner and others, 2014). Water samples that plotted off the LMWL were exposed to surface-water evaporation or other physical processes. Most samples collected in the fall plotted on or near the line, suggesting little evaporation had occurred. Some of the samples collected during the spring—including from the seep (station mar06) and the Marengo River at FR384 (station 21602) and FR194 (station 21703)—plot to the right of the line, suggesting some evaporation had occurred.

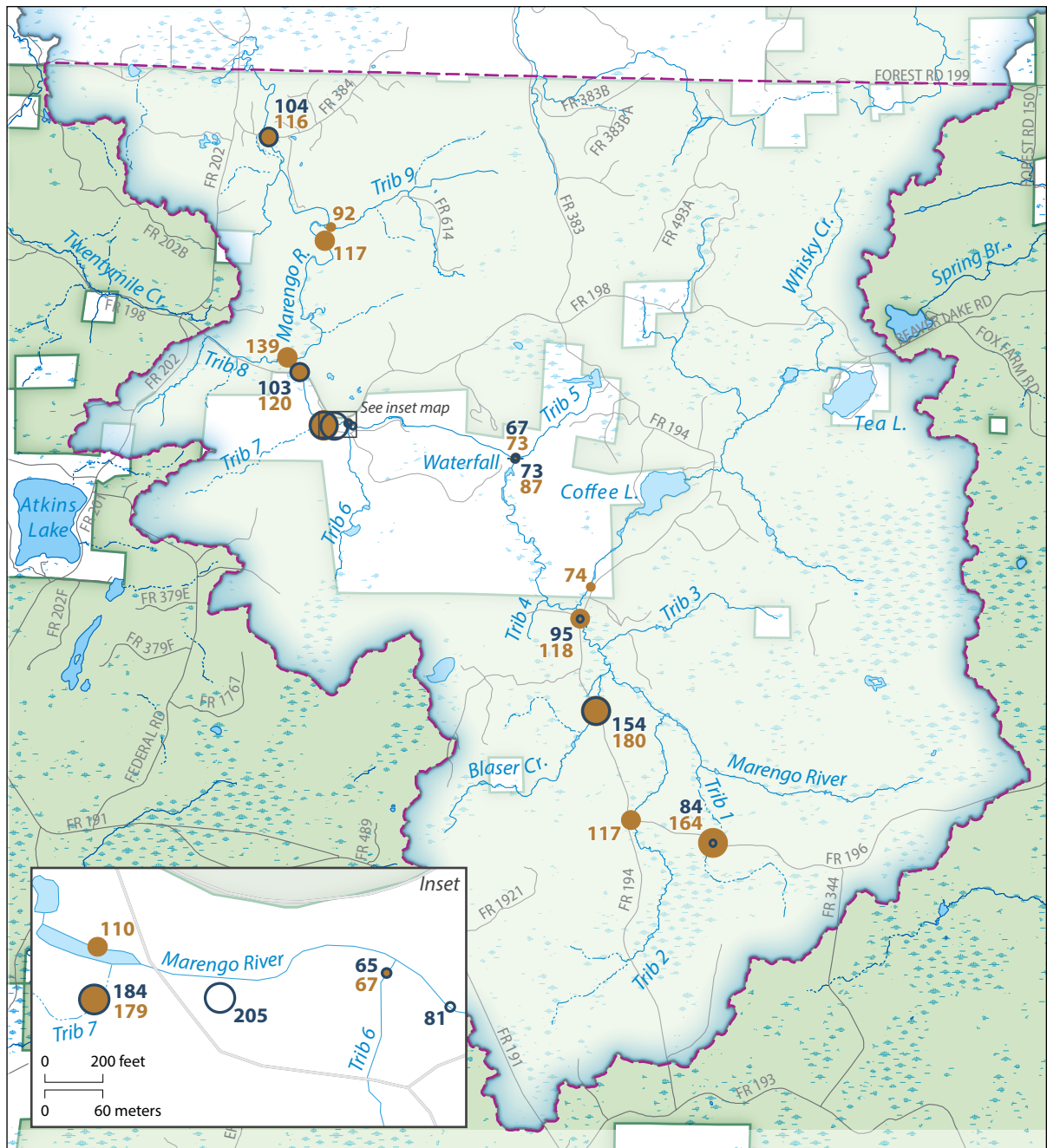
Table 4. Streamflow measurements in the study area.

Station ID ^a	Location	Date	Discharge (cfs)	Source
USGS #04026590	Marengo River at Altamont Road	8/30/2011	11.3	USGS
		8/21/2018	14.5	USGS
21602	Marengo River at FR384 bridge	6/1/2018	129.6	WGNHS
		8/7/2018	30.0	WGNHS
21757	Tributary 9	8/7/2018	0.3	WGNHS
mar01	Marengo River at North Country Trail	8/7/2018	29.8	WGNHS
21756	Tributary 8	8/27/2002	0.5	USFS
		9/2/2003	0.4	USFS
		8/8/2018	0.7	WGNHS
mar02 / USGS #04026580	Marengo River at FR198/Wisco Road	8/30/2011	9.7	USGS
		8/21/2018	12.0	USGS
mar10	Marengo River downstream of Tributary 7	5/29/2018	22.8	WGNHS
		7/16/2018	11.7	WGNHS
		8/8/2018	26.4	WGNHS
21755	Tributary 7	8/27/2002	3.1	USFS
		9/2/2003	3.6	USFS
		8/8/2018	4.4	WGNHS
21707	Marengo River between Tributaries 6 and 7	7/16/2018	8.2	WGNHS
21754	Tributary 6	8/27/2002	0.2	USFS
		9/2/2003	0.1	USFS
		8/8/2018	0.7	WGNHS
mar03	Marengo River downstream of Tributary 5	8/8/2018	21.8	WGNHS
21798	Tributary 5	8/8/2018	0.7	WGNHS
NA	Marengo River downstream of Whisky Creek	7/17/2018	4.0	WGNHS
21704	Whisky Creek	5/29/2018	17.4	WGNHS
		5/31/2018	62.3	WGNHS
		7/17/2018	1.3	WGNHS
		8/9/2018	10.4	WGNHS
21703	Marengo River at FR194	5/29/2018	21.9	WGNHS
		5/31/2018	65.0	WGNHS
		7/17/2018	3.0	WGNHS
		8/8/2018	4.9	WGNHS
21705	Tributary 3	8/27/2002	0.1	USFS
mar09	Blaser Creek at FR194	8/27/2002	1.0	USFS
		5/31/2018	5.3	WGNHS
		7/17/2018	2.0	WGNHS
		8/9/2018	1.8	WGNHS
NA	Tributary 2 at FR196	8/9/2018	1.5	WGNHS

Abbreviations: cfs, cubic feet per second; FR, Forest Road; ID, identification number; NA, not applicable; USFS, U.S. Forest Service; USGS, U.S. Geological Survey; WGNHS, Wisconsin Geological and Natural History Survey.

^aStation IDs shown on figure 9. Station 21707 does not have a collocated thermograph and is shown on figure 25.

Figure 21. Electrical conductivity measurements in the Marengo River study area. Sampling occurred during dry periods in May and August of 2018. Abbreviation: $\mu\text{S}/\text{cm}$, microsiemens per centimeter.



Electrical conductivity, $\mu\text{S}/\text{cm}$
Label on map indicates exact measurement

May 16-18	August 7-8
• <100	• <100
○ 100-150	• 100-150
○ >150	• >150

- Marengo watershed
- Study area
- National forest
- Wetland
- Roads
- Perennial stream
- Intermittent stream

0 1 mile
0 1 kilometer

National Forest boundaries from the USDA Forest Service, 2011. Hydrography from National Hydrography Dataset (U.S. Geological Survey, 2016).

Because temperature affects the isotope fractionation efficiency, water that has a more negative isotopic signature (plotting on the lower left of graph) indicates the source precipitation was colder (for example, from snowmelt runoff or recharge). The samples collected during the spring generally displayed more negative isotopic signatures than the samples collected during the fall. Because the air temperature during the spring rain event was actually warmer than it was during the fall event, the samples collected in the spring were likely influenced by recharge and (or) runoff from snowmelt still occurring during that event. The fall samples, which were not influenced by snowmelt runoff, may provide more insight into which samples were influenced by

snowmelt-recharged groundwater. The coldest fall signatures were from the seep (station mar06), Tributary 7 (station 21755), and Blaser Creek (station mar09), which is consistent with other groundwater indicators such as conductivity and temperature. In contrast, the sample from the Marengo River at FR194 (station mar09) displayed the least negative signature, suggesting that the flow was dominated by runoff.

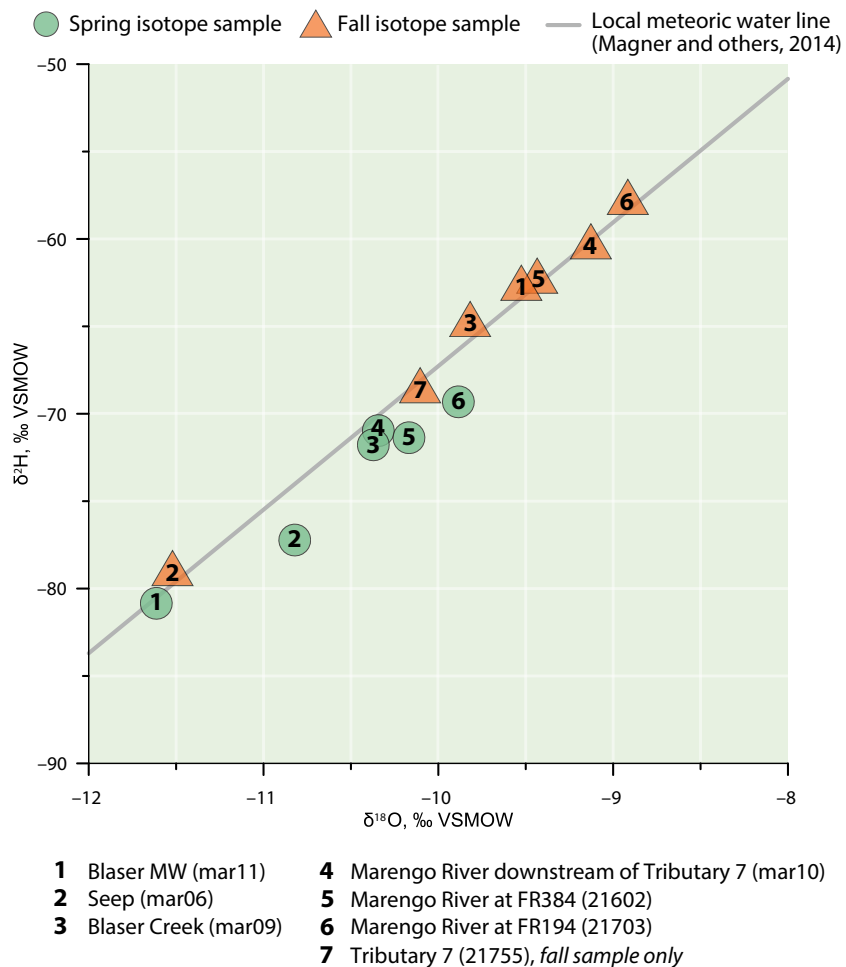
Of the two groundwater samples, the seep sample displayed a more consistent negative signature than the sample from the shallow Blaser monitoring well (station mar11). The Blaser monitoring well displayed the most negative signature for the spring sample, but it also indicated the greatest change in signature

between its spring and fall samples. Because the well is so shallow, the samples' positions along the LMWL likely reflect the surficial temperature changes of shallow recharge. In contrast, the consistency of the seep samples suggests a deeper or longer groundwater-flow path.

Groundwater interactions at Blaser Creek

The seepage meter and mini-piezometer tests both indicated that groundwater discharges into Blaser Creek. The specific discharge into Blaser Creek (volumetric flow per area of streambed), as measured by four seepage meter tests spaced less than 10 ft apart, ranged from 3.9×10^{-8} to 4.9×10^{-7} feet per second (ft/s). The test with the lowest specific discharge was suspected to be biased toward a

Figure 22. Results of stable isotope sampling in spring and fall of 2018. Abbreviations: FR, Forest Road; MW, monitoring well; VSMOW, Vienna Standard Mean Ocean Water; ‰, parts per thousand.



low value, possibly due to restrictions in the flow tube. The measured base-flow in Blaser Creek (1.5 cfs at station mar09) spread over the estimated upstream streambed surface area suggested a higher average specific discharge, on the order of 10^{-5} ft/s. Higher groundwater inputs were assumed to be upstream of the measurement location in sand and gravel deposits, consistent with simulated discharge in the groundwater-flow model (see *Targets* in chapter 4).

The elevation of shallow groundwater immediately below the creek, as measured with the mini-piezometer on three dates, was consistently higher than the creek stage, indicating groundwater was discharging into Blaser Creek. The vertical gradient (change in groundwater head per vertical distance) ranged from 0.07 to 0.16 ft/ft (feet per foot). Assuming the vertical flow fell within the range of measured specific discharge, the streambed sediment's vertical hydraulic conductivity (K_v) was calculated to be 0.02 to 0.3 feet per day (ft/d).

Discussion

The stream temperature in the Marengo River varied spatially and correlated with the differences in the hydrogeologic settings. High temperatures were observed above the waterfall and in the headwaters, where shallow till overlies low-relief crystalline bedrock. Some of these areas were already known to be poor trout habitat. Cooler temperatures were observed downstream of the fractured bedrock near the Atkins Lake–Marenisco fault and in the sandy glacial deposits of Blaser Creek. The groundwater discharge to Blaser Creek was consistent with observations of Michigan streams in similar hydrogeologic settings such as sand and gravel downgradient of glacial moraines (Wiley and others, 1997).

The varying groundwater temperatures and temporal patterns at the two groundwater-monitoring locations were attributed to differences in the groundwater-flow paths. The deeper, longer flow paths resulted in a cooler and steadier temperature signature at the groundwater seep compared to the flow path of shallow groundwater sampled in the headwater wetlands.



Above the Marengo River waterfall | Pete Chase

Chapter 4: Groundwater-flow model

The groundwater-flow modeling program GFLOW (Haitjema, 1995) was used to simulate the potential impacts of climate change on groundwater baseflow. A model of the study area simulating average groundwater flow during the late 20th century was created by refining a regional parent model covering the Great Divide Ranger District (Leaf and others, 2019). Changes to the model were guided by the geology, observed streamflows, and other characteristics of the watershed. The model was manually adjusted to match local and updated streamflow and groundwater well water-level measurements while honoring what is known about the hydrogeologic system. A manual calibration was considered sufficient for the primary purpose of simulating flow in the study area for use in the stream-temperature model (chapter 5). Although calibration using a formal inversion would likely statistically improve the model fit, it was unclear if it would result in a meaningful improvement given the small number of head targets in the study area and uncertainties from structural error. This chapter describes the model's development and performance.

Description of GFLOW model code

GFLOW is an analytic element modeling program that simulates groundwater flow in a laterally infinite aquifer with a specified bottom elevation. Hydraulic conductivity (K) was applied in user-specified zones, and recharge was applied either in zones or in a grid. GFLOW is a steady-state model; that is, it represents long-term average conditions and does not change with time. Streams and wells were input as unique elements in the model. Streams were represented in the model by elements called linesinks. Streams in the study area (near-field linesinks) incorporated data about stream stage, width, and resistance to flow with the aquifer. Baseflow, the groundwater component of streamflow, was calculated for these stream elements. Streams outside the study area (far-field linesinks) were given zero resistance, effectively setting the water-table elevation as equal to the stream stage and creating boundary conditions for the model. Further discussions of analytic elements are in Haitjema (1995) or Hunt (2006).

Analytic element models have the benefit of being relatively simple to create and modify, and they provide a continuous solution to the groundwater-flow equation (rather than being confined to a grid). However, areas with complex heterogeneity or three-dimensional flow patterns are not always well represented (Haitjema, 1995; Hunt and others, 2003). The analytic element code was selected for this project for ease of future use by the USFS and others and because poor data coverage limited the potential for creating a more complex model.

Although the user specifies hydraulic conductivity values in the model, the analytic element solution was based on transmissivity, the product of hydraulic conductivity and aquifer thickness. Therefore, transmissivity was emphasized in this report to avoid confusion.

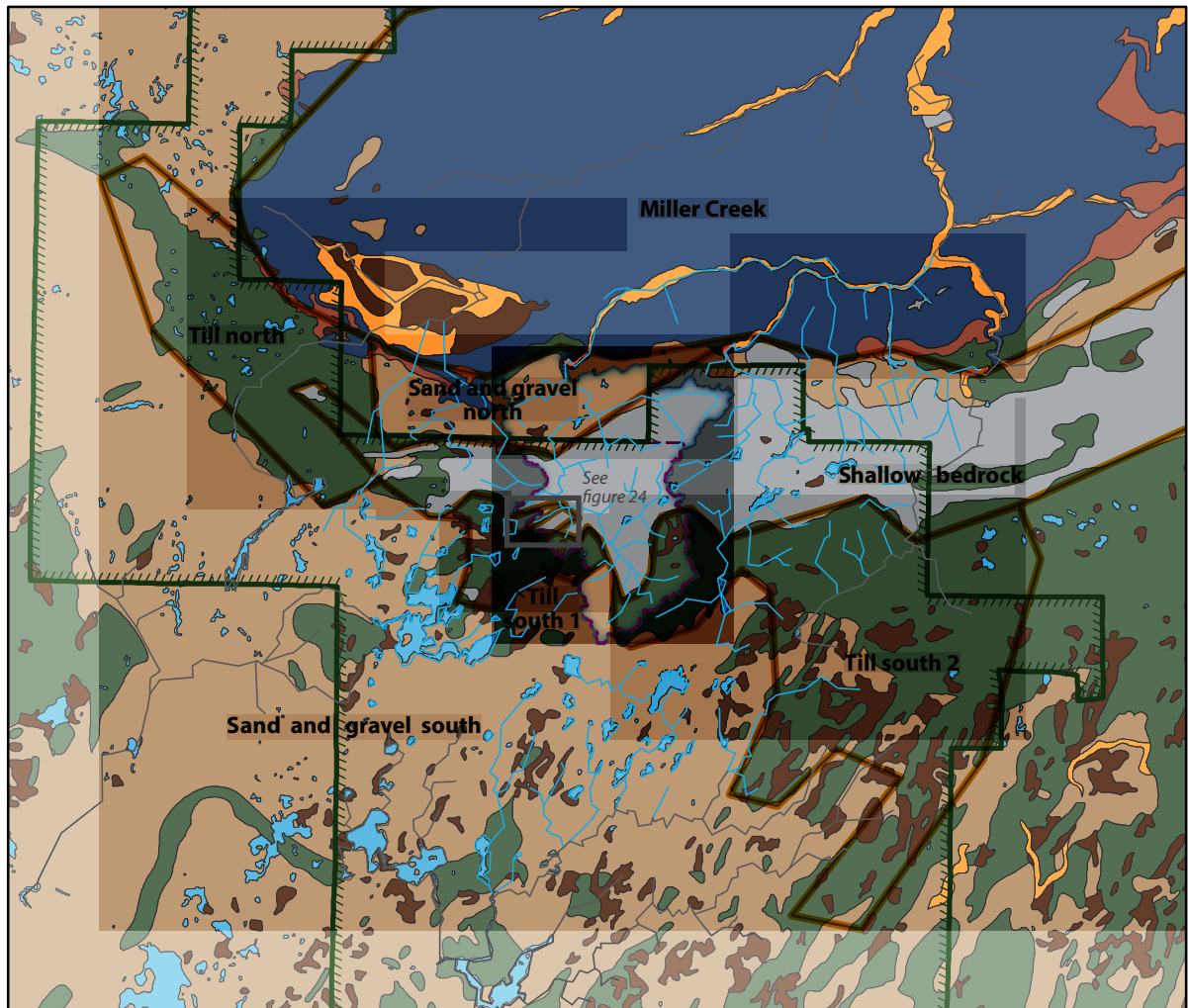
Conceptual model of Marengo River study area

The hydrogeologic setting in the region was conceptualized into a simplified system that could be readily represented in a computer model. The conceptual model followed the approach used for the parent GFLOW model but is described here for the Marengo River watershed area.

The area was divided into zones of differing aquifer transmissivity based on the geologic units present in the area (figs. 23–24). Streams were assumed to be in good connection with the aquifer system in both the glacial and bedrock zones. Zones representing glacial till and stream sediment (sand and gravel) deposits of the Copper Falls Formation, which is present north and south of the study area, were created based on mapping of Pleistocene deposits by Clayton (1984). Clay-rich till of the Miller Creek Formation is also present north of the study area.

The parent model was unable to simulate the high groundwater discharge observed in and downstream of Tributary 7. This high discharge occurred near the bedrock contact between the steeply northward-dipping bedrock layers of the Marquette Range Supergroup (fig. 4), suggesting that there was a contrast in transmissivity here. Two new zones representing shallow bedrock were added in

Figure 23. Transmissivity zones in the groundwater-flow model and surficial geologic units. Map shows names and boundaries of the transmissivity zones. Linesinks in the model are based on stream locations. See figure 24 for details of the high- and low-transmissivity bedrock zones in the rectangular area adjacent to the shallow bedrock zone. Generalized surficial sediments are modified from Clayton (1984).



GENERALIZED SURFICIAL SEDIMENTS

Post-glacial

- Sand and gravel
- Peat

Copper Falls Formation

- Sand and gravel
- Clayey sand and silty sand

Miller Creek Formation

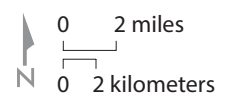
- Sand and gravel
- Silt and clay

Precambrian

- Bedrock, overlain by thin layer of sediments

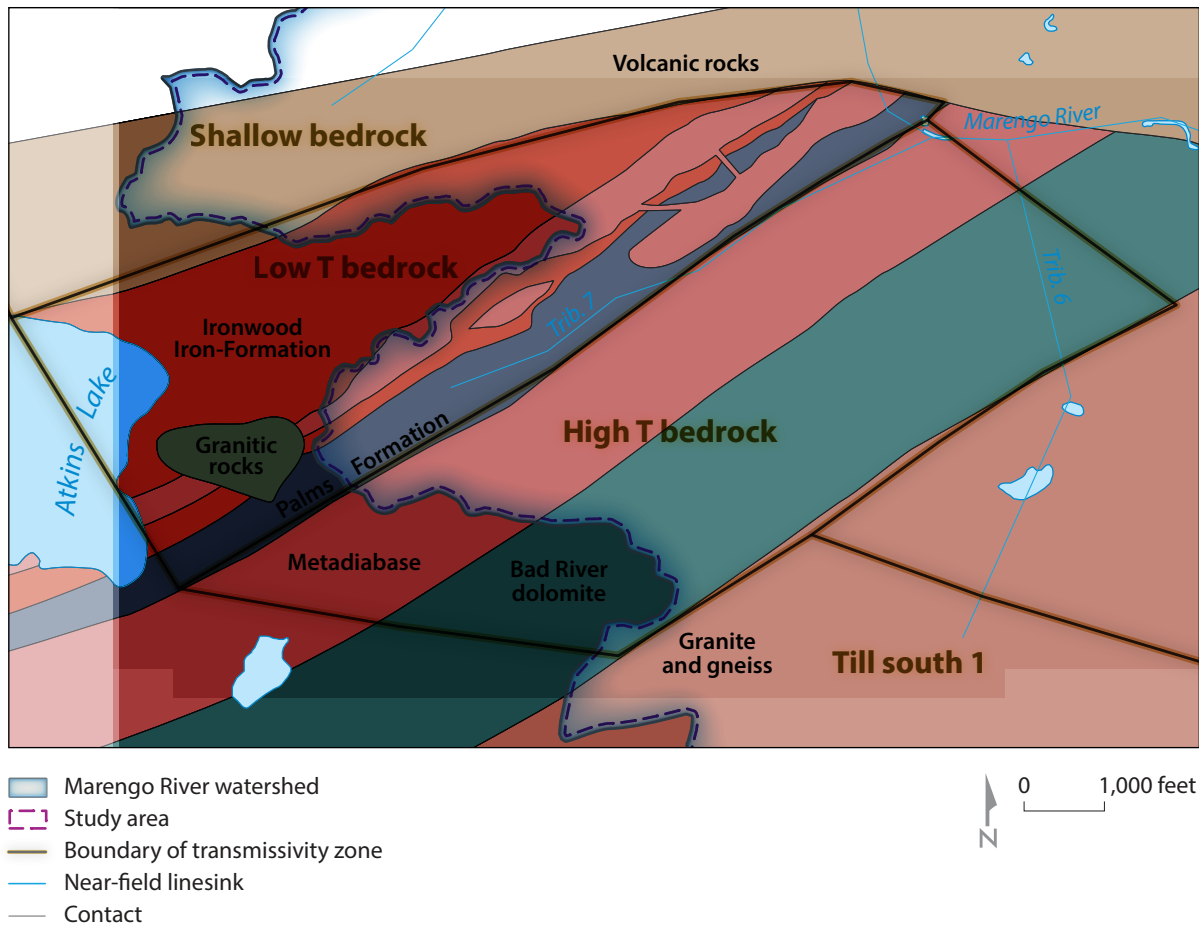
- Boundary of transmissivity zone
- Near-field linesink
- Far-field linesink
- Contact

- Marengo River watershed
- Study area
- National forest boundary, generalized



National Forest boundaries from the USDA Forest Service, 2011.

Figure 24. Detail of high- and low-transmissivity (T) zones in the groundwater-flow model, showing bedrock geologic units. Map shows names and boundaries of the transmissivity zones. See figure 23 for location.



the central part of the study area to better simulate groundwater flow near Tributary 7.

Swanson and Bahr (2004) demonstrated that high-permeability fractures in sandstones can produce steady, high volumes of spring groundwater flow. Using this conceptual model, substantial groundwater recharge and flow was inferred through bedrock fractures of a high-transmissivity zone that included the Bad River Dolomite and metadiabase, which constitute the first of the two added zones. The groundwater flow is diverted and discharges at the contact with a low-transmissivity zone that included the Palms Formation and Ironwood Iron-Formation (fig. 24),

which constitute the second added zone. The two added transmissivity zones generally followed the mapped units (Cannon and others, 2007) where bedrock was shallow.

The preliminary model runs with the high-transmissivity zone corresponding to the Bad River Dolomite resulted in a modeled groundwater flow that discharged directly to the Marengo River and bypassed Tributaries 6 and 7, which is out of agreement with field observations. Therefore, an additional model change was made. In this change, the fault was assumed to act as a hydrologic barrier to groundwater flowing perpendicular to the fault and a conduit for groundwater flowing parallel to the fault (see Caine

and others, 1996). These characteristics could be due to very low conductivity in the deformed rock located along either the fault or fractures parallel to the fault, which provide conduits for parallel flow. To represent this in the simplified GFLOW model, the simulated high-transmissivity zone was truncated south of the fault and river.

The aquifer's thickness varies throughout the study area. For the model, glacial aquifers were assumed to have a bottom elevation roughly equal to the bedrock surface, and in all areas except the high-transmissivity zone it was assumed that bedrock contributed a limited amount of transmissivity compared to the glacial materials.

In the high-transmissivity zone, it was assumed that only bedrock contributed to transmissivity. The top of bedrock is roughly 1,400 ft in the study area, except in the relatively narrow valley of the Marengo River (Fehling and others, 2018). Within the study area, the saturated thickness decreases northwards as the water table falls. North of the study area, the top of bedrock dips steeply northward to about 500 ft above sea level. In the fractured bedrock zones, flow was assumed to be limited to the top 300 ft of bedrock on the basis of fracture flow testing by Hart (2016), which yielded an approximate aquifer base of 1,100 ft. The GFLOW model did not support a sloping base elevation, and testing of stepwise changes in base elevation led to model instability. A constant aquifer base of 500 ft was therefore retained from the parent model. As a result, within the study area, the model simulated an aquifer that was thicker than reality with varying hydraulic conductivities adjusted to provide calibrated transmissivities. The calibrated hydraulic conductivities were reported both as simulated and effective values (see *Transmissivity*). Changes in head were expected to affect model transmissivity and true transmissivity differently. However, these differences were not expected to affect the results of this study because the simulated head changes were relatively small and represented a range of realistic expected changes in hydrology.

Recharge was applied over the model area to drive groundwater flow. See *Recharge*, below, for more details.

Overview of parent model

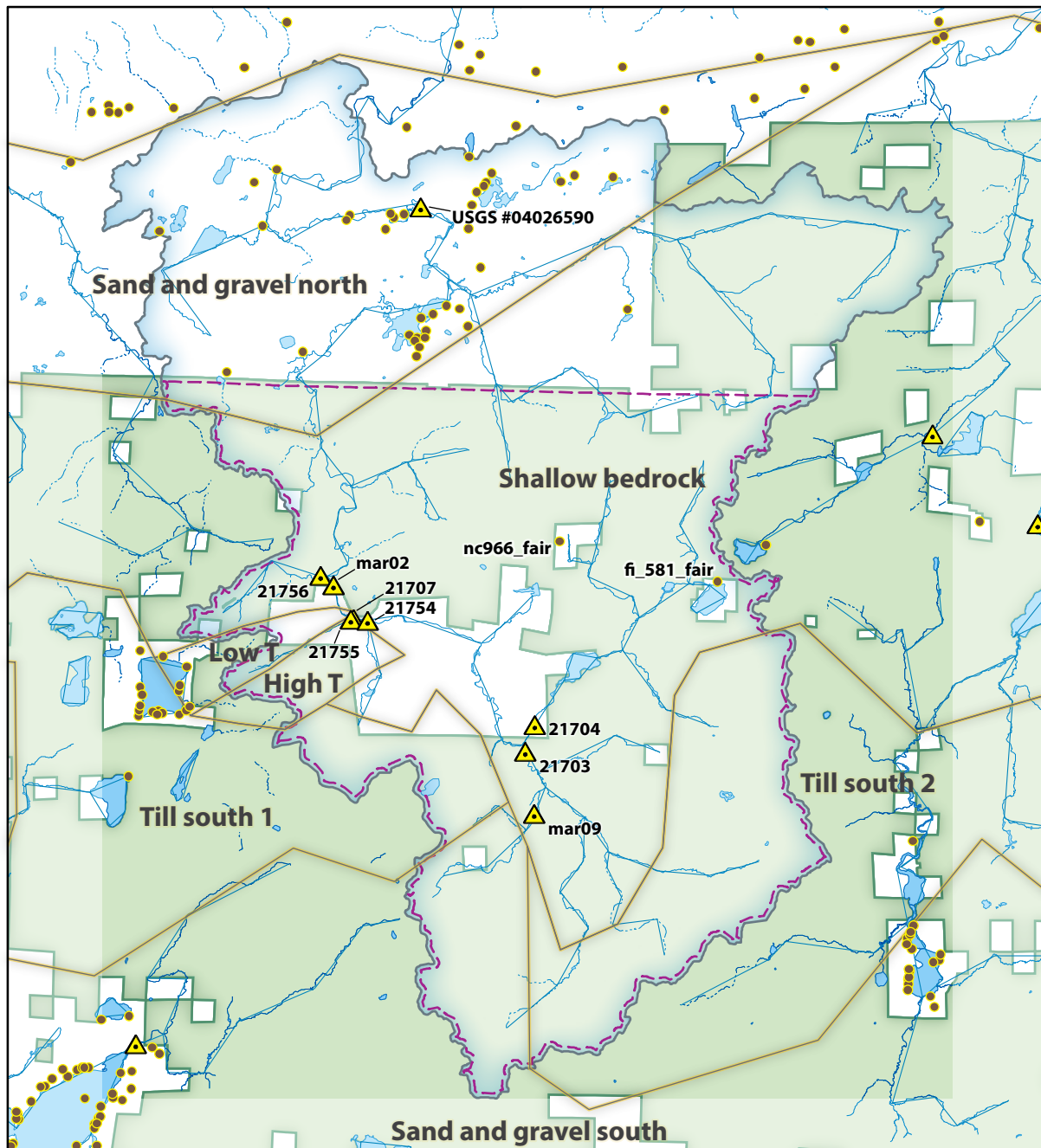
The parent model was developed using GFLOW to simulate groundwater in the Great Divide Ranger District of the Chequamegon-Nicolet National Forest, which contains the Marengo River headwaters at its northern edge (fig. 1). We used an internal copy of the parent model (A.T. Leaf and others, U.S. Geological Survey, unpublished data) that was later included in Leaf and others (2019). The parent model has the following characteristics:

- The groundwater recharge was applied in a 1,000-x-1,000-meter grid. Values were based on a soil-water-balance (SWB) (Westenbroek, Kelson, and others, 2010) model output that was calibrated to heads and flows. The recharge rate averaged 8.8 in./yr in the Great Divide Ranger District.
- Five zones were determined, representing areas of differing transmissivity. Two zones are present in the Marengo River study area: (1) till of the Copper Falls Formation had an approximate transmissivity of 2,400 square feet per day (ft²/d) (model $K = 2.7$ feet per day (ft/d)); (2) the shallow bedrock zone had an approximate transmissivity of 400 ft²/d (model $K = 0.5$ ft/d).
- The base elevation was set at 500 ft above sea level, which was artificially low, to improve model performance (see Fehling and others, 2018, for further discussion). As a result, the modeled hydraulic conductivity was not representative. Additionally, because the base elevation was constant but the water-table elevation varied, the simulated transmissivity varied within each zone. The assumption of an artificially low aquifer base was considered reasonable within our study area, where the conceptual aquifer base elevation was also approximately constant (see *Conceptual model of Marengo River study area*, above).
- Pumping from high-capacity wells was simulated in both the parent and refined models. Although there are high-capacity wells within the model domain, none of the wells are located within the Marengo River watershed.
- The resistance parameter of streams (equal to streambed thickness per vertical hydraulic conductivity of stream sediments) was fixed at 0.3 days.
- The model evaluated the steady-state average annual conditions during the late 20th century.

Targets

Measurements of streamflow and well records of water-table elevations were used as targets to evaluate the model's results (fig. 25). These targets represented the long-term average baseflow and water-level conditions, respectively. The parent model used two baseflow targets in the watershed from Gebert and others (2011). Those published values were estimated by applying a statewide regression equation (Gebert and others, 2007) to low-flow stream-discharge measurements. The regression compared individual measurements to a nearby continuous gaging station (in this case, the USGS stream gage in the Bad River at Odanah; see fig. 1). To produce additional baseflow targets in the study area, the same equation was applied to low-flow measurements obtained from 2018 field work, previous measurements from the USFS, and USGS measurements in the NWIS database. An average annual recharge for each measurement location was then estimated by dividing the baseflow by the groundwater-contributing area estimated from the GFLOW

Figure 25. Locations of the groundwater-flow model targets and the names and boundaries of transmissivity zones.



National Forest boundaries from the USDA Forest Service, 2011. Hydrography from National Hydrography Dataset (U.S. Geological Survey, 2016).

water table. A summary of low-flow measurements and the estimated baseflow and recharge is shown in table 5. Targets with multiple low-flow measurements have greater certainty.

The baseflow calculations were dependent on a realistic estimate of the groundwater divide. The surface-water divide is often used as a proxy for the groundwater divide

where no other information was available, but the proxy may lead to poor estimates of baseflow where the divides differ (Gebert and others, 2007). These differences occurred in Tributaries 6 and 7 and to some degree in parts of the larger study area. The average annual measured low-flow discharge in Tributary 7 divided by the drainage area (46

in.) was greater than the average annual rainfall (32 in.), suggesting the groundwater divide was substantially larger than the surface drainage area. Using the drainage area in baseflow calculations resulted in an estimate of 1.6 cfs, which was lower than the measured flows of 3.1–3.6 cfs. If spread over the drainage area, the flow measured at Tributary 6

Table 5. Baseflow targets.

Station ID ^a	Location	Average annual baseflow (cfs) ^b	Equivalent recharge rate (in./yr)	Groundwatershed area (mi ²) ^c	Drainage area (mi ²) ^d	Low-flow measurement ^e		
						Date	Flow (cfs)	Source
USGS #04026590	Marengo River at Altamont Road	21.8	7.0	42.2	50.5	8/30/2011	11.3	NWIS ^f
						8/21/2018	14.5	NWIS
21756	Tributary 8	0.5	9.2	0.7	0.9	8/27/2002	0.5	
						9/2/2003	0.4	
mar02 / USGS #04026580	Marengo River at FR198/Wisco Road	17.3	7.4	31.5	26.9	8/30/2011	9.7	NWIS
						8/21/2018	12.0	NWIS
mar10	Marengo River downstream of Tributary 7	14.9	6.8	30.3	26.6	7/16/2018	11.7	
21755	Tributary 7	3.2	10.7	4.1	1.0	8/27/2002	3.1	USFS ^g
						9/2/2003	3.6	USFS
						7/16/2018	3.5 ^h	
21707	Marengo River between Tributaries 6 and 7	11.3	6.1	25.3	25.5	7/16/2018	8.2	
21754	Tributary 6	0.2	5.8	0.6	1.5	8/27/2002	0.2	USFS
						9/2/2003	0.1	USFS
21704	Whisky Creek	2.1	5.3	5.4	7.5	7/17/2018	1.3	
21703	Marengo River at FR194	5.2	5.1	13.7	12.1	7/17/2018	3.0	
mar09	Blaser Creek at FR194	1.5	8.0	2.6	2.1	8/27/2002	1.0	USFS
						7/17/2018	2.0	

Abbreviations: cfs, cubic feet per second; FR, Forest Road; ID, identification number; in./yr, inches per year; mi², square miles; NWIS, National Water Information System; USFS, U.S. Forest Service; USGS, U.S. Geological Survey.

^aStation ID indicates name of collocated thermograph, shown in figure 9. Station 21707 shown in figure 25. USGS station included where applicable.

^bBaseflows calculated using statewide regression from Gebert and others (2007).

^cGroundwatershed area approximated from GFLOW particle tracking. "Groundwatershed" is defined as the area contributing groundwater discharge to one of these streams and their tributaries (Leaf and others, 2015).

^dDrainage area shown for reference only. Groundwatershed used to calculate average annual baseflow. Drainage areas estimated from Stream Stats at <https://water.usgs.gov/osw/streamstats/>.

^eLow-flow measurements used to calculate baseflow. Multiple measurements increase certainty in baseflow value.

^fNational Water Information System, available online at <https://waterdata.usgs.gov/nwis/sw>

^gUSFS measurements provided by Dale Higgins.

^hTributary 7 measurement on July 16, 2018, was assumed from difference between measurements in the Marengo River taken upstream and downstream of the confluence.

was only 2.7 in., which was lower than expected. Because the ground-water watershed areas were not known beforehand and could not be used to calculate the average annual baseflow, the low-flow measurements and the relative increase in flow between measurements were used to guide development of the GFLOW conceptual model and manually calibrate the model. The simulated groundwater divides were then substituted for the drainage areas in the regression equation to recalculate the average annual baseflow (table 5). Tributary 7 had a simulated groundwater watershed area that was four times greater than the surface-drainage area (fig. 26). Even so, the recalculated Tributary 7 target was still slightly lower than the measured baseflows; in general, the average annual baseflow was typically higher than baseflow measured during a dry period. The groundwater watershed area at most other measurement locations did not differ substantially from the surface-drainage area. Figure 26 also shows the generalized groundwater-flow paths. Flow paths to Tributary 7 were generally longer than those to the wetland headwaters.

Both of the flow targets from the parent model were modified for this study. The flow target on the Marengo River at Altamont Road (USGS #04026590) was decreased from 30.3 to 21.8 cfs on the basis of two new, consistent flow measurements. The new value was also more consistent with recent simulations of groundwater flow in the Bad River watershed (26.6 cfs in the parent model and 24.0 cfs in a larger model (Leaf and others, 2016)). The original target (Gebert and others, 2011) was based on unpublished measurements that could not be verified and therefore was not used for this study. The flow target off FR198 (station mar02/USGS #4026580) was updated with a second

measurement from 2018. Although the value did not change substantially, the measurement location was found to be incorrect and was moved from upstream to downstream of Tributary 7 (Eric Dantoin, USGS, personal communication). Because of the high volume of flows entering the stream near Tributary 7, this corrected target was much more consistent with other measurements and our understanding of the flow system.

Areas with a higher estimated recharge and higher groundwater discharge included Tributary 7, Blaser Creek, and Tributary 8. The average annual baseflow in the Marengo River increased by about 6 cfs from upstream of Tributary 7 to FR198, a distance of about 0.5 mi. This locally high groundwater discharge was consistent with the high estimated baseflow calculations for Tributary 7. The upper Marengo River (above FR194) and Whisky Creek had a lower estimated recharge. Streams with higher estimated recharge often exhibited lower temperatures and higher electrical conductivity, which is typical for groundwater-fed streams. Head targets were not changed from the parent model (fig. 25).

Model refinement and calibration

The regional parent model was refined and manually calibrated to add detail and improve model performance within the study area. Stepwise modeling employing formal parameter estimation (see Anderson and others, 2015) was considered to be beyond the scope of this project (also see *Discussion*, below). Changes were made with the intent to improve the match to measured heads, groundwater flows, and changes in flow between targets. This section summarizes changes made to the model.

Model extent

The model extent was reduced to focus on the study area (fig. 23). Streams and rivers outside the study area were also represented in the model. Large rivers outside of the study area that were not expected to affect hydrology in the study area were selected as far-field streams, which have a fixed water-table elevation.

Streams

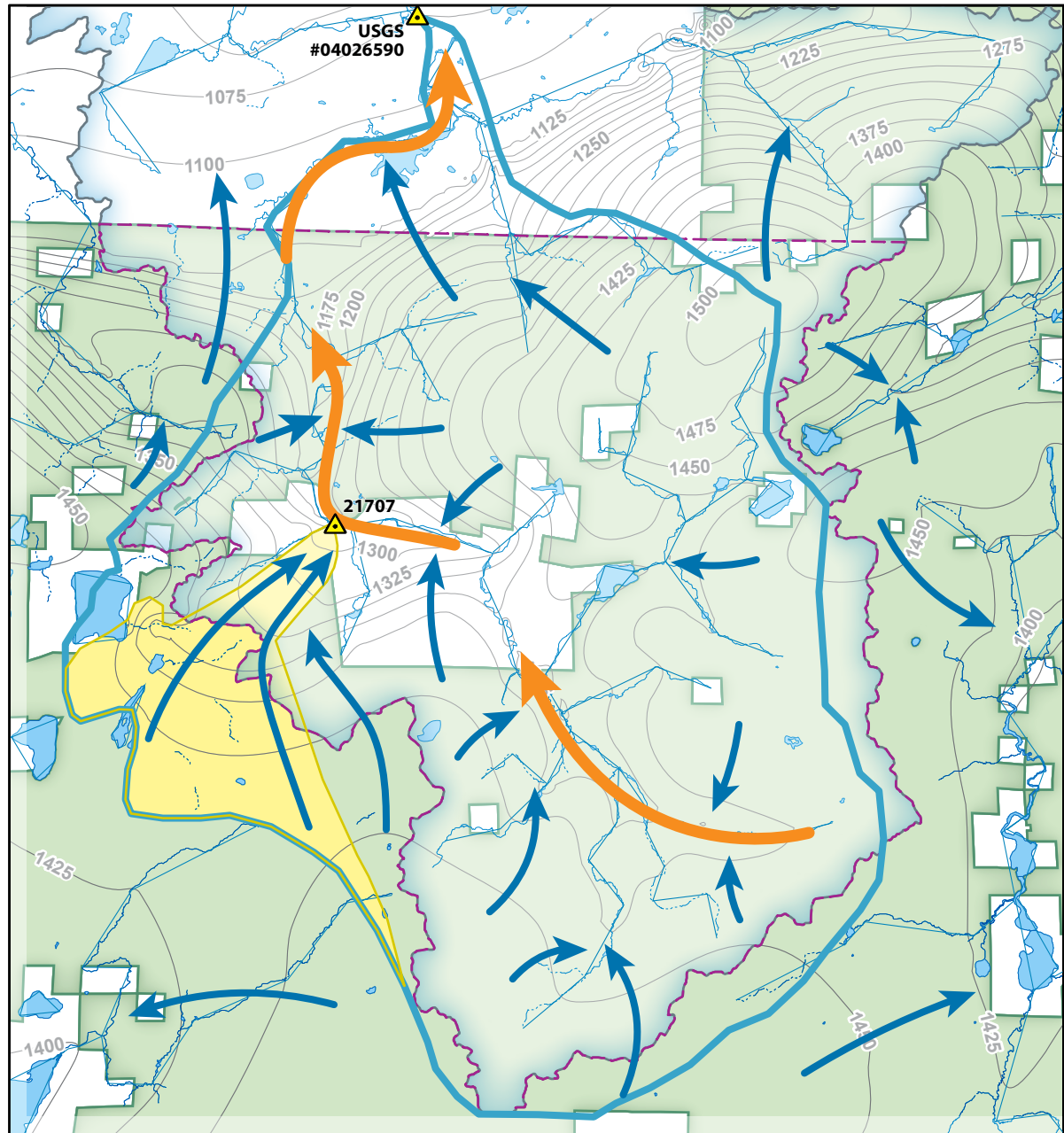
The representation of streams in the study area was improved by modifying their elevations and geometry according to light detection and ranging (lidar) imagery for Bayfield and Ashland Counties (State Cartographer's Office, 2017). Some small perennial streams were added to the model, and the geometry of selected streams was refined.

Recharge

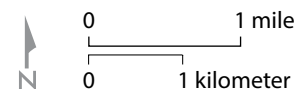
Recharge was modified to increase the detail of the recharge grid and to better match the distribution and magnitude of flows in the study area. The parent model simulated too much flow overall in the study area, too much flow in the uplands above the waterfall, and too little flow in Tributary 7. The original SWB grid was used as a base and changed to address the two flow discrepancies (above the waterfall and Tributary 7; see fig. 6).

The two areas with flow discrepancies were located in wetlands and fractured rock, respectively, both of which could potentially limit performance of the SWB model. The SWB model can overpredict recharge in wetlands because the model only accounted for evapotranspiration on days with precipitation, when in reality evapotranspiration in wetlands continues after precipitation events occur. Wet areas were observed in the

Figure 26. Simulated groundwater drainage area for two baseflow targets (station 21707 and USGS #04026590) compared to the surface watershed for the Marengo River, also showing generalized groundwater-flow paths and water table simulated by GFLOW groundwater-flow model.



- Marengo River flow direction
- Groundwater flow direction
- Linesink
- Water table contour, ft
- ▲ Baseflow target
- Groundwater drainage area for USGS #0426590
- Groundwater drainage area for Tributary 7 (station 21707)
- Marengo River watershed
- Study area
- National forest
- Perennial stream
- Intermittent stream



National Forest boundaries from the USDA Forest Service, 2011. Hydrography from National Hydrography Dataset (U.S. Geological Survey, 2016).

headwaters even in areas that were not mapped as wetlands (Wisconsin Department of Natural Resources, 2011), suggesting that evapotranspiration continues to be a substantial part of the water budget on days without precipitation. Additionally, the SWB model did not include a groundwater-discharge component, and so it cannot account for areas with upward gradients (Westenbroek, Kelson, and others, 2010; Hart and others, 2012). To reduce the excess flow in upland areas, recharge to all mapped wetland cells (Wisconsin Department of Natural Resources, 2011) was reduced to zero.

The SWB model estimated infiltration rates from soil data and could not represent focused recharge through shallow bedrock fractures, such as the infiltration of groundwater in the high-transmissivity zone that contributed substantial groundwater discharge to Tributary 7 (see *Conceptual model of Marengo River study area*, above, and fig. 24). Additional recharge in the high-transmissivity zone was simulated to account for this high observed discharge. The zone added a recharge rate of 6.6 in./yr above what the SWB model already included for an approximate total recharge rate of 15 in./yr. The total recharge rate in this zone was limited to approximately 15 in./yr to avoid overfitting the model with unrealistic recharge.

After addressing the two flow discrepancies, the SWB grid (30 × 30 m spacing) was aggregated to 120 × 120 m. For comparison, the parent model was aggregated to a grid size of 1,000 × 1,000 m. Averaged across the study area and including the added zone along Tributary 7, the annual simulated recharge rate was 7.8 in./yr. A map of the simulated recharge is shown in figure 27. For areas outside the study area that were

not covered by the recharge grid, the model applied the average recharge rate from the parent model (8.8 in./yr).

Transmissivity

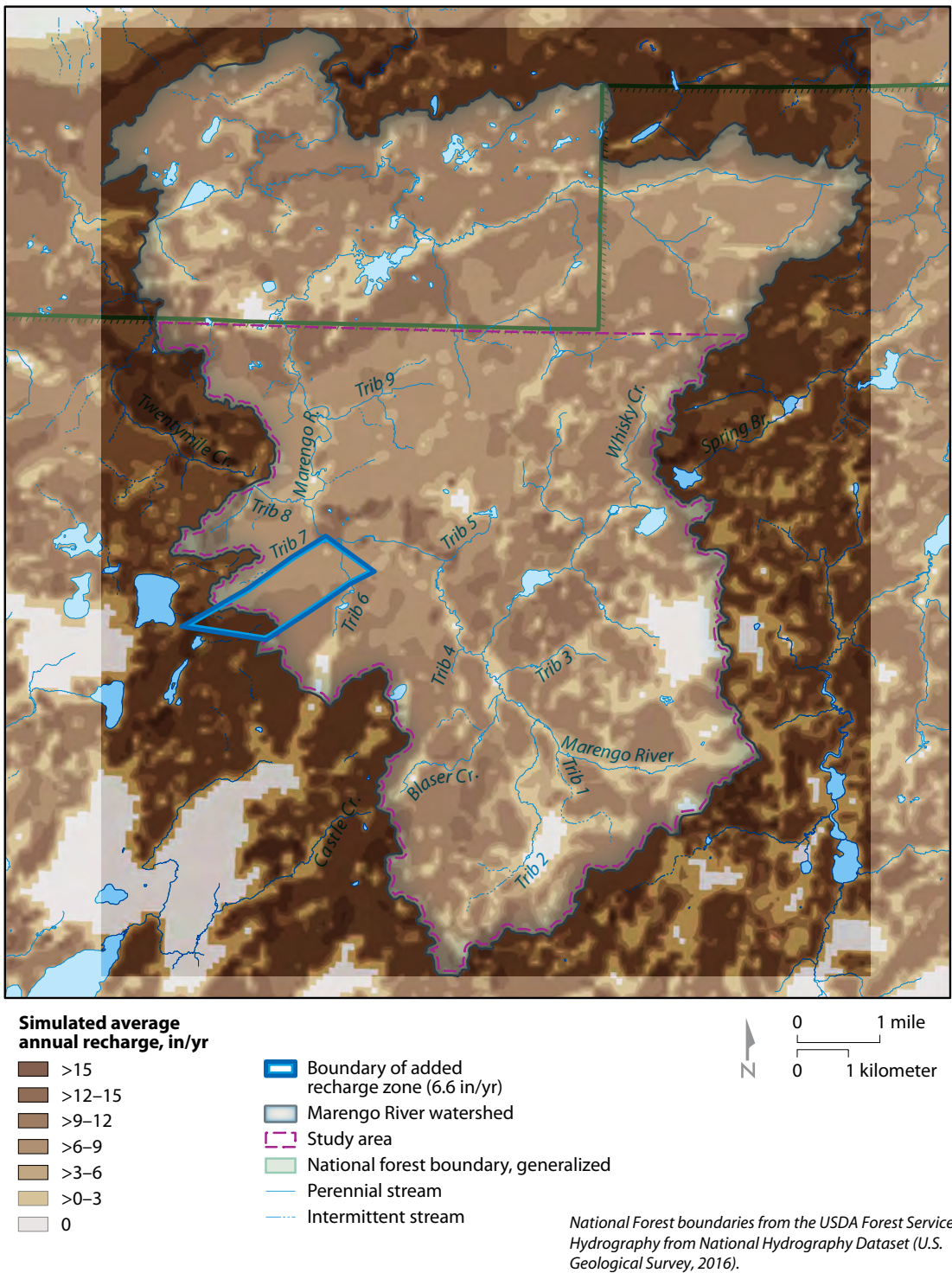
Details about transmissivity were added to both the glacial and shallow bedrock zones compared to the parent model (see *Conceptual model of Marengo River study area*, above). The model's transmissivity results are listed in table 6. Because the model had an artificially low base elevation, the model hydraulic conductivity is not representative. The table includes both simulated and average effective (representative) hydraulic conductivity, which was calculated on the basis of the approximate simulated and actual aquifer thickness.

The glacial deposits of the Copper Falls Formation, previously simulated as a single zone, were split into two distinct units: (1) sand and gravel and (2) till as mapped by Clayton (1984) (see fig. 23). This split resulted in several zones for each unit (for example, north and south till). All zones within each unit were assigned the same effective value for hydraulic conductivity to account for real changes in aquifer thickness. For the sand and gravel zones, an effective $K = 36$ ft/d was assigned on the basis of (1) the calibrated values for the sand and gravel ($K = 30$ ft/d from the Washburn model (Fehling and others, 2018)) and (2) the original till zone in the Copper Falls Formation in the parent model ($K = 40$ ft/d). The northern till zone was assigned the simulated hydraulic conductivity, rather than the higher effective hydraulic conductivity from the parent model, which improved model performance and was consistent with the more detailed Bad River model (Leaf and others, 2015). The southern till zones were assigned hydraulic conductivity values to match the northern till's effective hydraulic con-

ductivity. The hydraulic conductivity of the Miller Creek Formation, which is outside the study area, was not changed from the parent model.

The shallow bedrock consists of three zones: shallow bedrock, high-transmissivity bedrock, and low-transmissivity bedrock (fig. 24; also see *Conceptual model of Marengo River study area*, above). To improve the match to measured heads in the headwaters, where simulated heads were too low, the modeled hydraulic conductivity of the shallow bedrock zone was reduced from $K = 0.53$ to $K = 0.25$ ft/d. The high- and low-transmissivity zones were manually calibrated to best match measured baseflows. Little published information is available on the hydrogeologic properties of individual bedrock units in this watershed, and what is available may not reflect the hydraulic effect of the Atkins Lake–Marenisco fault. Although direct comparisons are difficult, the calibrated values in the GFLOW model are nonetheless consistent with values of similar units reported by Leaf and others (2015) in the Bad River watershed model. The Bad River watershed model simulated the Marquette Supergroup as a single zone that includes slightly different formations than are present in the Marengo River study area (the Palms Formation of the Menominee Group, Tyler Formation of the Baraga Group, and Ironwood Iron-Formation of the Menominee Group). The hydraulic conductivity of this zone ranged from $K = 0.025$ –13 ft/d. The Archean bedrock was simulated as a single zone using $K = 0.33$ –12 ft/d (table 6).

Figure 27. Simulated average annual recharge in the groundwater-flow model. Abbreviation: in./yr, inches per year.



Model performance

The results from the manually calibrated model were compared to the measured values of head and baseflow to evaluate the model's performance. The model's performance is shown in figures 28–30 and appendix tables 2.1–2.2, and the simulated baseflows are illustrated on plate 1. Flows in the study area, as well as increases in flow between targets, were generally well represented, with residuals (the difference between the measured and simulated values) of less than 3 cfs. The average recharge in the study area was less than the average over the parent model, which was consistent with the spatial distribution of recharge mapped from the SWB results (Fehling and others,

2018). The model simulated too much flow in the upper Marengo River (at FR194), possibly as a result of a simulated recharge rate that was too high despite the elimination of wetland recharge. A higher model transmissivity would have decreased flows in the headwaters; however, it would have negatively affected the model heads.

Although there were only two head targets in the study area, they are reasonably well simulated (fig. 29, appendix table 2.2) as are targets outside of the study area. The flow of the Marengo River at Altamont Road was simulated to be slightly low, and heads north of the model domain were too high. Changes to transmissivity zones improved the high simulated heads north of the

study area, although a bias was still present. Increasing the hydraulic conductivity of the sand and gravel lowered the heads but decreased flow even more in the Marengo River at Altamont Road. The model simulated a losing stream here, which is feasible based on a measured flow increase of only 0.2 cfs between the North Country Trail and FR384. The difficulty in matching heads and flows near Altamont Road, as well as the overly high flows in the headwaters, suggested that there is heterogeneity or a structural error (such as a sloping aquifer base) in the shallow bedrock zone that was not captured in this model.

Table 6. Model transmissivity zones.

Zone (see figures 23 and 24)	Average simulated saturated thickness ^a (ft)	Simulated K^b (ft/d)	Approximate simulated transmissivity (ft ² /d)	Representative actual saturated thickness ^c (ft)	Average effective K (ft/d)	Description	Effective K from parent model	Effective K from Bad River model ^d
Sand and gravel, north	640	8.0	5,100	140	36	Sand and gravel of Copper Falls Formation	30–40	2.95–95
Sand and gravel, south	860	2.7	2,300	60	38			
Till, north	700	2.7	1,900	100	19	Till of Copper Falls Formation	40	3.5–23.3
Till, south 1 and 2	990	1.7	1,700	90	19			
Shallow bedrock	840	0.25	200	240	0.83	Fractured crystalline bedrock	40	0.33–12 ^e
High- transmissivity bedrock	890	15.0	13,400	290	46	Bad River dolomite and metadiabase	—	—
Low- transmissivity bedrock	890	0.10	100	290	0.34	Palms Formation and Ironwood Iron- Formation	—	0.025–13 ^f
Miller Creek Formation	330	2.8	900	230	3.9	Clay-rich till of Miller Creek Formation	20	0.78–1.3

Abbreviations: ft, feet; ft/d, feet per day; ft²/d; square feet per day; K , hydraulic conductivity; —, no data.

^aCalculated as average simulated water table in a zone minus the base elevation of 500 ft.

^bSimulated hydraulic conductivity is not representative of the aquifer because of the artificially low base elevation. The effective hydraulic conductivity is shown in the column labeled "Average effective K ." ≠

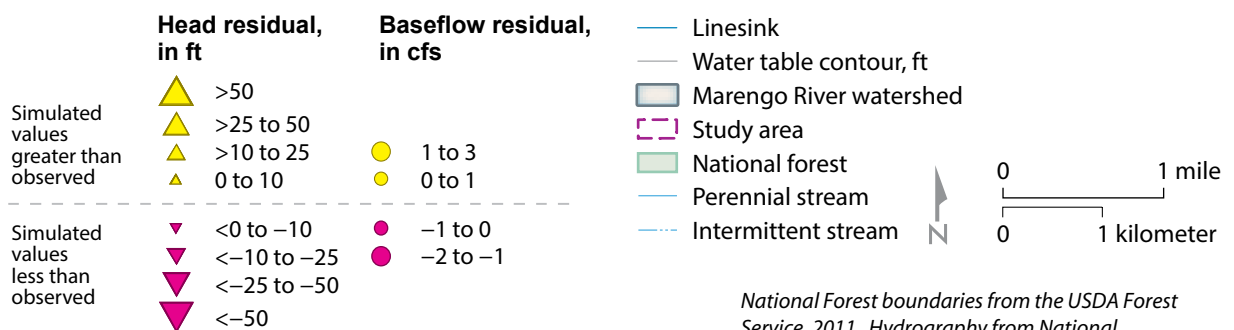
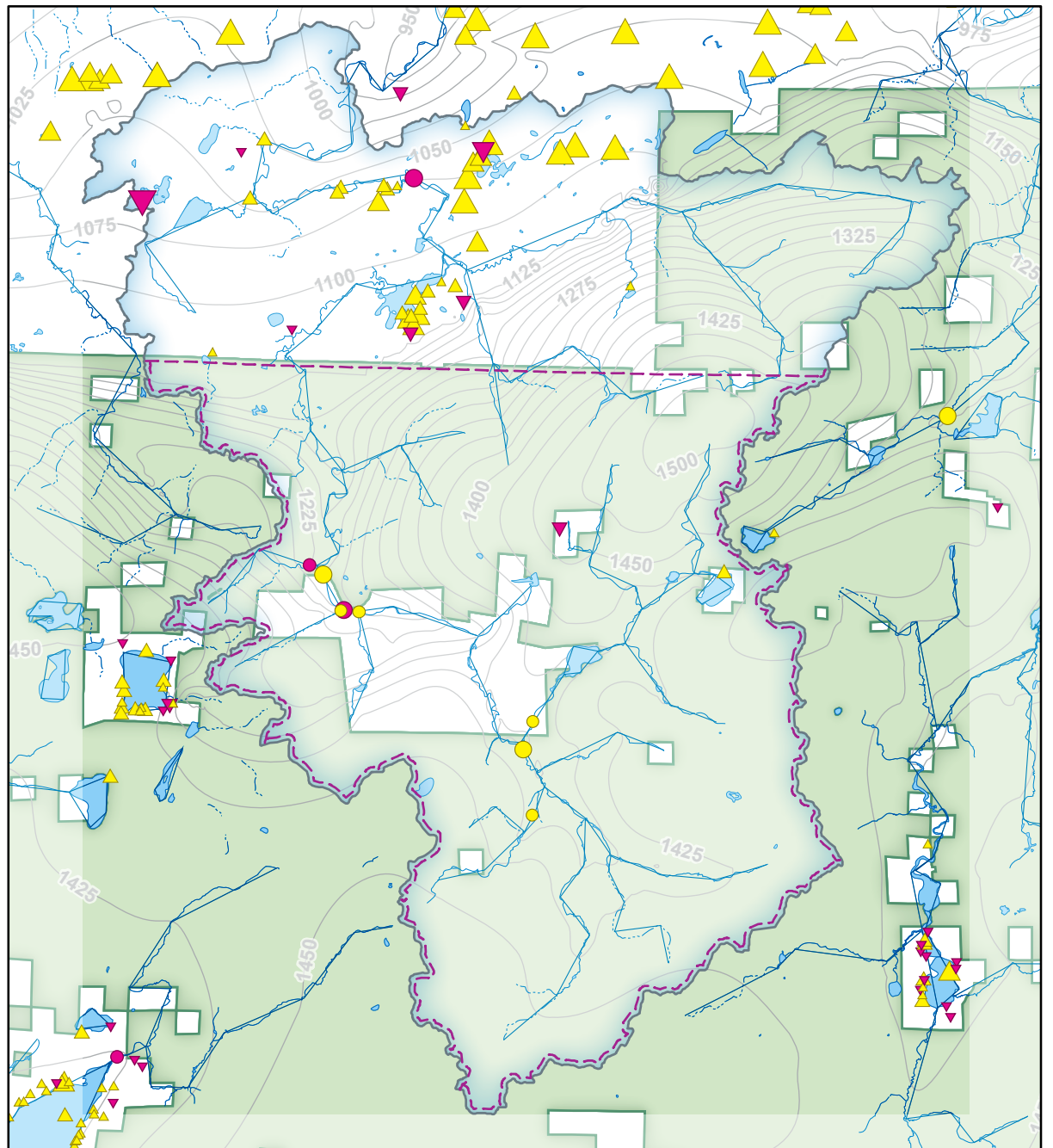
^cGlacial aquifer base elevations are assumed to be top of bedrock. Bedrock aquifer base elevations are assumed to be 300 ft below land surface.

^dFrom Leaf and others (2015).

^eArchean units only.

^fIncludes Tyler and Palms Formations and Ironwood Iron-Formation.

Figure 28. Map showing groundwater-flow-model results. Abbreviations: cfs, cubic feet per second; ft, feet.



Discussion

This study introduces a new conceptual model of the hydrogeology near the Atkins Lake–Marenisco fault. The two contrasting transmissivity zones and the significance of the focused recharge near Tributary 7 also influence future predicted flow patterns. Changing the conditions in a steady-state model necessarily introduces uncertainty, and a different conceptual model that fits current conditions might not produce the same results.

The simulated groundwatersheds (recharge areas) differ substantially from the surface-drainage areas in some parts of the model. The recharge area feeding Tributary 7 is four times larger than the surface watershed and is characterized by relatively long groundwater-flow paths.

As with any model, the groundwater-flow model includes several assumptions and limitations. The aquifer is simulated as laterally infinite, which is generally reasonable on a regional basis where the aquifer is thin relative to its areal extent. The aquifer is simulated as homogeneous and isotropic within zones with sharp transitions at the edges; in reality, however, the aquifer transmissivity varies throughout the watershed. The model uses a constant base elevation that is lower than reality. This assumption is reasonable within our study area due to a roughly constant conceptual aquifer base and small expected changes in saturated thickness. Because horizontal flow is assumed, areas with a significant vertical component of flow are not well represented. The conceptual model of two contrasting transmissivity zones is a simplified version of reality, and the model cannot account for anisotropic flows along the fault or in discrete fractures. The assumptions of the SWB model carry over to the groundwater-flow model as well; these are discussed in

Figure 29. Graph comparing the simulated and observed heads. The data points are from stations shown in figure 28 and are plotted against a 1:1 line. Abbreviation: ft, feet.

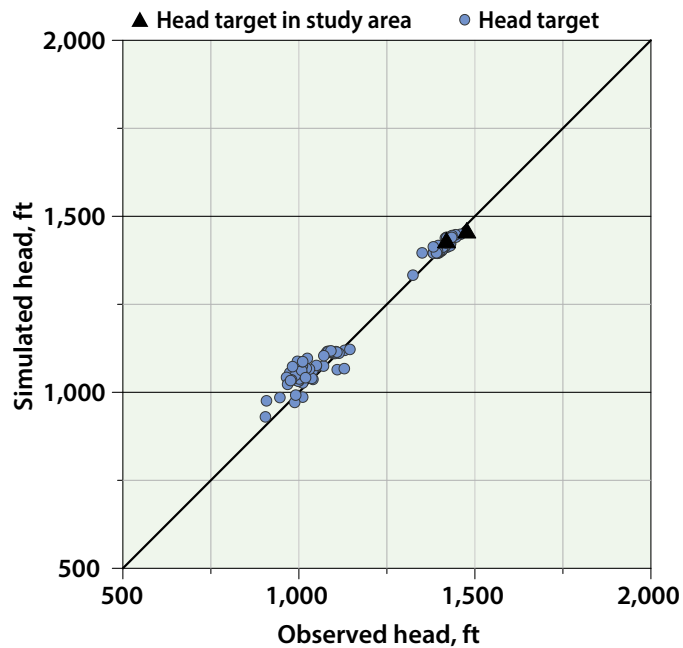
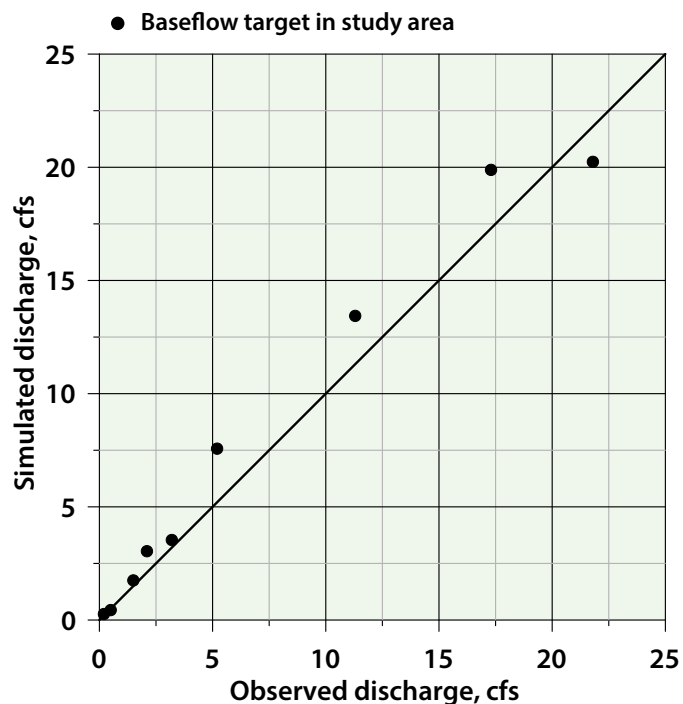


Figure 30. Graph comparing the simulated and observed baseflows in the Marengo River study area plotted against a 1:1 line. Abbreviation: cfs, cubic feet per second.



Fehling and others (2018). Calibration of the model is limited by the lack of monitoring wells that constrain water-table elevations in the study area; however, numerous stream-stage elevations help constrain the groundwater surface. Because the model was manually calibrated, there is likely a set of parameter values that yield an improved statistical model fit; however, it is unclear that this improvement would be meaningful given the small number of head targets in the study area and uncertainties from the model structure (such as zone locations and base elevation). The adjustments to the model were considered sufficient to simulate local changes in flow that were incorporated into the stream-temperature model. Further improvements to the model, such as additional data collection or development of a finite difference model, were considered to be beyond the scope of this project. Despite the limitations of this model, this approach is useful for illustrating hydrogeologic patterns relevant to trout habitat in the study area, such as the spatial correlation of high transmissivity to increased groundwater discharge and cooler stream temperatures.

Climate change scenarios for baseflow

The groundwater-flow model was used to simulate possible changes to average annual baseflow in the future. Changing precipitation and snowmelt may alter the timing and magnitude of groundwater recharge to the aquifer, which may in turn affect baseflow. A SWB model developed to predict changes in recharge for a statewide stream-temperature study (Westenbroek, Stewart, and others, 2010; Stewart and others, 2014) was used to evaluate possible changes to recharge in the Marengo River study

area. This section discusses the selection of climate (recharge) scenarios and subsequent results.

Climate-change scenarios

The climate's impact on recharge, and therefore on baseflow, is difficult to predict due to uncertainty in how the magnitude and timing of precipitation may change. In Wisconsin, a future climate likely includes more extreme rain events, more frequent droughts, somewhat higher average precipitation, and more precipitation falling during the winter (WICCI, 2011). However, although most models predict that precipitation will increase, the resulting increases in recharge could be mitigated by higher evapotranspiration rates during the warmer and longer growing season or by increased surface runoff during high-intensity precipitation events. In a detailed climate study of Trout Lake in northern Wisconsin, Hunt and others (2013) found that changes in evapotranspiration resulted in only moderate changes in average annual recharge. It is also uncertain how changes in temperature and the timing of precipitation will affect recharge. Winter precipitation is expected to increase, and more of it is expected to fall as rain as temperatures increase (WICCI, 2011). This precipitation is less likely to be used for plant transpiration compared to summer rainfall, which would increase recharge; however, the excess could run off if the ground is frozen. Hunt and others (2013) found that periodic winter thaws at Trout Lake were likely to result in a more gradual recharge instead of a pulse during the spring melt. Such changes in the timing of recharge may also affect the temporal patterns of baseflow.

To account for this uncertainty, a range of possible future recharge scenarios in the Marengo River study area was simulated on the basis of results from a statewide SWB model developed by Westenbroek, Stewart, and others (2010). The future statewide recharge scenario was simulated by running the SWB model with statistically downscaled daily air temperature and precipitation values from 10 general circulation models (GCMs) under the moderate A1B emissions scenario and 3 time periods: 1989–2000, 2046–2065, and 2081–2100 (Stewart and others, 2015). The statewide average annual recharge grids for the 30 model-time period combinations (provided by Stephen Westenbroek, USGS, written communication) were evaluated for areal average recharge within the study area (fig. 31). The baseline GCMs for 1989–2000 resulted in recharge rates ranging from 7.1 to 8.2 in./yr and a mean of 7.7 in./yr, which was consistent with the GFLOW average simulated recharge rate of 7.8 in./yr. The mean of all the GCMs suggested a slight (6%) increase in Marengo River area recharge by 2081–2100. However, the range in the simulated recharge increased with time, indicative of the uncertainty discussed above.

The recharge in the groundwater model was scaled to simulate a range of possible future changes to baseflow. The highest and lowest SWB-simulated average recharge rates were 6.7 in./yr and 9.5 in./yr, a change of –12% and +21%, respectively, compared to the mean SWB-simulated recharge rate for 1989–2000 (7.7 in./yr). The recharge rate in the groundwater-flow model was therefore simulated with a percent change of –12% and +21% compared to the original groundwater-flow model grid recharge rate (7.8 in./yr). This is not to suggest that the recharge

rate will stay within these exact bounds, but it is meant to represent a range of what might realistically be expected. The bounds were consistent with the range of $\pm 15\%$ found by Pruitt (2013) in a study of steady-state recharge under multiple climate models in the Foulds Creek watershed, located about 50 mi to the southeast in the Chequamegon-Nicolet National Forest. The simulated recharge rates in other Wisconsin studies that measure the climate change impacts on recharge also fell within this range (for example, Hunt and others, 2013, 2016).

Results

The simulated baseflows for the three climate-change scenarios (base, +21% recharge, and -12% recharge) are shown on plates 1–3 and in appendix table 2.3. Headwater tributaries

are generally affected the most in terms of percent change because groundwater discharge in tributaries constitutes a larger proportion of streamflow. The distribution of baseflow changes with these scenarios as well; the Tributary 7 and Blaser Creek baseflow remains fairly consistent. In these areas, the groundwater-capture zones are slightly smaller when the recharge is higher. Although the distribution of baseflow in the study area changes, the mass balance of the larger model is met; that is, the largest downstream baseflow changes by the same amount as the recharge. The initial 1,500 ft of Whisky Creek and Tributary 6 are simulated to go dry in the -12% scenario (plate 3), although Tributary 6 is undersimulated in the base model as well. The model does not directly simulate wetlands, but

the simulated lower water levels would probably correlate to some reduction in the wetlands' extent for the reduced recharge scenario.

Discussion

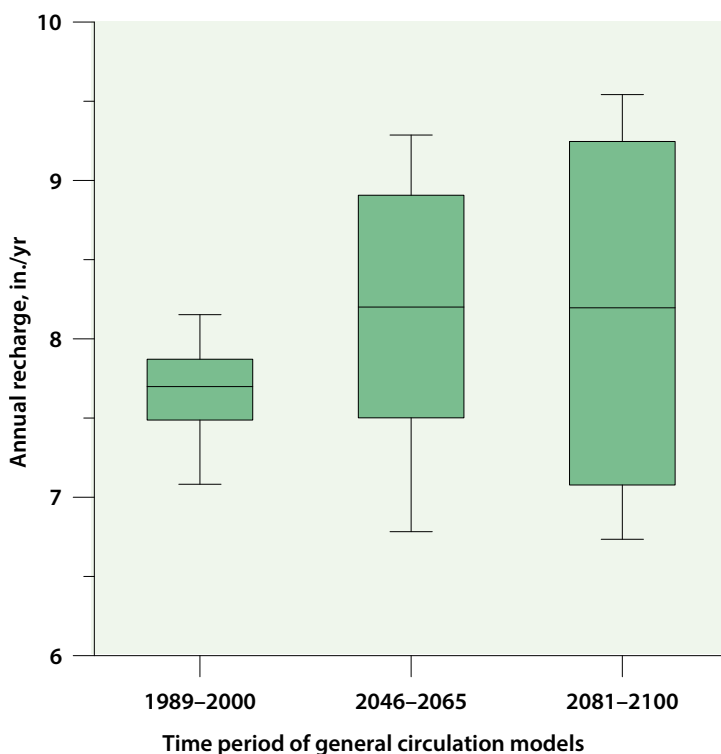
Tributary 7 and Blaser Creek, both areas of important groundwater discharge and higher transmissivities, maintain more consistent baseflow for both an increase and decrease in annual recharge. The baseflow in warm portions of the watershed, including Whisky Creek and Marengo River at FR194, changes more than the associated recharge magnitude. For the increased recharge scenario, therefore, higher relative baseflows are simulated in warmer parts of the watershed compared to baseflows in groundwater-dominated reaches.

The simulated water table is lowered in the reduced recharge scenario, causing some simulated headwater streams to go dry. A lower water table also may likely result in the loss of wetlands. However, the extent of this effect is uncertain because of the lack of head targets in the study area to constrain the water table.

Subannual changes in climate are accounted for in the SWB model, which operates on a daily time scale. Changes in the timing of precipitation may affect the timing and magnitude of baseflow, stream temperature, and groundwater temperature. An exploration of the intricacies of these effects was outside the scope of this study, however, and the simplified annual recharge values were used as inputs for the steady-state GFLOW model.

The changes in recharge were assumed to be uniform across the model. Other feedbacks from climate change, such as vegetation changes or flooding from high groundwater levels, were not simulated.

Figure 31. Simulated annual recharge from 10 general circulation models (GCMs) within the Marengo River study area over one past and two future periods. For a list of the GCMs, see table 3 in Stewart and others (2015). GCMs downscaled by Notaro and others (2011). Abbreviation: in./yr, inches per year.



Chapter 5: Stream-temperature modeling

The simulated baseflows from the groundwater-flow model, GFLOW, were used along with other parameters to develop and calibrate a heat-flux model that simulates stream temperatures during summer baseflow conditions, which is often considered a critical period for trout (for example, Bartholow, 1989; Gaffield and others, 2005; Deitchman and Loheide, 2012). The heat-flux model uses weather data and physical features of the stream to simulate the temperature along the length of a stream. The model was used to (1) simulate future scenarios on the basis of air temperature from climate models and baseflow from groundwater-model scenarios and (2) examine the relative importance of factors that affect stream temperature. To understand how changing stream temperatures might affect trout, the climate-change scenario results were compared to thermal tolerance limits developed by Wehrly and others (2007), which account for the influence of both daily temperature fluctuations and long-term patterns.

Description of model code

The water temperatures were simulated using the computer code SNTMP (Stream Network Temperature Model; Bartholow, 2010). The model was developed using a modified version of this code with a graphical interface, TRPA Stream Temperature for Windows (TRPA Fish Biologists, 2018, TRPA Stream Temperature for Windows: Arcata, Calif., at <http://trpafishbiologists.com/software-2/> accessed on February 15, 2018; no longer available). SNTMP is a mechanistic and successive steady-state heat-transport model that calculates the environmental heat flux to simulate daily mean water temperatures along a dendritic

stream network. The model's inputs include a linear stream network and information on stream geometry, meteorology, and hydrology. The model's outputs include the daily mean temperature at specified locations along the stream network. The model assumes that all input data can be represented by daily averages and that the stream is well mixed (that is, there are no vertical or lateral temperature gradients). SNTMP simulates dry periods when streamflow is approximately constant.

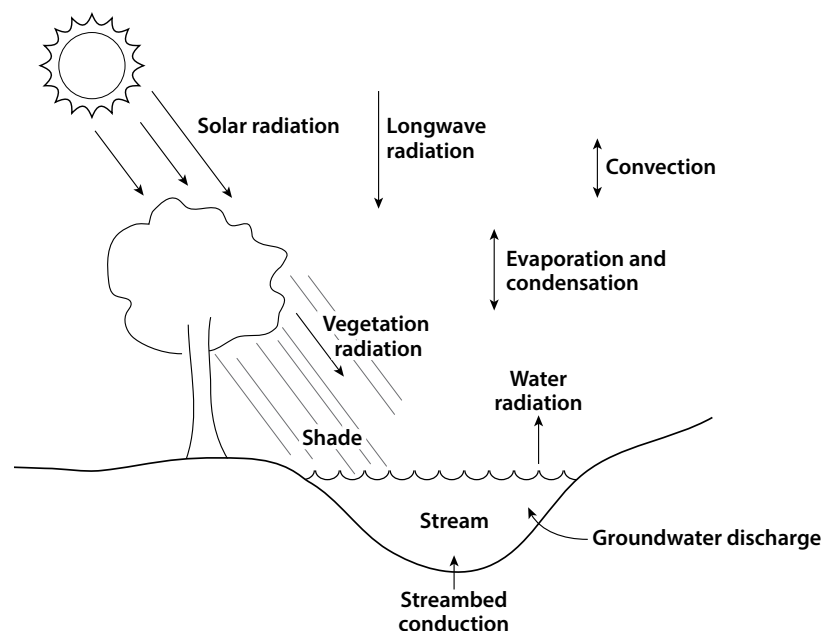
The water temperature in a stream is affected by heat fluxes and groundwater discharge to the stream (fig. 32). The heat fluxes approximated by the stream-temperature model include solar radiation corrected for shade, longwave radiation, evaporation and condensation, convection due to temperature differences between water and air, and streambed conduction (Theurer and others, 1984).

Measurements related to groundwater discharge and groundwater temperature are entered by the user. The daily mean stream temperature is computed using a heat transport equation (1) that applies the basic principles of conservation of mass and energy to a control volume of the stream:

$$\delta T / \delta x = [(q_{gw} / Q)(T_{gw} - T)] + [(WH_n) / (Q\rho c_p)]$$

where T is the water temperature, in degrees Celsius; x is the length of the stream, in meters; q_{gw} is the groundwater discharge per unit length of stream, in square meters per second; Q is the streamflow, in cubic meters per second; T_{gw} is the groundwater temperature, in degrees Celsius; W is the stream width, in meters; H_n is the net heat flux, in watts per square meter; ρ is the water density, in kilograms per cubic meter; and c_p is the specific heat of water, in joules per kilogram per degree Celsius. Note that

Figure 32. Heat fluxes simulated in the stream-temperature model (SNTMP). Groundwater discharge is also shown for clarity. Modified from Theurer and others (1984).



although these variables are reported in metric units for consistency within the equation, most analyses in this study used units of feet for length and cubic feet per second for discharge. The model is discretized into reaches with constant groundwater discharge, groundwater temperature, width, and shade parameters. The most upstream reaches must be assigned an initial temperature unless the starting flow is zero. The stream temperature can then be computed at any location along the stream using a first-order solution to equation 1 (not included here for brevity; see Theurer and others, 1984).

Model construction

The SNTMP model consists of information about the stream geometry, hydrology, and meteorology. Two baseflow periods totaling 43 days were modeled: July 2–31, 2018, and August 11–23, 2018. Days with rainfall greater than 0.5 in. were not modeled. The calibration period was selected to represent the highest stream temperatures for most of the watershed (figs. 14–16). Slightly higher peak and sustained temperatures were observed in the Marengo River at FR198 during some runoff events (see *Flooding*) and during an unseasonably warm period in May. Because many sensors were not deployed until June, there were not sufficient input data to simulate the warm May period in SNTMP. This section describes the model inputs and data sources.

Stream geometry

Stream geometry consists of the stream-network layout, stream width, stage, and shading parameters. The stream network was developed on the basis of the groundwater-flow model layout with slight modifications to represent measurement locations (fig. 33). Reaches are typically a few thousand feet long, up to about 7,500 ft. Because lakes are difficult to

model in SNTMP, Whisky Creek was simulated as a point-flow discharge to the Marengo River with a specified temperature based on sensor measurements. The stream width for each reach was taken from field measurements where available; aerial photography was used to supplement and check for consistency. SNTMP indirectly simulates channel geometry by allowing daily width values to vary with discharge according to this equation (2):

$$W = A \times Q^B$$

where W is width, in feet; Q is discharge, in cubic feet per second, and A and B are constants that define the width-discharge relation for a particular stream reach. An inspection of this equation shows that when $B = 0$, the width is constant. When $B > 0$, the width increases with increasing discharge. The model was divided into four zones of similar channel shape: main channel, tributary, wetland, and wetland tributary. The B -value for each zone was considered to be a calibration term, and A was calculated assuming that a discharge equal to the average annual baseflow simulated in GFLOW would result in a stream width equal to the width that was either measured or estimated from aerial photographs. Lidar data was used to estimate stream elevations and their gradients. The streambed thermal conductivity, used to

calculate streambed heat conduction, was set at the default of 1.65 watts per meter-Celsius ($W/m^\circ C$).

Shade

SNTMP includes an algorithm for calculating the percentage of shade over the stream surface, which is used to correct for solar radiation that does not reach the stream. The algorithm accounts for both topographic and vegetative shading. These are combined to estimate percent shade, or how much of the stream surface is covered by shade each day. The parameters used to calculate percent shade are illustrated on figure 34.

Topographic shading is calculated from the topographic altitude (the angle from the stream surface to the horizon) and the stream azimuth (its compass orientation). The topographic altitude was estimated from topographic maps or from streambank-height measurements in flatter areas. The stream azimuth was entered as part of the stream geometry.

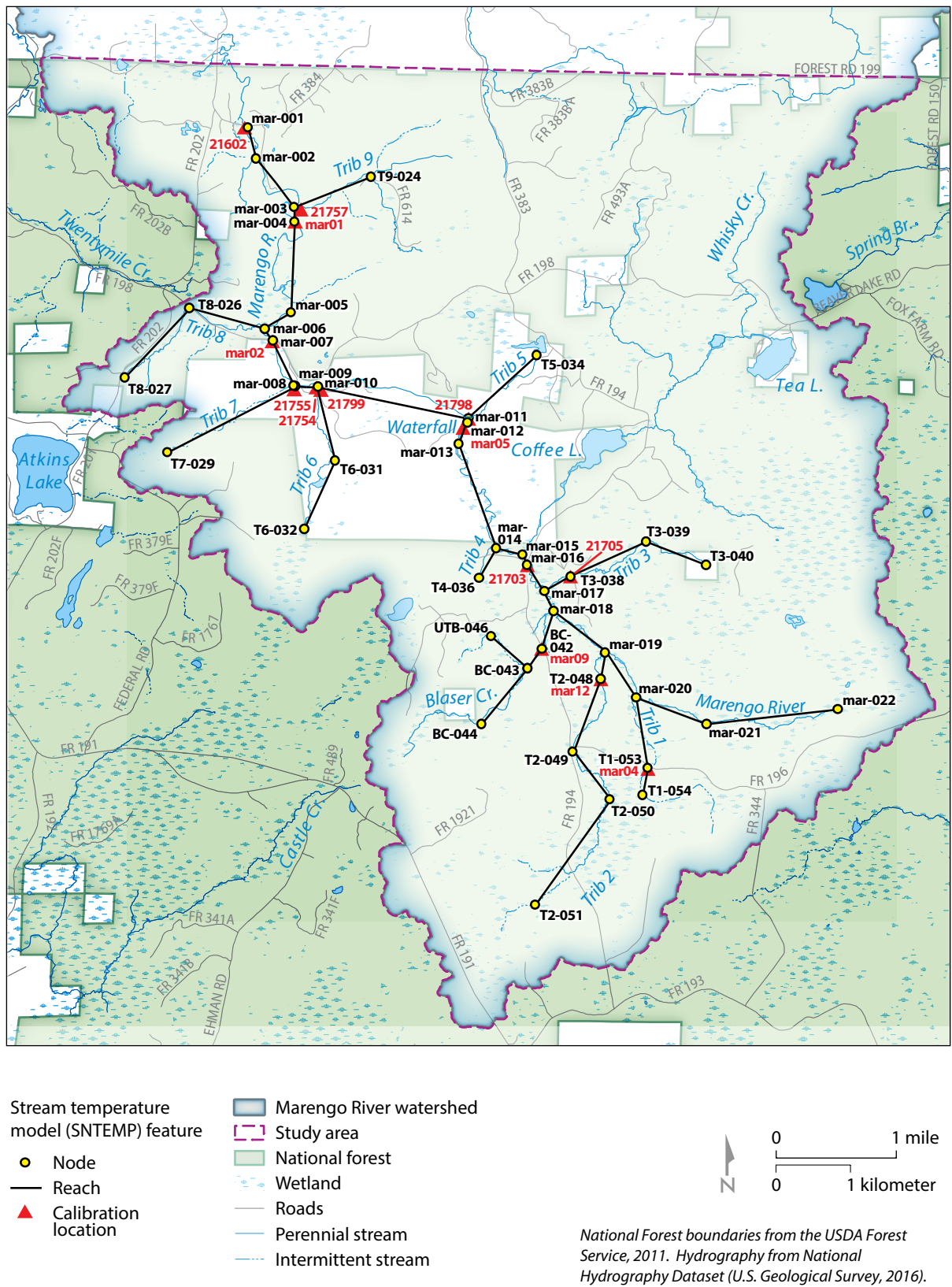
Vegetative shading is calculated from the canopy height, width, distance from the stream, and vegetation density (the percent of light filtered from vegetation). Field measurements and aerial photography were used to develop typical parameters (table 7) for three different vegetation types found in the watershed: forest, wetland, and brush (mostly tag alder shrubs). These parameters were then averaged for each reach on the

Table 7. Shade parameters for each vegetation type.

Shade parameters	Brush	Grass	Forest
Height (ft)	15	4	24
Crown width (ft)	10	0.5	15
Vegetation density (%)	55	45	70
Vegetation offset (ft)	2	2	5

Abbreviation: ft, feet.

Figure 33. Layout of the stream-temperature model (SNTMP) for the Marengo River study area.



basis of the relative percentage of each vegetation type. This approach allows the model to (1) maintain a similar layout to GFLOW, (2) limit the computational time compared to creating a reach for each shade change, and (3) apply physical measurements to areas of the watershed that are difficult to access. The vegetation density was used as a calibration parameter.

Hydrology

Hydrologic data consist of daily groundwater discharge and groundwater temperature for each reach. Groundwater discharge is assumed to be uniformly distributed along each modeled reach. Because the model only simulates baseflow, the groundwater discharge for each reach is summed to total the baseflow in the stream. Simulated baseflows from the GFLOW model (plate 1) were used to develop the spatial distribution of groundwater discharge in the SNTMP model. This distribution was assumed to be representative throughout the calibration period. Each day, all discharge values were scaled on the basis of estimated flows at a single location on the main stem

just below Tributary 7 (station mar10; see fig. 35). Flows at this location were calculated from a stage-discharge relationship and daily measured stream depths. The streamflow at this location is calculated as (equation 3)

$$Q = 23.622 \times d^{2.958}$$

where Q is streamflow, in cubic feet per second; and d is depth, in feet. The relationship was developed from three data points with flows less than 30 cfs, within the range expected during the calibration period; higher flows are not likely to be well simulated. The nearest downstream gage at the Bad River (USGS 4027000; fig. 1), which covers a much larger watershed, shows similar overall patterns in flow but lags behind changes in stage and is not always consistent with the magnitude of these changes.

Groundwater-temperature inputs for most reaches use daily mean temperature measured at the Blaser Creek monitoring well, which is assumed to represent groundwater flow in shallow till. The reaches from Tributary 7 downstream to the Marengo River at FR198 use the temperature measured in the groundwater seep, which is assumed to represent the cooler

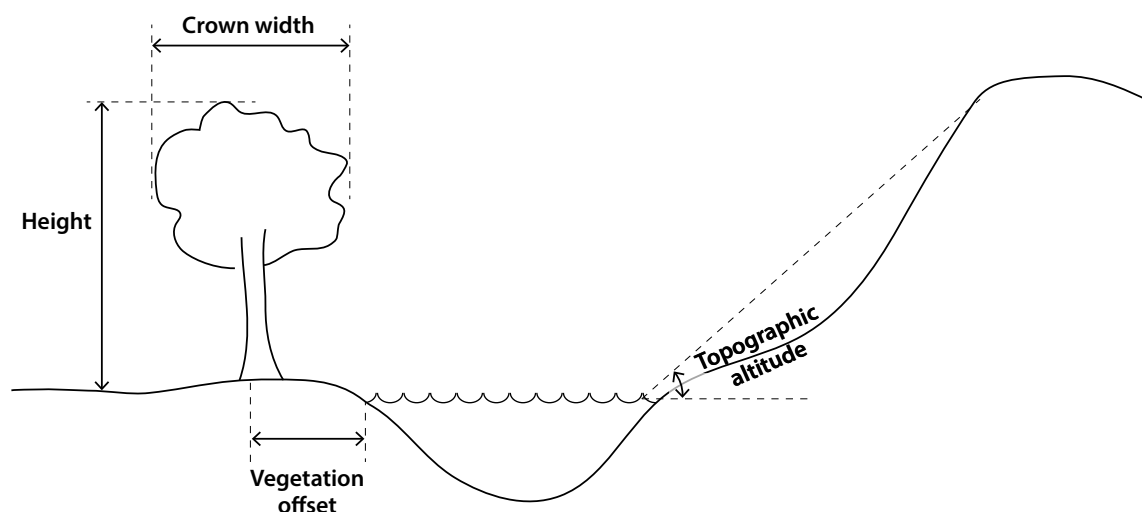
groundwater from a fracture flow. These locations were selected based on geology and simulated groundwater-flow paths (fig. 26).

Calibration

The stream-temperature model was manually calibrated to reflect the conceptual model while matching observed values as best as possible. Fourteen stations were used to compare simulated and observed-daily mean temperatures (fig. 33). The objectives of calibration were (1) minimal error between observed and simulated values, (2) high correlation between observed and simulated values, and (3) minimal spatial bias. Particular attention was paid to measurement locations with greater flow and certainty (main channel of Marengo River) and locations with a known trout population (Marengo River at FR198 and at the North Country Trail (stations mar02 and mar01, respectively)).

Calibration focused on seven parameters: vegetation density of the three vegetation types, and the width B term (from equation 2) for four zones. The vegetation density was found to not be particularly sensitive and was

Figure 34. Topographic, hydrographic, and vegetative features used for the shading parameters in the stream-temperature model (SNTMP).



left at the initial values. The vegetation geometry was developed from measurements and was not varied during calibration. However, model runs with a uniform shade value did not perform well, indicating that differences in geometry between the three types of vegetation does influence stream temperature. The width terms were initially set at $B = 0.2$, the model-recommended parameter for typical channels. The calibrated width term was changed to $B = 0$ for wetlands and wetland tributaries, indicating a rectangular channel; the initial value of $B = 0.2$ was retained for the main channel of the Marengo River and its tributaries.

Although baseflows were not considered to be a calibrated parameter, the preliminary model runs show the significance of baseflows for predicting stream temperature. For example, the preliminary GFLOW model results that did not include the high-transmissivity zone, which simulated too little baseflow in Tributary 7; when these baseflows were used in the SNTEMP model, Tributary 7 was simulated with stream temperatures more

than 3°C too high. The sensitivity of the SNTEMP model to baseflows, as well as to groundwater temperature and air temperature, are tested in the climate-change scenarios.

Model performance

The final model has a root-mean-square error (RMSE) of 1.6°C and a mean temperature error for all the calibration targets of -0.2°C. The temperature in calibration locations along the main channel of the Marengo River below the waterfall is modeled well, with mean errors below 0.6°C and correlation coefficients between daily observed and simulated temperatures above 0.6 (fig. 36, appendix table 3.1). Mean errors above 2°C are limited to low-flow Tributaries 5 and 6. The stream temperature of the Marengo River's main channel is overall simulated slightly high; the tributaries have both positive and negative mean errors, but the differences are varied and not related to a single parameter. The final model is a balance where all targets are simulated relatively well while maintaining low mean errors in the main channel.

The model simulates temporal changes well in most locations (fig. 37; also see correlation coefficients in appendix table 3.1). Figure 37 compares simulated results at sites upstream and downstream of the focused groundwater-discharge area near Tributary 7 that influences the trout habitat near FR198. Because the SNTEMP model does not account for the influence of the previous day's temperature, some simulated stream temperatures are overly sensitive to air temperature and are simulated with greater daily variation than observed. As a result, the short term (1-day) maximum daily means may be conservatively high. See further discussion in *Results*, below. Blaser Creek has a low correlation coefficient that is possibly due to a changing stream geometry (from the construction of beaver dams), which is not captured in the model.

Figure 35. Modeled daily discharge, measured daily stage, and measured flow in 2018 for the Marengo River downstream of Tributary 7 (station mar10 in figure 9 and table 1). Abbreviations: cfs, cubic feet per second; ft, feet.

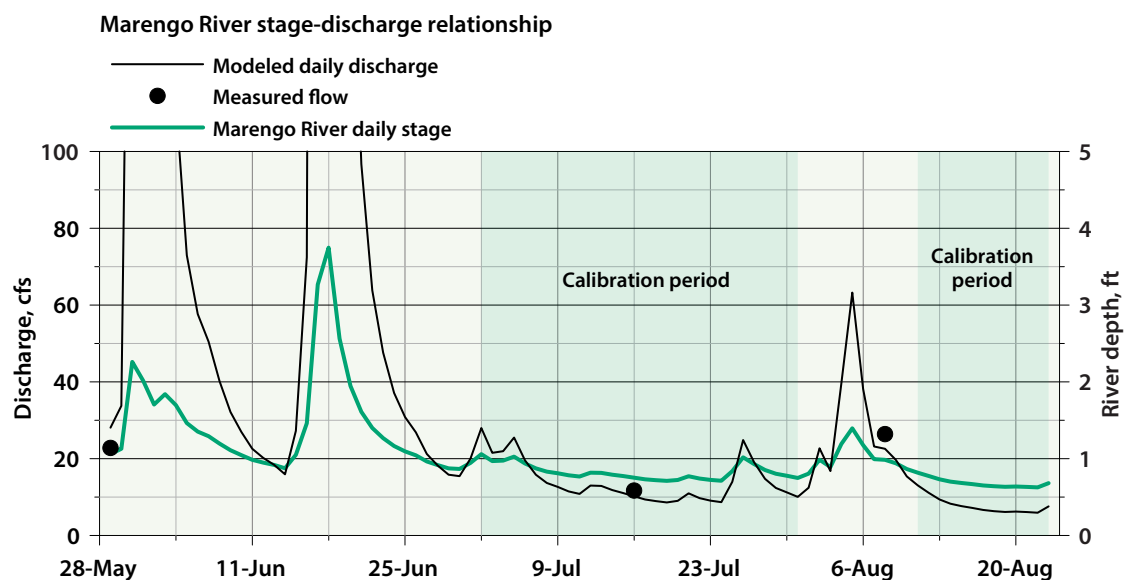
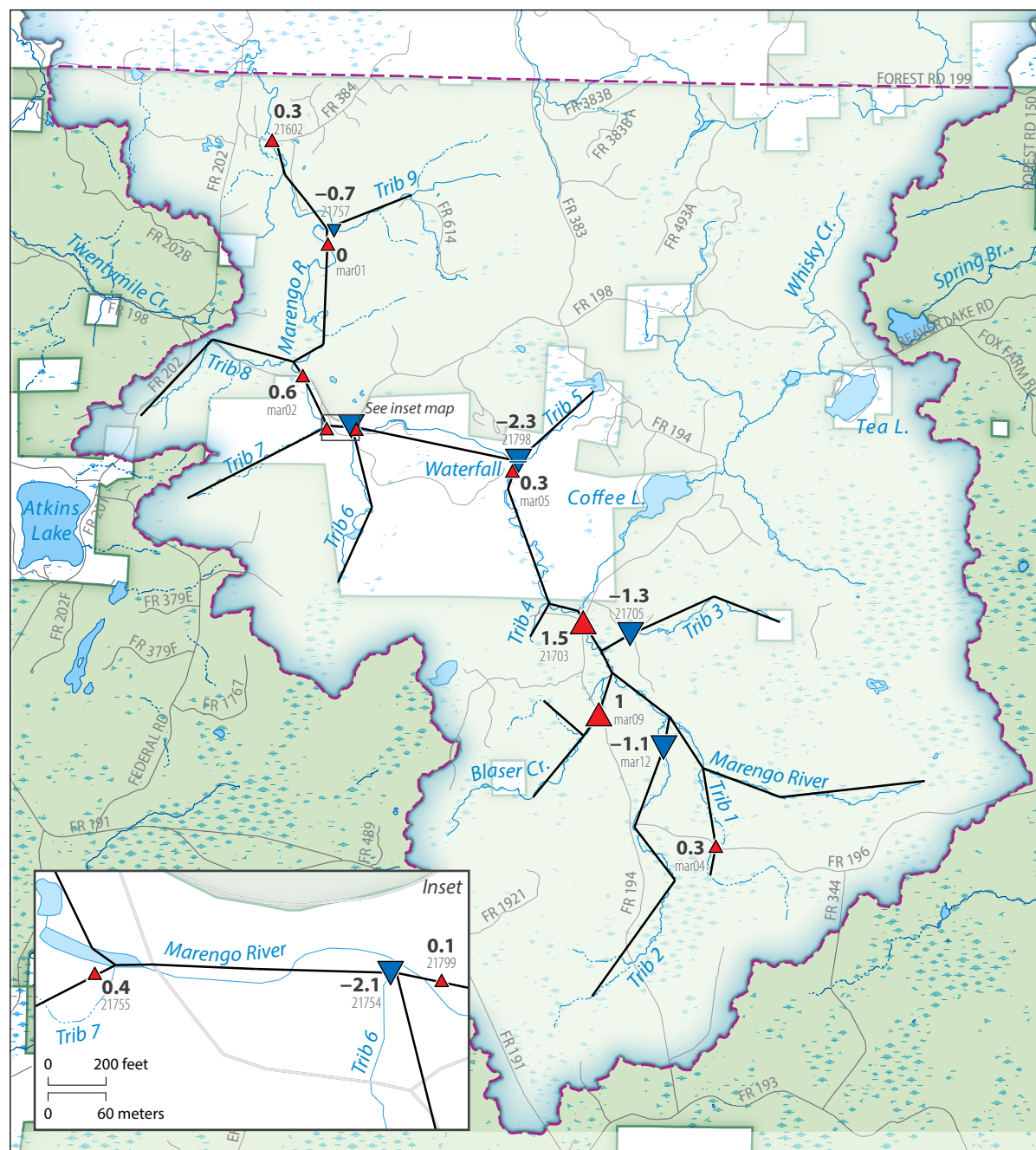


Figure 36. Map showing the results of the stream-temperature model (SNTEMP). Abbreviation: °C, degrees Celsius.



National Forest boundaries from the USDA Forest Service, 2011. Hydrography from National Hydrography Dataset (U.S. Geological Survey, 2016).

Scenarios for stream temperature

Climate-change scenarios

Climate change in the stream-temperature model is represented by changes to air temperature, groundwater temperature, and groundwater discharge. This section describes the changes to each of these parameters. Solar radiation and all other parameters were assumed to remain the same as in 2018.

The measured daily mean air temperatures from the 2018 calibration period were modified to represent equally probable future air temperatures using the University of Wisconsin Probabilistic Downscaling dataset (Notaro and others, 2014; Daniel Vimont, UW-Madison, written communication). A suite of general circulation models (GCMs) was evaluated for the average air temperature over the calibration period. Of these GCMs, three models representing

approximately the 10th, 50th, and 90th percentiles of average air temperature were then selected to represent low-, medium-, and high-air-temperature scenarios, respectively (fig. 38, table 8). The 2018 data were then scaled such that, given a particular temperature on a particular day in 2018 with an estimated probability, that day was assigned a future temperature with the same probability obtained from the GCM probability distribution. The GCMs represent the time period 2041–2060 under a high-emissions scenario (representative concentration pathway (RCP) 8.5; Moss and others, 2010). The probability distribution of this time period is similar to the moderate emissions scenario (RCP 4.5; Moss and others, 2010) for 2081–2100. These air temperatures could be expected in roughly 30 years under high emissions or 70 years with moderate emissions. Air temperatures are projected to increase between

2.1°C and 4.9°C relative to the average temperature of the 2018 calibration period (table 8).

Future groundwater temperatures depend on thermal sensitivity (the increase in groundwater temperature per degree of air temperature increase over a specified duration of time). Numerous climate studies conservatively assume a thermal sensitivity of 1, meaning that groundwater temperature increases the same amount as air temperature (for example, Deitchman and Loheide, 2012). The modeled and observed groundwater temperatures in thin, shallow aquifers can respond quickly to increasing air temperatures (Kurylyk and others, 2014; Menberg and others, 2014). Kurylyk and others (2014) found that the modeled thermal lag was less than 5 years, and thermal sensitivities ranged from 0.55 to 1. Groundwater with longer flow paths, such as those discharging to Tributary 7, can be expected

Figure 37. Simulated and measured daily mean water temperatures for the Marengo River at FR198 and upstream of Tributary 6 (stations mar02 and 21799, respectively, on figure 9 and table 1) during calibration period. Abbreviations: °C, degrees Celsius; FR, Forest Road.

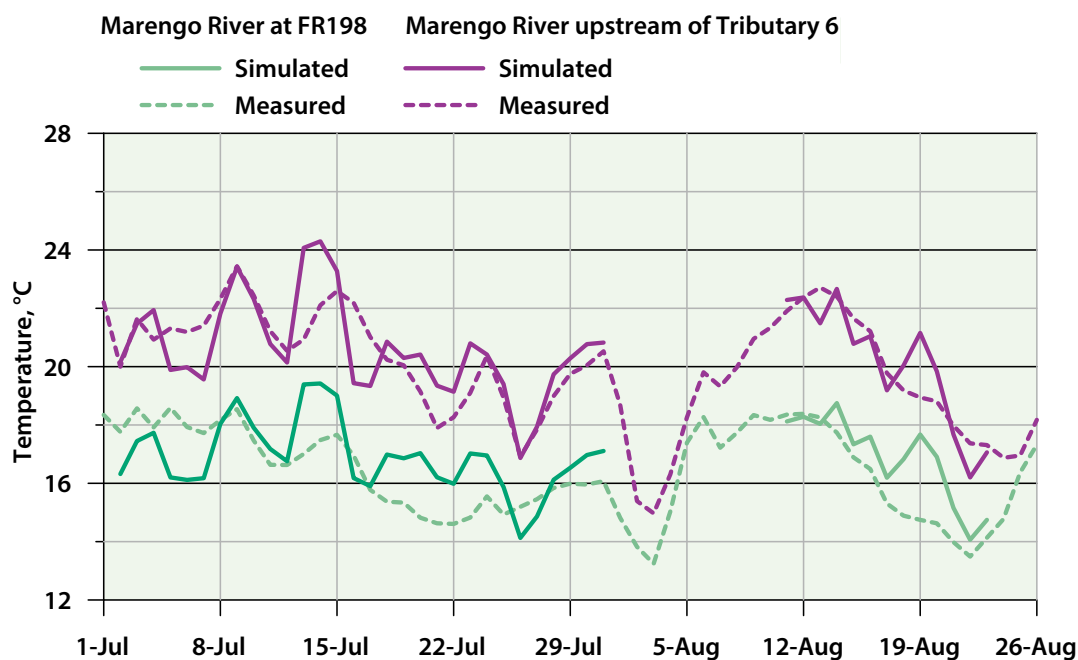


Figure 38. Air temperatures for the low-, medium-, and high-air-temperature scenarios developed from three general circulation models, also showing air temperatures measured during the 2018 calibration period. The gap in data was not included in the calibration period. Abbreviation: °C, degrees Celsius.

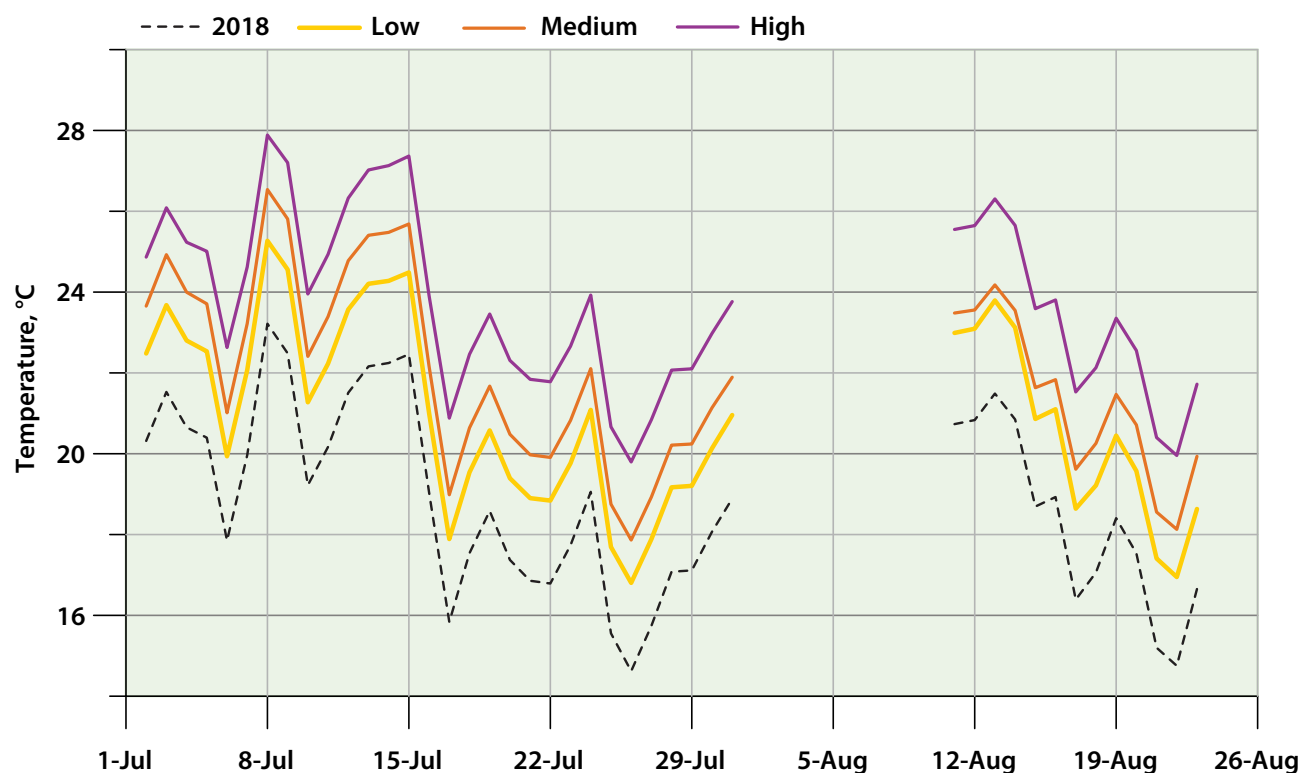


Table 8. Average projected air temperatures compared to the 2018 calibration period for low-, medium-, and high-air-temperature general circulation models.

Air-temperature model	General circulation model	General circulation model originating group	Average daily air temperature, °C	Increase in daily average air temperature, °C
2018 measured			18.8	—
Low	MRI-ESM1	Meteorological Research Institute, Japan	20.9	2.1
Medium	CanESM2	Canadian Centre for Climate Modelling and Analysis	21.9	3.1
High	GFDL-CM3	National Oceanic and Atmospheric Administration (NOAA) Geophysical Fluid Dynamics Laboratory (GFDL)	23.7	4.9

Abbreviations: C, degrees Celsius; —, not applicable.

Note: The listed general circulation models (GCMs) are for the time period 2041–2060 and representative concentration pathway (RCP) 8.5 high-emissions scenario (Moss and others, 2010). These models are similar to the RCP 4.5 (moderate emissions, Moss and others, 2010) for the 2081–2100 time period.

to maintain cold temperatures for a longer period of time. The timing of the recharge—and whether or not it is from snowmelt—may also affect future groundwater temperatures. For the climate-change scenarios, the thermal sensitivity is simulated to range from 0 to 1. The thermal sensitivity values are also applied to Whisky Creek, which is simulated to discharge into the Marengo River with a known flow and temperature. Although model runs with a thermal sensitivity of 0 likely underestimate the temperature in Whisky Creek, the two values provide limits for the range of future temperatures.

The three baseflow climate-change scenarios discussed in the chapter 4 were used to represent the possible range in groundwater discharge: no change (base), +21% recharge, and –12% recharge. The groundwater-flow model simulates a baseflow increase of 18% and a decrease of 10% in the main channel just below Tributary 7 at station mar10 for the two new scenarios (appendix table 2.3). The discharge time series from 2018 was therefore scaled by the same amount. The spatial distribution of flow was also updated for both scenarios (plates 2 and 3).

Management scenarios

Several different management scenarios were simulated to evaluate the benefit of possible management strategies. All management scenarios were compared to the climate-change scenario with medium air temperature, a thermal sensitivity of 1, and no change to groundwater discharge. The first scenario simulates installing in-channel structures by decreasing the average stream width from 21.6 to 15 ft between nodes mar-017 and mar-016 (fig. 33). This 1,900-ft section is fairly easy to access from FR194 and has little shade, so reducing the width is expected to decrease the temperature. The second scenario simulates

the removal of a large beaver dam and narrowing the upstream portion by decreasing the width between nodes mar-020 and mar-019. This section is harder to access but contains one of the larger beaver dams in the headwaters. The average width of the 2,300-ft reach was reduced from 25 to 20 ft. The third scenario simulates decreasing the stream width upstream of Tributary 7, from mar-010 to mar-009, from 31 to 20 ft over the 880-ft length. The fourth and final scenario simulates the removal of tag alder shrubs and revegetating with wetlands downstream of FR194 in the headwaters, from mar-016 to mar-014, which is about 1,900 ft. This scenario was selected because although tag alder is typically an undesirable species, it provides shade and removing it could increase temperatures.

Flooding

Although precipitation is not simulated in the SNTMP, it does affect stream temperature (Carlson and others, 2019). After large rain events in the Marengo River study area, the stream temperatures in the main channel converge toward a uniform temperature for several days (figs. 14–17) and can result in higher long-term average temperatures in groundwater-discharge areas. Wisconsin is projected to see an increase in extreme precipitation as well as increasing temperatures (WICCI, 2011). Recent regional flooding events in 2016 and 2018 suggest that these changes are already occurring. The future temperature of the precipitation and runoff are therefore an unknown that could substantially influence trout habitat.

The effect of a large rain event on stream temperatures was evaluated using measured stream temperatures following a rain event from July 15 to 18, 2018. To evaluate how a rain event of this magnitude might affect stream temperatures in the

future, a future flooding scenario was created by increasing the 2018 stream temperatures by the same amount as the medium-air-temperature climate-change scenario. Because the stream is likely dominated by runoff following a rain event, this effectively and conservatively assumes that runoff has a thermal sensitivity of 1 (increases by the same magnitude as air temperature). In reality, temperatures following a future flooding event caused by a rain event of similar magnitude would probably be somewhere in between the 2018 measurements (runoff thermal sensitivity = 0) and the scenario with increased runoff temperatures (runoff thermal sensitivity = 1). Although this exercise only examines one rain event, it provides insight into the current thermal effects of flooding and the range of possible changes.

Evaluating potential impact to trout

Because the effects of stream temperatures on trout habitat are dependent on time scale, the scenario results were compared to the trouts' thermal tolerance limits for different periods. Wehrly and others (2007) used field data from 285 sites in Michigan and Wisconsin to generate thermal tolerance curves (considered to be the 95th percentile of sites with trout present) for daily mean and daily maximum temperatures. The results from the climate-change scenarios were used to calculate a moving average of daily mean temperature for periods of 1, 3, 7, 14, 21, 28, 35, and 42 days. The maximum for each of these periods was then compared to the thermal tolerance curves from Wehrly and others (2007). Although the calibration period is actually two separate time periods, this analysis assumes the dates are continuous.

Results

The mean daily stream temperatures of the Marengo River under the altered climate-change scenarios are projected to increase by 0.8°C to 4.6°C at FR198 (station mar02) relative to those simulated for the calibration period in 2018 (fig. 39, table 9). This range in the increase in temperature illustrates the uncertainty in climate models and thermal sensitivity. Air temperature has the greatest influence on stream temperature at these two stations, increasing stream temperature up to 2.5°C more in the high-air-temperature scenario compared to the low-air-temperature scenario. Thermal sensitivity is also influential, especially for the Marengo

River at FR198 because of the large volume of groundwater discharged at that location. When the thermal sensitivity is 0, the temperature increases less at FR198 compared to upstream of Tributary 6 (station 21799; fig. 39). However, when the thermal sensitivity is 1, the temperature at FR198 increases more than it does upstream of Tributary 6. The change in simulated temperature at FR198 demonstrates that the extent to which groundwater can buffer increases in air temperature depends greatly on the thermal sensitivity. The worst-case scenario at FR198 is an increased recharge with a thermal sensitivity of 1, which simulates a mean stream temperature 1.7°C higher than the scenario with a thermal sensitivity

of 0. The worst-case scenario for the Marengo River upstream of Tributary 6 is also for a thermal sensitivity of 1, but the flow scenario does not make a difference (table 9). Streamflow has the least overall influence on temperature. Typically, low streamflows are associated with higher stream temperatures because the volume of flow decreases relative to the surface area exposed to sunlight. In this case, however, the low-recharge scenario decreases the simulated temperatures at FR198. This result is an artifact of the simulated change in the distribution of groundwater discharge and the simplifying assumption of two distinct groundwater temperatures: the low-recharge scenario disproportionately decreases discharge in reaches

Figure 39. Simulated mean temperature of the Marengo River during the calibration period and for six climate-change scenarios at FR198 and upstream of Tributary 6 (stations mar02 and 21799, respectively, in figure 9 and table 1). Scenarios include a thermal sensitivity of 0 to 1 and low, medium, and high projected air temperatures. Abbreviation: °C, degrees Celsius.

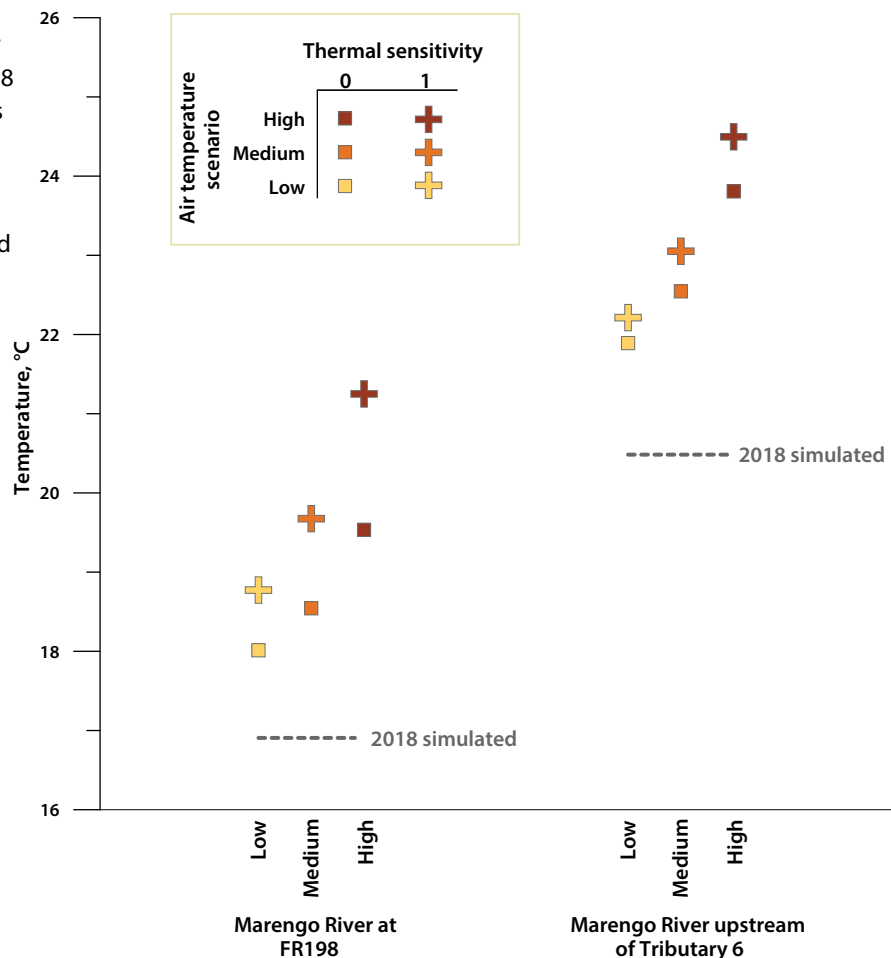


Table 9. Mean simulated daily mean stream temperatures for climate-change scenarios.

Groundwater discharge	Groundwater thermal sensitivity	High-, medium-, or low-air-temperature scenario	Temperature of Marengo River at FR198, °C	Temperature of Marengo River upstream of Tributary 6, °C
2018 simulated			16.9	20.5
No change	0	Low	18.0	21.9
		Medium	18.5	22.5
		High	19.5	23.8
	1	Low	18.8	22.2
		Medium	19.7	23.1
		High	21.2	24.5
+21% recharge	0	Low	18.3	21.8
		Medium	18.8	22.5
		High	19.8	23.7
	1	Low	19.0	22.2
		Medium	19.9	23.0
		High	21.5	24.5
–12% recharge	0	Low	17.7	21.9
		Medium	18.3	22.6
		High	19.2	23.8
	1	Low	18.5	22.2
		Medium	19.4	23.0
		High	21.0	24.5

Table 10. Change in average simulated stream temperatures for management scenarios.

Management scenario	Change in headwaters (Marengo River at FR194, station 21703)	Change downstream of Tributary 7 (Marengo River at FR198, station mar02)
Reduce width in headwaters	–0.2°C	None
Remove beaver dam	–0.2°C	None
Reduce width upstream of Tributary 7	None	–0.1°C
Remove tag alder shrubs downstream of FR194	None	None

simulated with warm groundwater, leading to lower simulated stream temperatures in some locations. In reality, the temperature of groundwater discharge will be different at each location.

The management scenarios have a modest effect on stream temperatures (table 10). Both scenarios that decrease the stream width in the headwaters reduce the mean temperature relative to the 2018 base case simulation by 0.2°C at FR194 (station 21703) but have no effect at FR198 (station mar02). This is a small but measurable impact compared to the projected increases in temperature, and a more substantial effort would be required to propagate temperature reductions below the waterfall. Reducing the stream width upstream of Tributary 7 results in a decrease of 0.1°C at FR198. This location is well shaded, and changing the width might have less of an impact. Removing the tag alder shrubs has no measurable effect at any temperature station, possibly because the Whisky Creek flows are simulated with a thermal sensitivity of 1, and these warm streamflows entering downstream of the simulated change overwhelm any temperature increase from the removal of the tag alder shrubs.

The simulated temperatures were compared to trout thermal tolerance limits from Wehrly and others (2007) (figs. 40–43). Figures 40–41 illustrate the maximum mean daily temperature averaged over several period lengths for six scenarios (base recharge only). These figures show how trout can tolerate higher temperatures for short periods of time. The simulated temperatures for the Marengo River at FR198 (station mar02) for these six scenarios remain below the thermal tolerance limit (fig. 40). The same scenarios upstream of Tributary 6 (station 21799; fig. 41) exceed the thermal tolerance limit

for all scenarios. The temperature is more stable over different periods at FR198 than upstream of Tributary 6. As discussed in *Model performance* in chapter 5, the simulated 2018 values are typically higher than the measured values, especially at the 1-day maximum daily means. That the simulated 2018 values are too high suggests that the maximum 1-day mean temperatures simulated for the climate-change scenarios may also be conservatively high. Even so, the temperatures that are averaged over longer time periods are closer to the thermal limit for almost all locations. The thermal tolerance limit is first exceeded at longer time periods (28–42 days) for all locations except for Tributary 1 (fig. 33). Long-term increases in temperature are therefore more likely to affect trout habitat.

Under the low- and medium-air-temperature scenarios, the Marengo River from FR198 downstream to FR384 is projected to remain below the thermal tolerance limit (fig. 42). For the high-air-temperature scenario, all but Tributary 7 and Blaser Creek are projected to exceed the thermal tolerance limit (fig. 43). The Marengo River at FR198 is only simulated to exceed the thermal tolerance limit when the thermal sensitivity is 1 and the recharge is increased by 21%.

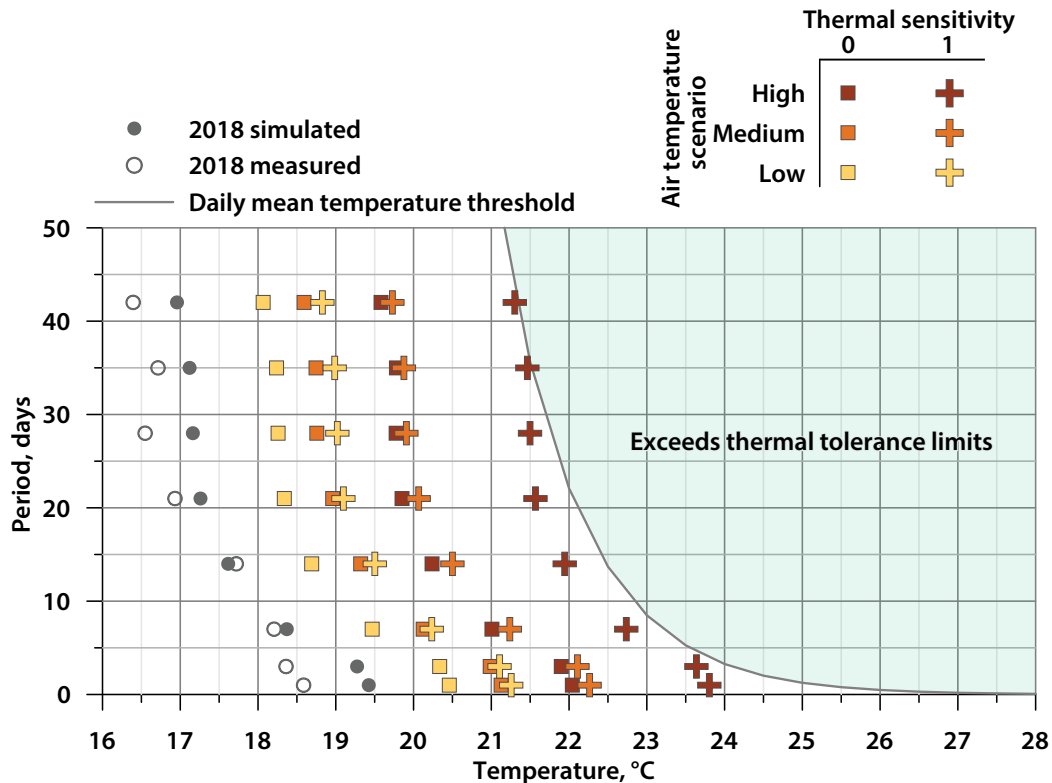
The simulated future rain event is projected to be cooler than the simulated baseflow if the thermal sensitivity of the runoff is 0 and warmer than the simulated baseflow if the thermal sensitivity is 1 (fig. 44). This rain event, even though it lasts only a few days, leads to long-term temperatures that are closer to the trouts' thermal toler-

ance limit. The flood is not projected to exceed the thermal tolerance limit for the simulated medium-air-temperature scenario.

Discussion

Evaluating the potential effect of climate change on trout viability is an inherently difficult task. Future stream temperatures will depend on many factors, including the timing, duration, and spatial patterns of air temperature and precipitation. The climate-change scenarios are not a formal prediction of a specific future year, nor do they account for all possible variations of these factors. For example, different durations of heat waves were not simulated. Instead, this analysis is intended as a comparative tool to illustrate the sensitivity

Figure 40. Simulated and measured temperatures of the Marengo River at FR198 (station mar02 in figure 9 and table 1) compared to trout thermal tolerance limits from Wehrly and others (2007). Scenarios include a thermal sensitivity of 0 to 1 and low, medium, and high projected air temperatures. Abbreviation: °C, degrees Celsius.



of stream temperatures to different parameters and demonstrate the scale of possible changes.

Air temperature has the highest simulated effect on stream temperature and is also an uncertain parameter for the future climate-change scenarios. The GFLOW model and SNTEMP model also introduce uncertainty to the simulated future stream temperatures. Stream temperature increases in all locations for all future climate-change scenarios.

Groundwater can buffer the effects of increased air temperature, but the extent of buffering depends on thermal sensitivity. The influence of thermal sensitivity on simulated results emphasizes the importance of continued research into understanding how groundwater temperature will change in the future. In the Marengo River watershed, the

thermal sensitivity is likely higher in areas with shallow groundwater that respond to seasonal variation, such as in the headwaters. Near Tributary 7, groundwater temperatures were observed to be relatively steady, suggesting deeper groundwater-flow paths and a low thermal sensitivity. However, the age of the groundwater is uncertain. Travel times through fractures can be on the order of years or less. If this is the case, a shift from snowmelt recharge to rainfall recharge might propagate through the aquifer quickly compared to aquifers with longer travel times.

The projected stream temperatures suggest that higher temperatures that are sustained over several weeks may be more detrimental to trout habitat than short-term variations. Daily thermal maxima are an important parameter for trout; however, areas

with high groundwater influence and little daily variation in stream temperature (such as at FR198) may be more susceptible to long-term changes.

A stream’s width and its width-to-depth ratio can be important. Deep pools can provide temperature stratification that are important to trout, even when there is no groundwater discharge (Matthews and others, 1994). Conversely, parts of the stream that are both shallow and wide have a greater surface area exposed to sunlight and they warm more readily (Deitchman and Loheide, 2012). The width is simulated in SNTEMP but is averaged over the reach, and the stream is assumed to be well mixed. The influence of local differences in width or thermally stratified pools is not captured in the model.

Figure 41. Simulated and measured temperatures of the Marengo River upstream of Tributary 6 (station 21799 in figure 9 and table 1) compared to trout thermal tolerance limits from Wehrly and others (2007). Scenarios include thermal sensitivity of 0 to 1 and low, medium, and high projected air temperatures. Abbreviation: °C, degrees Celsius.

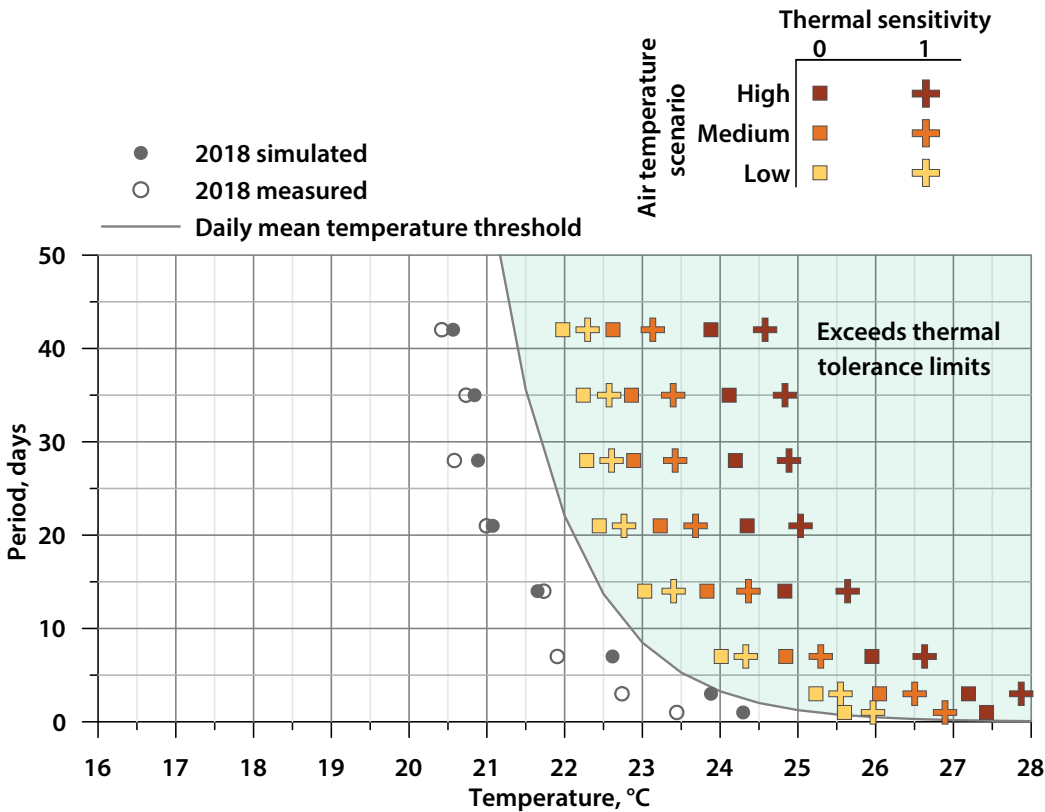
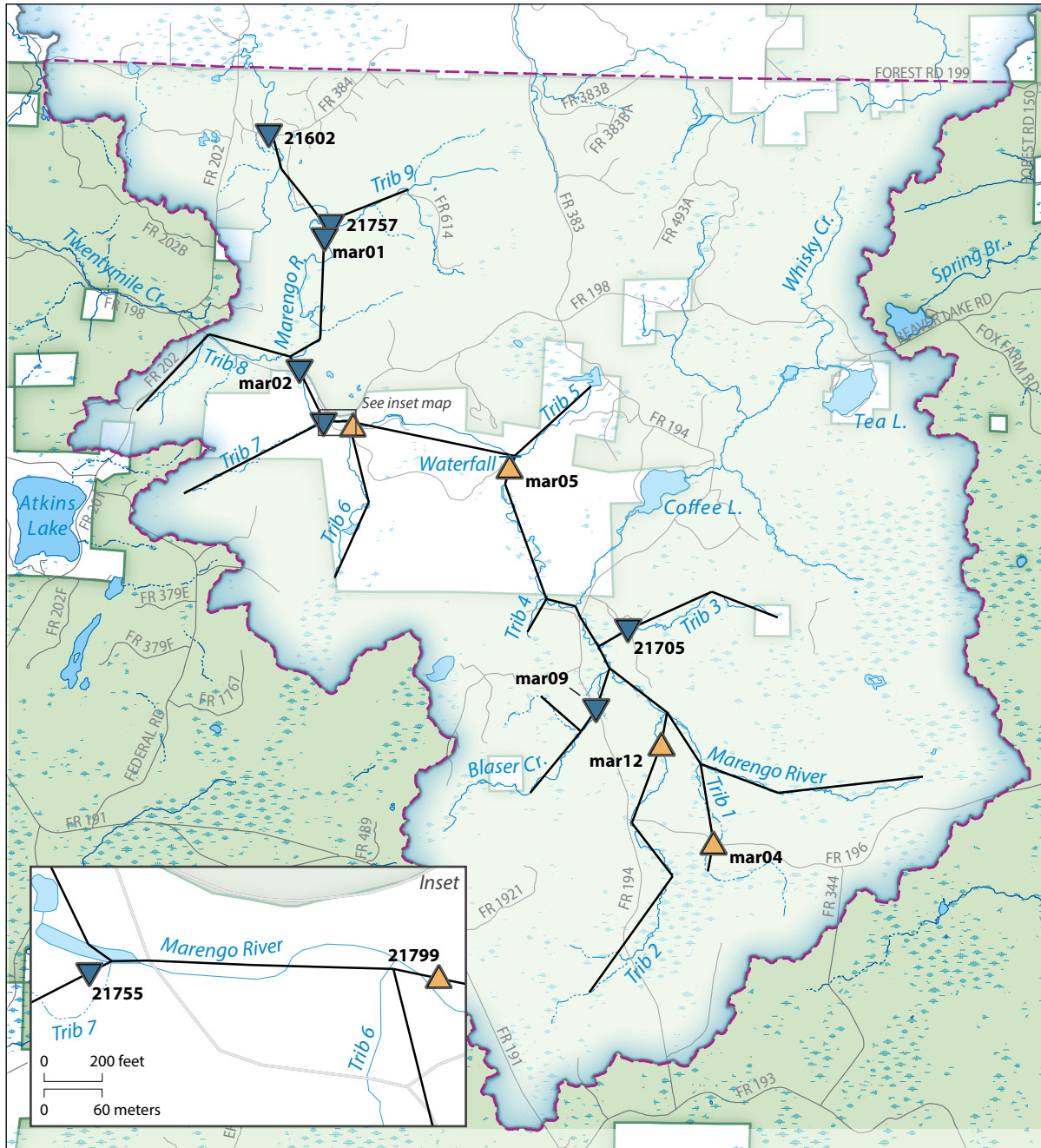


Figure 42. Modeled locations where the trout thermal tolerance limits from Wehrly and others (2007) in stream water were exceeded for the low- and medium-air-temperature scenarios. Abbreviation: SNTMP, Stream Network Temperature Model.



Exceeds thermal tolerance limits?

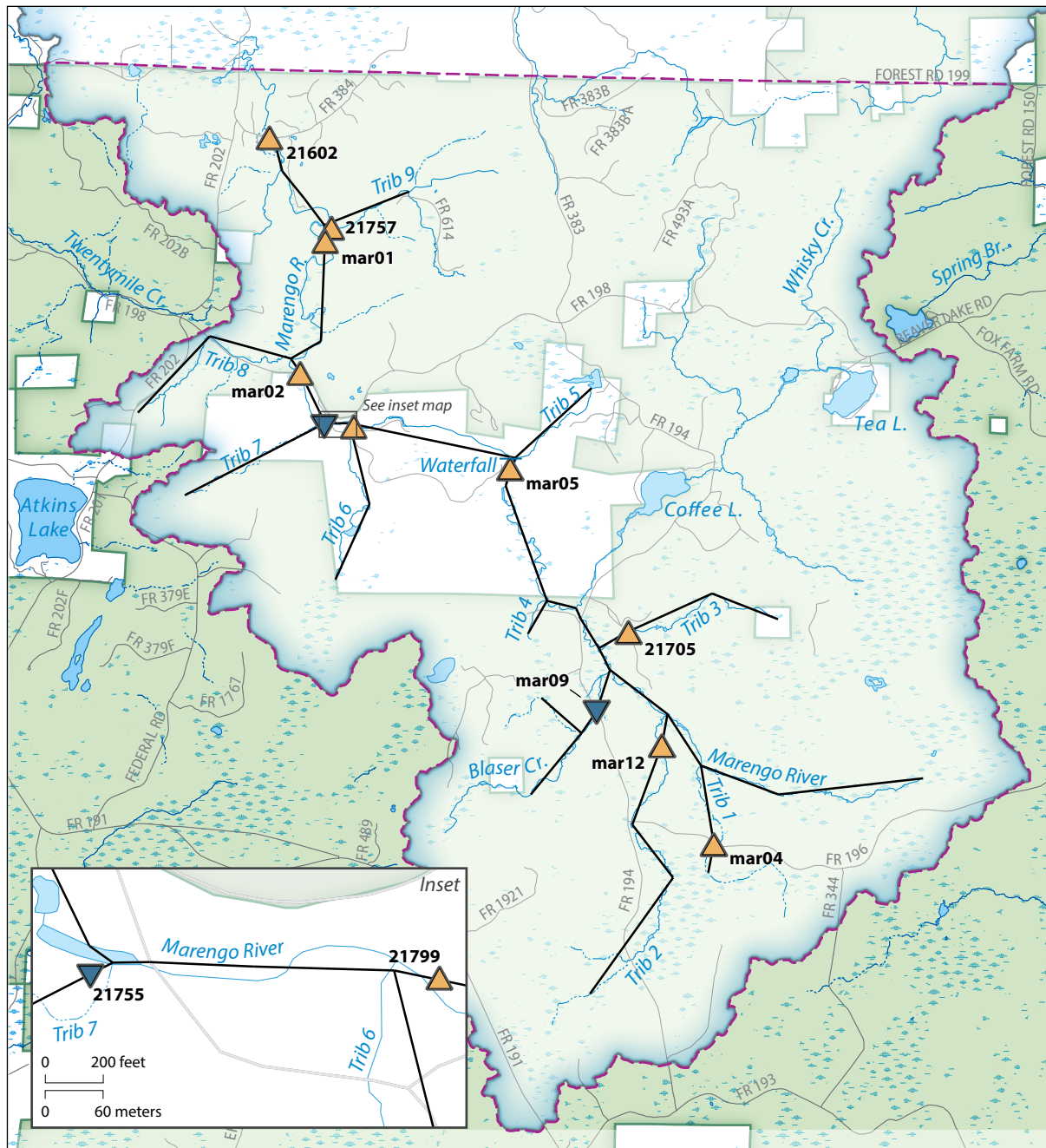
- ▲ Yes
- ▼ No

- SNTMP model reach
- Marengo River watershed
- ▭ Study area
- National forest
- Wetland
- Roads
- Perennial stream
- Intermittent stream



National Forest boundaries from the USDA Forest Service, 2011. Hydrography from National Hydrography Dataset (U.S. Geological Survey, 2016).

Figure 43. Modeled locations where the trout thermal tolerance limits from Wehrly and others (2007) in stream water were exceeded for the high-air-temperature scenario. Abbreviation: SNTMP, Stream Network Temperature Model.



Exceeds thermal tolerance limits?

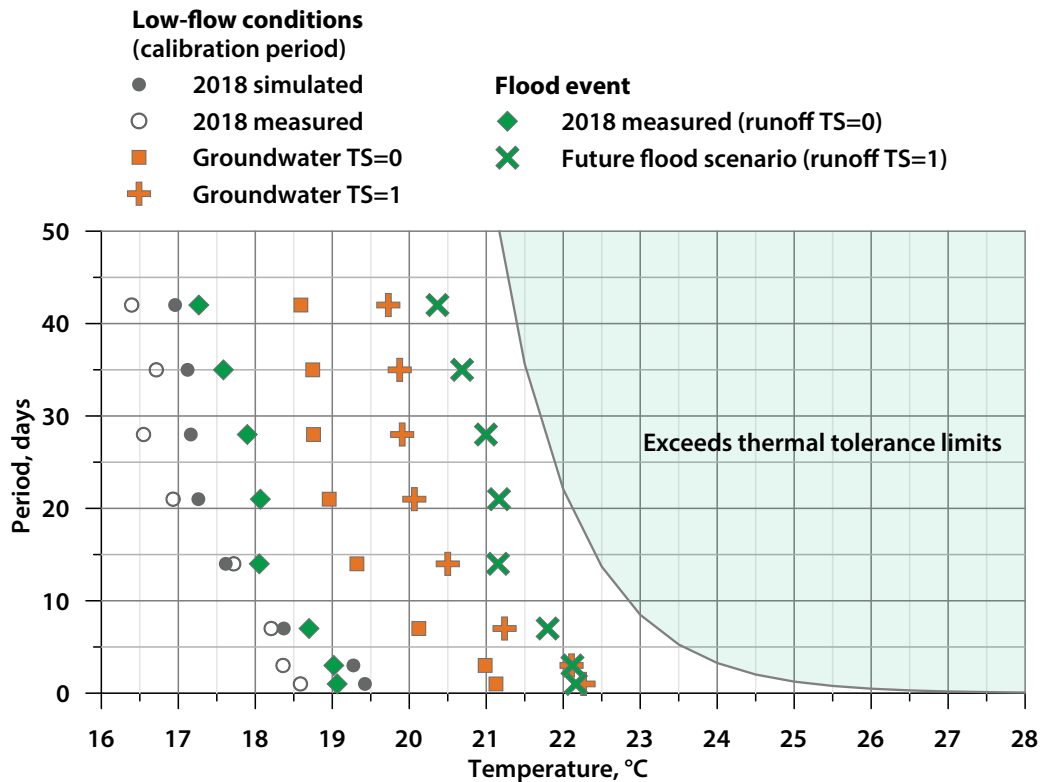
- ▲ Yes
- ▼ No

- SNTMP model reach
- Marengo River watershed
- ▭ Study area
- National forest
- Wetland
- Roads
- Perennial stream
- Intermittent stream

0 1 mile
0 1 kilometer

National Forest boundaries from the USDA Forest Service, 2011. Hydrography from National Hydrography Dataset (U.S. Geological Survey, 2016).

Figure 44. Simulated and measured temperatures of the Marengo River at FR198 (station mar02 in figure 9 and table 1) during low flow (calibration period) and during flooding compared to the trout thermal tolerance limits from Wehrly and others (2007). All scenarios used a medium-air-temperature projection. The flooding scenarios assumed a runoff thermal sensitivity (TS) of 1; the low-flow scenarios used a groundwater thermal sensitivity of 0 and 1. Abbreviation: °C, degrees Celsius.



Although low-flow periods are often considered critical factors that affect stream temperature, flooding is projected to have a similar thermal impact in this watershed. As with baseflow, the long-term increases in runoff temperature are projected to have a greater effect on trout habitat suitability compared to short-term increases. The relative importance of flooding compared to baseflow depends on a number of factors, including the thermal sensitivity of both runoff and baseflow. The runoff temperatures are more directly affected by summer air temperatures than groundwater temperatures because groundwater typically is deeper and may be derived from snowmelt recharge. As a result, runoff temperatures may increase more rapidly than baseflow stream tem-

peratures. In the short term, stream temperature in groundwater discharge areas such as those near FR198 may increase more during flooding than during dry, hot baseflow periods.

The stream-temperature model SNTemp operates on a successive steady-state basis; that is, SNTemp assumes that the steady-state (daily average) conditions remain the same for the time it takes for water to travel from the top of the system to the most downstream node. This leads to uncertainty if that travel time is longer than a day because the model does not account for the influence of previous day's temperatures. The travel times for this model were estimated to be on the order of one to several days. As a result, there is a greater variation in the simulated daily tem-

peratures than the measured daily temperatures. Although this variation leads to higher simulated daily peaks (such as the maximum 1-day and 3-day mean temperature shown in figs. 40–41), the long-term temperature increases are simulated to be more critical for trout habitat. SNTemp also uses average input values for each day and reach. Parameters that change on a subdaily time scale are not captured in the model. Similarly, the influence of small variations in stream geometry, groundwater temperature, or groundwater discharge may not be simulated. The model assumes a thorough mixing both vertically and transversely. Flows are dependent on the groundwater-flow model and a stage-discharge relationship with somewhat limited data.

Some of the uncertainties described above are overshadowed by the uncertainty in climate models. The model representing the 90th percentile of GCMs has more than twice the air temperature increase as the 10th percentile (4.9°C compared to 2.1°C). The large range in climate-change scenarios was selected to help offset the uncertainty in earlier assumptions.

Trout habitat is influenced by many factors in addition to average stream temperature, including stream geometry, pests, food sources, and fish passage. For instance, even where average temperatures exceed the thermal tolerance limits, trout might find protected pockets of cooler water. Spring flooding during

the emergence of fry (young trout) is a critical period for trout in this watershed. Extreme flooding not only increases the temperature, it also increases turbidity, decreases oxygen availability, and threatens the habitat through erosion. This analysis does not address the complicating factors of warming, such as disease, pests, or a decline in food sources. For example, Mitro (2016) found that brook trout populations were outcompeted by brown trout after a warm, dry season that increased the gill lice population, which infected higher numbers of brook trout. Although this study focuses on trout habitat in the main channel of the Marengo River, even its unmapped

headwater streams might provide biodiversity (Meyer and others, 2007), and climate change is likely to affect the habitat and ecosystem function in its upper headwaters as well.



Measuring electrical conductivity in the Marengo River | Catherine Christenson

Chapter 6: Conclusions

The Marengo River watershed is a heterogeneous system that is highly influenced by its hydrogeologic setting. The stream temperature varies spatially, largely due to geologically driven changes in groundwater discharge. Groundwater discharge is focused in two main parts of the watershed: (1) Blaser Creek and (2) the vicinity of Tributary 7, including in the main channel from Tributary 7 downstream to FR198. Evidence suggests that shallower groundwater discharges to Blaser Creek and deeper groundwater discharges to Tributary 7. The shallow groundwater is warmer and has a greater seasonal variation in temperature than the deeper groundwater. Tributary 7 is also distinguished by the volume and focused nature of the groundwater discharge. The average annual baseflow increases by about 50% (6 cfs) from upstream of Tributary 6 to FR198 (upstream and downstream of Tributary 7). This focused cold-water input corresponds to trout habitat observed in the main channel downstream of Tributary 7. The simulated groundwater watershed (recharge area) for Tributary 7 is four times larger than the surface drainage area. A conceptual model with contrasting transmissivity zones near the Atkins Lake–Marenisco fault improves simulations of the focused groundwater discharge. Estimates of effective hydraulic conductivity from the groundwater flow model are 46 ft/d for the high-transmissivity zone (including Bad River Dolomite) and 0.34 ft/d for the low-transmissivity zone. These values are likely influenced by the presence of the fault and the history of deformation in this area.

Potential climate change impacts were simulated using the groundwater-flow and stream-temperature models. Recharge is projected to

either increase or decrease; a suite of GCMs through 2100 simulate the future average annual recharge to be between 6.7 and 9.5 in./yr, representing a change of –12% to +21% compared to the mean SWB-simulated recharge for

1989–2000 of 7.7 in./yr. This change in recharge is simulated to influence the distribution of flow, with the high-discharge areas near Tributary 7 and Blaser Creek remaining fairly constant for both the increase and decrease in overall recharge. The

stream temperature model illustrates the sensitivity of the baseflow stream temperature to different parameters and demonstrates the scale of possible changes. The future baseflow stream temperatures were simulated using a range of climate-change scenarios expected in 30 to 70 years compared to a dry period in 2018. The stream baseflow temperatures are projected to increase everywhere in the watershed compared to 2018. The mean daily stream temperatures in the main channel downstream of Tributary 7 at FR198, where trout habitat has been observed, are simulated to increase between 0.8°C and 4.6°C relative to the 2018 calibration period. This location remains below the trout thermal tolerance limits for the low- and medium-air-temperature scenarios but exceeds the thermal tolerance limit for the high-air-tem-

perature scenario. Air temperature has the greatest simulated effect on stream temperature, followed by groundwater thermal sensitivity. Simulations with a low thermal sensitivity, indicating a small or delayed



Sampling groundwater at Mineral Lake campground well | Anna Fehling

increase in groundwater temperature, provide a more effective buffer against the effects of increased air temperatures than simulations with high thermal sensitivity. It is expected that the groundwater temperature near Tributary 7 may increase less rapidly than the shallower groundwater in the headwaters. Flooding is also projected to increase temperatures downstream of Tributary 7. The magnitude of the increases depends on future runoff temperatures but is likely to be similar to the impacts during baseflow conditions. Sustained temperature increases from flooding and low-flow conditions are projected to have a greater effect on trout than short-term increases.

Implications for management

The management scenarios from this study help inform possible management strategies to improve trout habitat under climate change (see *Management scenarios* in chapter 5). The reader is referred to Avery (2004), Roni and others (2011), and Palmer and others (2014) for a more general discussion of stream restoration approaches, goals, and history. This section discusses the following strategies: (1) Protecting recharge areas, (2) in-stream restoration, (3) shade or riparian management, (4) beaver control, and (5) culvert improvements.

Because of the importance of groundwater discharge for keeping stream temperatures within trout thermal tolerance limits, protecting the surface watershed and groundwatersheds should be a priority for groundwater-discharge areas such as Tributary 7 and Blaser Creek. This priority is especially noteworthy given the difference between the surface-drainage area and the groundwatershed (*fig. 26*). Recharge areas can be protected by avoiding activities that increase runoff or evapotranspiration. Soil compaction from logging or development and other activities that increase runoff could reduce the focused groundwater discharge upstream of trout habitat.

In-stream restoration to narrow and deepen stream channels has been a successful trout habitat management strategy in Wisconsin (Avery, 2004). However, narrowing the stream width was simulated to have only a minor local effect on stream temperature in the study area, especially if groundwater temperatures increase as a result of climate change. In-stream structures and the potential effects from deepening streams (such as

exposing gravel beds or increasing groundwater discharge) were not evaluated as part of this study.

Shade has been identified as an important parameter for reducing stream temperatures in central and southwestern Wisconsin (Gaffield and others, 2005; Cross and others, 2013). Under the climate-change scenarios, modest simulated changes in shade did not have an effect on stream temperature in the study area. However, the response of stream temperatures to an early heat wave in May suggests that shade and (or) sun angle can be important in this watershed, and activities such as logging would likely have an adverse effect on trout. Nonetheless, much of the riparian corridor and watershed, especially near trout habitat areas, is either already protected or located in undeveloped private land.

Beavers are widely considered to be detrimental to trout populations, mainly because stream temperatures are warmer downstream of beaver dams (Johnson-Bice and others, 2018). Simulated beaver dam removal in the study area resulted in slightly reduced local stream temperatures. However, although beaver dam removal in Wisconsin has been shown to increase trout habitat (Avery, 2004), a review of 21 beaver-salmonid studies in Michigan, Minnesota, and Wisconsin found that the actual effects of beaver on trout can vary substantially in heterogeneous settings and is not always well documented (Johnson-Bice and others, 2018; also see McRae and Edwards, 1994). Although beaver dams can increase stream temperatures and reduce connectivity, they can also provide benefits to trout and the watershed as a whole. The possible positive functions of beaver dams include detaining storm water; inducing recharge; maintaining flow during droughts; exposing gravel beds

downstream; and providing deep, low-energy pools for trout habitat (Johnson-Bice and others, 2018).

Although this study did not investigate the effects of roads, culverts, or fish passage, others have identified these as important factors affecting trout habitat (Roni and others, 2011). Specifically, culvert improvement can improve connectivity, reduce erosion, increase biodiversity, and improve storm resilience (Sue Eggert, USFS, unpublished data). A culvert improvement program has been implemented in the larger Marengo River watershed (American Society of Adaptation Professionals, 2017).

Research implications and suggestions for future work

The local hydrogeology often has important implications for understanding system changes, especially in heterogeneous settings. In this study area, the simulated changes in baseflow distribution buffer the effects of increasing or decreasing the annual recharge. Other areas with substantial groundwater discharge, similar to the area near Tributary 7, may exceed the trout thermal tolerance limits at longer periods and may be strongly influenced by the groundwater thermal sensitivity. Flooding is a potential critical event that can affect a stream's temperature in groundwater-dominated areas, which can be overwhelmed by warmer runoff. Future work should include an investigation of the thermal sensitivities of groundwater and runoff, which may influence future stream temperature in areas with high groundwater discharge and during flood events, respectively. Lastly, stream temperatures in this watershed are mostly influenced by air temperature. Continued research into climate change and adaptation strategies will be critical for effective resource management.

Appendix 1: Chemistry

Table 1.1. Field chemistry measurements, listed in order from downstream to upstream.

Location	Station ID ^a	Date	Temperature, °C	pH	Conductivity, $\mu\text{S}/\text{cm}$
Marengo River at FR384	21602	5/16/2018	17.2	8.4	104
		6/1/2018	16.8	7.5	63
		8/7/2018	19.2	7.9	116
		9/27/2018	11.3	—	75
Tributary 9	21757	8/7/2018	17.2	7.9	92
Marengo River at North Country Trail	mar01	6/1/2018	16.8	7.5	62
		8/7/2018	18.9	8.0	117
		9/27/2018	11.2	—	74
Tributary 8	21756	8/8/2018	16.3	7.7	139
Marengo River at FR198/Wisco Road	mar02	5/16/2018	15.7	8.1	103
		8/8/2018	17.9	7.9	120
		9/25/2018	13.3	—	70
Marengo River downstream of Tributary 7	mar10	5/29/2018	22.6	7.8	97
		7/16/2018	19.6	8.2	—
		8/8/2018	18.0	7.6	110
		9/25/2018	13.5	—	64
Tributary 7	21755	5/17/2018	8.2	8.3	184
		8/8/2018	9.8	8.5	179
Seep	mar06	5/17/2018	6.1	7.6	205
		7/16/2018	—	7.5	—
		9/25/2018	8.9	—	192
Tributary 6	21754	5/17/2018	11.4	7.7	65
		8/8/2018	17.6	7.9	67
Marengo River upstream of Tributary 6	21799	5/17/2018	14.2	6.7	81
Tributary 5	21798	5/17/2018	13.9	6.8	67
		8/8/2018	19.9	7.7	73
		9/26/2018	11.5	—	49
Marengo at waterfall	mar03	5/17/2018	16.4	6.8	73
		8/8/2018	23.0	7.8	87
		9/26/2018	12.3	—	58
Marengo River above the waterfall	mar05	5/31/2018	18.9	6.8	55
		9/26/2018	12.2	—	59
Whisky Creek	21704	5/30/2018	21.2	7.2	52
		7/17/2018	23.3	7.1	—
		8/9/2018	21.0	7.5	74
		9/26/2018	13.4	—	61

Abbreviations: FR, Forest Road; NA, not applicable; $\mu\text{S}/\text{cm}$, microsiemens per centimeter; —, no data.

^aStation identification numbers are shown in table 1 and figure 9. Beaver Lake and Mineral Lake wells are shown in figure 1.

^bTwo field measurements were taken in Tributary 2 where it intersects FR196 (in addition to measurements at the thermograph location (mar12)).

Table 1.1. Field chemistry measurements, listed in order from downstream to upstream, *(continued)*.

Location	Station ID ^a	Date	Temperature, °C	pH	Conductivity, μS/cm
Marengo River at FR194	21703	5/18/2018	12.1	6.8	95
		5/30/2018	18.9	7.1	92
		5/31/2018	16.9	6.6	58
		7/17/2018	17.2	7.2	—
		8/8/2018	21.2	7.3	118
		9/26/2018	11.2	—	60
Tributary 3	21705	5/30/2018	20.5	6.7	43
		9/26/2018	10.9	—	39
Blaser Creek at FR194	mar09	5/18/2018	8.5	6.7	154
		5/31/2018	16.4	7.3	89
		7/17/2018	15.8	7.7	—
		8/9/2018	13.2	7.5	180
		9/26/2018	10.7	—	96
Blaser monitoring well	mar11	9/26/2018	12.4	—	104
Tributary 2 at FR196 ^b	NA	5/18/2018	11.4	6.8	85
		8/9/2018	19.7	—	117
Tributary 2 at mar12	mar12	5/30/2018	20.4	7.1	96
		9/26/2018	12.5	—	66
Tributary 1	mar04	5/18/2018	12.0	6.8	84
		5/31/2018	19.2	6.6	65
		8/9/2018	17.7	7.0	164
		9/26/2018	13.7	—	78
Beaver Lake well	NA	5/30/2018	8.0	7.2	164
		9/25/2018	8.4	—	155
Mineral Lake well	NA	5/30/2018	7.7	7.2	178
		9/25/2018	7.8	—	130

Abbreviations: FR, Forest Road; NA, not applicable; μS/cm, microsiemens per centimeter; —, no data.

^aStation identification numbers are shown in table 1 and figure 9. Beaver Lake and Mineral Lake wells are shown in figure 1.

^bTwo field measurements were taken in Tributary 2 where it intersects FR196 (in addition to measurements at the thermograph location (mar12)).

Table 1.2. Chemistry laboratory results.

		Sample results, mg/L											
Station ID ^a	Date ^b	Alka- linity	Chloride	Cal- cium	Copper	Iron	Magnesium	Manganese	Phosphorus	Potassium	Sodium	Sulfate	Zinc
Limit of detection		20	0.5	0.05	0.001	0.01	0.05	0.001	0.003	0.050	0.5	0.2	0.002
21602	6/1	26	ND	7.4	0.002	0.33	2.66	0.008	0.015	0.37	1.0	2.0	0.005
	9/27	31	ND	8.2	0.004	0.65	3.09	0.013	0.021	0.66	1.0	1.8	0.005
mar10	5/31	23	ND	6.1	0.002	0.39	2.27	0.010	0.017	0.38	0.9	2.0	0.009
	9/25	24	1.6	8.4	0.027	0.62	3.67	0.014	0.026	1.56	1.6	1.8	0.014
mar06	5/29	100	ND	24.6	0.001	ND	7.05	ND	0.010	0.67	2.0	4.2	0.013
	9/25	100	ND	25.6	0.003	0.10	7.40	0.002	0.019	0.82	2.1	3.8	0.003
21703	5/30	39	ND	9.9	0.002	0.51	4.00	0.037	0.021	0.47	1.2	2.4	0.011
21703	9/26	23	ND	6.5	0.004	0.59	2.81	0.020	0.020	0.63	0.8	1.4	0.007
mar09	5/31	39	ND	9.8	0.002	0.24	3.53	0.006	0.020	0.46	1.3	2.6	0.006
	9/26	39	ND	10.1	0.004	0.35	3.87	0.014	0.021	0.64	1.3	2.3	0.006
mar11	5/31	42	ND	13.9	0.020	0.75	3.38	0.119	0.030	0.66	1.2	8.3	0.046
	9/26	40	0.8	12.3	0.010	0.57	3.91	0.066	0.037	0.65	1.2	4.8	0.021

Abbreviations: mg/L, milligrams per liter; ND, no data.

Note: Nitrate+nitrite, arsenic, and lead were not detected in any sample and are not listed in this table. The limits of detection are 0.1 mg/L, 0.005 mg/L, and 0.005 mg/L, respectively.

^aStation identification numbers are shown in table 1 and figure 9. Associated locations are listed in appendix table 1.1.

^bAll dates are in 2018.

Appendix 2: Groundwater-flow model performance

Table 2.1. Model performance—Baseflow targets.

Location	Station ID ^a	Measured, cfs	Simulated, cfs	Absolute difference ^b , cfs	Percent difference ^c
Marengo River at Altamont Road	USGS #04026590	21.8	20.2	−1.6	−7%
Tributary 8	21756	0.5	0.4	−0.1	−12%
Marengo River at FR198	mar02	17.3	19.9	2.6	15%
Tributary 7	21755	3.2	3.5	0.3	10%
Marengo River between Tributaries 6 and 7	21707	11.3	13.4	2.1	19%
Tributary 6	21754	0.2	0.3	0.1	31%
Whisky Creek	21704	2.1	3.0	0.9	45%
Marengo at FR194	21703	5.2	7.6	2.4	46%
Blaser Creek at FR194	mar09	1.5	1.7	0.2	17%

Abbreviations: cfs, cubic feet per second; FR, Forest Road; ID, identification number; USGS, U.S Geological Survey.

^aStation identification numbers are shown in figure 25.

^bDifference calculated as simulated minus measured. Positive values indicate the target is simulated too high; negative values indicate the target is simulated too low.

^cThe percent difference may appear inconsistent due to rounding errors.

Table 2.2. Model performance—Head target elevations in watershed.

GFLOW label	Measured ^a , ft	Simulated, ft	Absolute difference, ft
nc966_fair	1477	1460	16.7
fi581_fair	1419	1432	−13.4

Abbreviations: ft, feet; GFLOW, groundwater flow model.

^aAll elevations are above mean sea level.

Table 2.3. Simulated baseflow for climate-change scenarios: base, +21%, and –12% recharge.

Location	Station ID ^a	Flow, cfs						
		Base	+21% case	Change	% change ^a	–12% case	Change	% change ^b
Marengo River at Altamont Road	USGS #04026590	20.2	26.7	6.4	32%	16.6	–3.6	–18%
Tributary 8	21756	0.4	0.6	0.1	34%	0.4	–0.1	–19%
Marengo River at FR198	mar02	19.9	23.4	3.5	18%	17.9	–2.0	–10%
Tributary 7	21755	3.5	3.8	0.2	6%	3.5	–0.1	–2%
Marengo River between Tributaries 6 and 7	21707	13.4	16.7	3.2	24%	11.5	–1.9	–14%
Tributary 6	21754	0.3	0.5	0.3	106%	0.0	–0.3	–103%
Marengo River at FR194	21703	7.6	9.1	1.6	21%	6.7	–0.9	–11%
Whisky Creek	21704	3.0	4.0	0.9	31%	2.5	–0.5	–18%
Blaser Creek at FR194	mar09	2.1	2.1	0.0	0%	2.1	0.0	0%

Abbreviations: cfs, cubic feet per second; FR, Forest Road; ID, identification number; USGS, U.S. Geological Survey.

^aStation identification numbers are shown in figure 25.

^bThe percent change may appear inconsistent due to rounding errors.

Appendix 3: Stream-temperature model performance

Table 3.1. Error in simulated mean daily temperature by location, in degrees Celsius (°C).

Location ^a	Station ID ^b	SNTEMP reach name ^c	Mean error ^d	RMSE	Correlation coefficient	Maximum error
Marengo River at FR384	21602	From mar-002 to mar-001	0.3	1.0	0.8	2.6
Tributary 9	21757	From T9-024 to mar-003	−0.7	1.0	0.9	−2.4
Marengo River at North Country Trail	mar01	From mar-005 to mar-004	0.0	1.0	0.8	2.4
Marengo River at FR198	mar02	From mar-008 to mar-007	0.6	1.3	0.6	2.9
Tributary 7	21755	From T7-029 to mar-009	0.4	0.6	0.5	1.2
Tributary 6	21754	From T6-031 to mar-010	−2.1	2.2	0.9	−3.4
Marengo River upstream of Tributary 6	21799	From mar-011 to mar-010	0.1	1.1	0.8	3.1
Marengo River at waterfall	mar05	From mar-012 to mar-011	0.3	1.1	0.8	3.2
Tributary 5	21798	From T5-034 to mar-012	−2.3	2.6	0.5	−5.0
Marengo River at FR194	21703	From mar-017 to mar-016	1.5	2.0	0.7	4.3
Tributary 3	21705	From T3-039 to T3-038	−1.3	1.9	0.7	−4.9
Blaser Creek	mar09	From BC-043 to BC-042	1.0	1.7	0.2	3.5
Tributary 2	mar12	From T2-049 to T2-048	−1.1	1.8	0.7	−4.4
Tributary 1	mar04	From T1-054 to T1-053	0.3	1.4	0.7	−4.1

Abbreviations: FR, Forest Road; ID, identification number; RMSE, root-mean-square error; SNTEMP, Stream Network Temperature Model.

^aLocations with partial records do not reflect the entire calibration period. These include Marengo at the North Country Trail, Tributary 7, Tributary 6, and Tributary 5.

^bStation identification numbers are shown in table 1 and figure 9.

^cReaches and their node endpoints are shown on figure 33.

^dErrors calculated as model minus observed. Positive errors indicate the model temperature is too warm.

References

- American Society of Adaptation Professionals, 2017, Preparing for extreme rainfall on the Chequamegon-Nicolet National Forest: American Society of Adaptation Professionals, available at <https://adaptationprofessionals.org/wp-content/uploads/2020/01/USFS-Snapshot-11-1-17.pdf>, accessed March 5, 2020.
- Anderson, M.P., Woessner, W.W., and Hunt, R.J., 2015, Applied groundwater modeling—Simulation of flow and advective transport (2d ed.): San Diego, Calif., Academic Press Inc., 564 p.
- Avery, E.L., 2004, A compendium of 58 trout stream habitat development evaluations in Wisconsin—1985–2000: Wisconsin Department of Natural Resources Research Report 187, 96 p.
- Bartholow, J., 2010, Stream network and stream segment temperature models software: U.S. Geological Survey web page accessed February 14, 2018, at <https://pubs.er.usgs.gov/publication/96233>.
- Bartholow, J.M., 1989, Stream temperature investigations: field and analytic methods. Instream Flow Information Paper No. 13: U.S. Fish and Wildlife Service Biological Report, v. 89, no. 17, 139 p.
- Bell, J.M., 2006, The assessment of thermal impacts on habitat selection, growth, reproduction, and mortality in brown trout (*Salmo trutta* L.): A review of the literature: Prior Lake, Minn., Applied Ecological Services, 23 p.
- Bjørnerud, M., and Cannon, W.F., 2011, Midcontinent microcosm: Geology of the Atkins Lake-Marengo Falls area, in Fitz, T., Mills, A., Wilson, K., Bodette, C., and Cramer, D., eds., Proceedings, Institute on Lake Superior Geology, 57th annual meeting, Ashland, Wisc., May 18–20, 2020, Field trip guidebook: Institute on Lake Superior Geology, v. 57, pt. 2, p. 31–47.
- Caine, J.S., Evans, J.P., and Forster, C.B., 1996, Fault zone architecture and permeability structure: Geology, v. 24, no. 11, p. 1025–1028.
- Cannon, W.F., Kress, T.H., and Sutphin, D.M., 1997, Digital geologic map and mineral deposits of Minnesota, Wisconsin, and Michigan, version 3: U.S. Geological Survey Open-File Report 97–455, <https://pubs.usgs.gov/of/1997/of97-455/>.
- Cannon, W.F., LaBerge, G.L., Klasner, J.S., and Schulz, K.J., 2007, The Gogebic iron range—A sample of the northern margin of the Penokean fold and thrust belt: U.S. Geological Survey Professional Paper 1730, 44 p.
- Cannon, W.F., Woodruff, L.G., Nicholson, S.W., Hedgman, C.A., and Barber-Delach, R.D., 1999, Digital bedrock geologic map of the Ashland and the northern part of the Ironwood 30'x 60' quadrangles, Wisconsin and Michigan: U.S. Geological Survey Open-File Report 99–546, <https://pubs.usgs.gov/of/1999/of99-546/>.
- Carlson, A.K., Taylor, W.W., and Infante, D.M., 2019, Modeling effects of climate change on Michigan brown trout and rainbow trout—Precipitation and groundwater as key predictors: Ecology of Freshwater Fish, v. 29, no. 3 p. 433–449, <https://doi.org/10.1111/eff.12525>.
- Clayton, L., 1984 [plate: 1985], Pleistocene geology of the Superior Region, Wisconsin: Wisconsin Geological and Natural History Survey Information Circular 46, 40 p., 1 pl., <https://wgnhs.wisc.edu/pubs/000296/>.
- Cross, B.K., Bozek, M.A., and Mitro, M.G., 2013, Influences of riparian vegetation on trout stream temperatures in central Wisconsin: North American Journal of Fisheries Management, v. 33, p. 682–692.
- Diebel, M., Ruesch, A., Menuz, D., Stewart, J., and Westenbroek, S., 2015, Ecological limits of hydrologic alteration in Wisconsin streams: Wisconsin Department of Natural Resources web page accessed April 2, 2018, at <https://www.wri.wisc.edu/research/ecological-limits-of-hydrologic-alteration-in-wisconsin-streams/>.
- Deitchman, R., and Loheide, S.P., II, 2012, Sensitivity of thermal habitat of a trout stream to potential climate change, Wisconsin, United States: Journal of the American Water Resources Association, v. 48, p. 1091–1103, <https://doi.org/10.1111/j.1752-1688.2012.00673.x>.
- Fehling, A.C., Bradbury, K.R., Leaf, A.T., Pruitt, A., Hunt, R.J., Mauel, S.M., Schoephoester, P.R., and Juckem, P.F., 2018, Characterization of groundwater resources in the Chequamegon-Nicolet National Forest, Wisconsin: Washburn/Great Divide Unit: Wisconsin Geological and Natural History Survey Technical Report 004-4, 60 p., <https://wgnhs.wisc.edu/pubs/tr0044/>.
- Frankson, R., Kunkel, K., and Champion, S., 2017, Wisconsin state climate summary: NOAA Technical Report NESDIS 149-WI, <https://statesummaries.ncics.org/wi>.

- Gaffield, S.J., Potter, K.W., Wang, L., 2005, Predicting the summer temperature of small streams in southwestern Wisconsin: Journal of the American Water Resources Association, v. 41, no. 1, p. 25–36.
- Gat, J.R., 1996, Oxygen and hydrogen isotopes in the hydrologic cycle: Annual Review of Earth and Planetary Sciences, v. 24, p. 225–262, <https://doi.org/10.1146/annurev.earth.24.1.225>.
- Gebert, W.A., Radloff, M.J., Considine, E.J., and Kennedy, J.L., 2007, Use of streamflow data to estimate base flow/ground-water recharge for Wisconsin: Journal of the American Water Resources Association, v. 43, no. 1, p. 220–236, <https://doi.org/10.1111/j.1752-1688.2007.00018.x>.
- Gebert, W.A., Walker, J.F., and Kennedy, J.L., 2011, Estimating 1970–99 average annual groundwater recharge in Wisconsin using streamflow data: U.S. Geological Survey Open-File Report 2009–1210, 14 p., available at <https://pubs.usgs.gov/of/2009/1210/>.
- Haitjema, H.M., 1995, Analytic element modeling of groundwater: San Diego, Calif., Academic Press, 394 p.
- Hart, D., 2016, A comparison of fracture transmissivities in granite water wells before and after hydrofracturing: Hydrogeology Journal, v. 24, no. 1, p. 21–33, <https://doi.org/10.1007/s10040-015-1315-5>.
- Hart, D.J., Schoephoester, P.R., and Bradbury, K.R., 2012, Groundwater recharge in Dane County, Wisconsin—Estimating recharge using a GIS-based water-balance model: Wisconsin Geological and Natural History Survey Bulletin 107, 11 p., <https://wgnhs.wisc.edu/pubs/b107/>.
- Hunt, R.J., 2006, Ground water modeling applications using the analytic element method: Groundwater, v. 44, p. 5–15, <https://doi.org/10.1111/j.1745-6584.2005.00143.x>.
- Hunt, R.J., Haitjema, H.M., Krohelski, J.T., and Feinstein, D.T., 2003, Simulating ground water-lake interactions: Approaches and insights: Ground Water, v. 41, no. 2, p. 227–237, <https://doi.org/10.1111/j.1745-6584.2003.tb02586.x>.
- Hunt, R.J., Strand, M., and Walker, J.F., 2006, Measuring groundwater-surface water interaction and its effect on wetland stream benthic productivity, Trout Lake Watershed, northern Wisconsin, USA: Journal of Hydrology, v. 320, p. 370–384.
- Hunt, R.J., Walker, J.F., Selbig, W.R., Westenbroek, S.M., and Regan, R.S., 2013, Simulation of climate-change effects on streamflow, lake water budgets, and stream temperature using GSFLOW and SNTMP, Trout Lake Watershed, Wisconsin: U.S. Geological Survey Scientific Investigations Report 2013–5159, <https://pubs.usgs.gov/sir/2013/5079/>.
- Hunt, R.J., Westenbroek, S.M., Walker, J.F., Selbig, W.R., Regan, R.S., Leaf, A.T., and Saad, D.A., 2016, Simulation of climate change effects on streamflow, groundwater, and stream temperature using GSFLOW and SNTMP in the Black Earth Creek Watershed, Wisconsin: U.S. Geological Survey Scientific Investigations Report 2016–5091, 117 p., <https://dx.doi.org/10.3133/sir20165091>.
- Johnson-Bice, S.M., Renik, K.M., Windels, S.K., and Hafs, A.W., 2018, A review of beaver-salmonid relationships and history of management actions in the Western Great Lakes (USA) region: North American Journal of Fisheries Management, v. 38, p. 1203–1225.
- Krabbenhoft, D.P., Anderson, M.P., Bowser, C.J., and Valley, J.W., 1990, Estimating groundwater exchange with lakes: 1. The stable isotope mass balance method: Water Resources Research, v. 26, no. 10, p. 2445–2453.
- Kurylyk, B.L., MacQuarrie, K.T.B., and Voss, C.I., 2014, Climate change impacts on the temperature and magnitude of groundwater discharge from shallow, unconfined aquifers: Water Resources Research, v. 50, p. 3253–3274.
- Leaf, A.T., Fehling, A., Bradbury, K.R., Hunt, R.J., and Juckem, P.F., 2019, GFLOW model used to characterize the groundwater resources of the Great Divide Unit of the Chequamegon-Nicolet National Forest, Wisconsin: U.S. Geological Survey Water Mission Area NSDI Node, <https://doi.org/10.5066/F708648W>.
- Leaf, A.T., Fienen, M.N., Hunt, R.J., and Buchwald, C., 2016, MODFLOW-NWT model used to evaluate groundwater/surface-water interactions in the Bad River Watershed, Wisconsin: U.S. Geological Survey, web page accessed May 13, 2020, at <https://dx.doi.org/10.5066/F7Z0368H>.
- Leaf, A.T., Fienen, M.N., Hunt, R.J., and Buchwald, C.A., 2015, Groundwater/surface-water interactions in the Bad River Watershed, Wisconsin: U.S. Geological Survey Scientific Investigations Report 2015–5162, 110 p., <https://dx.doi.org/10.3133/sir20155162>.
- Loheide, S.P., II, and Gorelick, S.M., 2006, Quantifying stream-aquifer interactions through the analysis of remotely sensed thermographic profiles and in situ temperature histories: Environmental Science & Technology, v. 40, no. 10, p. 3336–3341.
- Lyons, J., Stewart, J.S., and Mitro, M., 2010, Predicted effects of climate warming on the distribution of 50 stream fishes in Wisconsin, U.S.A.: Journal of Fish Biology, v. 77, p. 1867–1898, <https://doi.org/10.1111/j.1095-8649.2010.02763.x>.

- Lyons, J., Wang, L., and Simonson, T.D., 1996, Development and validation of an index of biotic integrity for coldwater streams in Wisconsin: *North American Journal of Fisheries Management*, v. 16, p. 241–256.
- Lyons, J., Zorn, T., Stewart, J., Seelbach, P.W., Wehrly, K., and Wang, L., 2009, Defining and characterizing coolwater streams and their fish assemblages in Michigan and Wisconsin, USA: *North American Journal of Fisheries Management*, v. 29, p. 1130–1151.
- Magner, J., Zhang, L., Engel, L., and Jaspersen, J., 2014, Stable isotopes in NSLS watershed management, in Sandstrom, P.V., ed., *Proceedings of the MN Lake Superior Watershed Stream Science Symposium*, Duluth, Minn., January 7–8, 2014: Duluth, Minn., Laurentian Resource Conservation and Development Council, 35 p., http://www.lrcd.org/uploads/1/6/4/0/16405852/magner_1-7-14_stable_isotope.pdf.
- Matthews, K.R., Berg, N.H., Azuma, D.L., and Lambert, T.R., 1994, Cool water formation and trout habitat use in a deep pool in the Sierra Nevada, California: *Transactions of the American Fisheries Society*, v. 123, p. 549–564.
- McRae, G., and Edwards, C.J., 1994, Thermal characteristics of Wisconsin headwater streams occupied by beaver: implications for brook trout habitat: *Transactions of the American Fisheries Society*, v. 123, p. 641–656.
- Menberg, K., Blum, P., Kurylyk, B.L., and Bayer, P., 2014, Observed groundwater temperature response to recent climate change: *Hydrology and Earth System Sciences*, v. 18, p. 4453–4466.
- Meyer, J.L., Strayer, D.L., Wallace, J.B., Eggert, S.L., Helfman, G.S., and Leonard, N.E., 2007, The contribution of headwater streams to biodiversity in river networks: *Journal of the American Water Resources Association*, v. 43, no. 1, p. 86–103.
- Mitro, M.G., 2016, Brook Trout, Brown Trout, and ectoparasitic copepods *Salmincola edwardsii*: Species interactions as a proximate cause of Brook Trout loss under changing environmental conditions: *Transactions of the American Fisheries Society*, v. 145, p. 1223, <https://doi.org/10.1080/00028487.2016.1219676>.
- Mitro, M.G., Lyons, J.D., Stewart, J.S., Cunningham, P.K., and Griffin, J.D.T., 2019, Projected changes in Brook Trout and Brown Trout distribution in Wisconsin streams in the mid-twenty-first century in response to climate change: *Hydrobiologia*, v. 840, no. 1, p. 215–226, <https://doi.org/10.1007/s10750-019-04020-3>.
- Moss, R.H., Edmonds, J.A., Hibbard, K.A., Manning, M.R., Rose, S.K., van Vuuren, D.P., Carter, T.R., Emori, S., Kainuma, M., Kram, T., Meehl, G.A., Mitchell, J.F.B., Nakicenovic, N., Riahi, K., Smith, S.J., Stouffer, R.J., Thomson, A.M., Weyant, J.P., and Wilbanks, T.J., 2010, The next generation of scenarios for climate change research and assessment: *Nature*, v. 463, no. 7282, p. 747–56.
- Natural Resources Conservation Service, 2018, Watershed boundary dataset for Wisconsin: U.S. Department of Agriculture, Natural Resources Conservation Service, <http://datagateway.nrcs.usda.gov>.
- Nicholson, S.W., Cannon, W.F., Woodruff, L.G., and Dicken, C.L., 2004, Bedrock geologic map of the Port Wing, Solon Springs and parts of Duluth and Sandstone 30' × 60' quadrangles, Wisconsin: U.S. Geological Survey Open-File Report 2004–1303, <https://doi.org/10.3133/ofr20041303>.
- Notaro, M., Lorenz, D.J., Vimont, D., Vavrus, S., Kucharik, C., and Franz, K., 2011, 21st century Wisconsin snow projections based on an operational snow model driven by statistically downscaled climate data: *International Journal of Climatology*, v. 34, no. 5, p. 1615–1633.
- Notaro, M., Lorenz, D., Hoving, C., and Schummer, M., 2014, Twenty-first-century projections of snowfall and winter severity across central-eastern North America: *Journal of Climate*, v. 27, no. 17, p. 6526–6550, <https://doi.org/10.1175/JCLI-D-13-00520.1>.
- Ojakangas, R.W., Morey, G.B., and Green, J.C., 2001, The Mesoproterozoic Midcontinent Rift System, Lake Superior Region, USA: *Sedimentary Geology*, v. 141–142, p. 421–442, [https://doi.org/10.1016/S0037-0738\(01\)00085-9](https://doi.org/10.1016/S0037-0738(01)00085-9).
- Palmer, M.A., Hondula, K.L., and Koch, B.J., 2014, Ecological restoration of streams and rivers—Shifting strategies and shifting goals: *Annual Review of Ecology, Evolution, and Systematics*, v. 45, p. 247–269.
- Pruitt, A.H., 2013, Potential impacts of climate change on groundwater/surface water interaction, Chequamegon-Nicolet National Forest, Wisconsin: Madison, University of Wisconsin, unpub. M.S. thesis, 190 p.
- Reidmiller, D.R., Avery, C.W., Easterling, D.R., Kunkel, K.E., Lewis, K.L.M., Maycock, T.K., and Stewart, B.C., eds., 2018, Impacts, risks, and adaptation in the United States, v. II of Fourth National Climate Assessment: Washington, D.C., U.S. Global Change Research Program, <https://doi.org/10.7930/NCA4.2018>.
- Roni, P., Hanson, K., and Beechie, T., 2011, Global review of the physical and biological effectiveness of stream habitat rehabilitation techniques: *North American Journal of Fisheries Management*, v. 28, no. 3, p. 856–890.
- Rosenberry, D.O., and LaBaugh, J.W., 2008, Field techniques for estimating water fluxes between surface water and ground water: U.S. Geological Survey Techniques and Methods 4–D2, 128 p., <https://pubs.usgs.gov/tm/04d02/>.

- Snyder, C.D., Hitt, N.P., and Young, J.A., 2015, Accounting for groundwater in stream fish thermal habitat responses to climate change: Ecological Applications, v. 25, p. 1397–1419. <https://doi.org/10.1890/14-1354.1>.
- State Cartographer's Office, 2017, Elevation/lidar data: Madison, University of Wisconsin website, accessed May 2017, at <https://www.sco.wisc.edu/data/elevationlidar/>.
- Stewart, J.S., Westenbroek, S.M., Mitro, M.G., Lyons, J.D., Kammel, L.E., and Buchwald, C.A., 2015, A model for evaluating stream temperature response to climate change in Wisconsin: U.S. Geological Survey Scientific Investigations Report 2014–5186, 64 p., <https://dx.doi.org/10.3133/sir20145186>.
- Swanson, S.K., and Bahr, J.M., 2004, Analytical and numerical models to explain steady rates of spring flow: Groundwater, v. 42, no. 5, p. 747–759, <https://doi.org/10.1111/j.1745-6584.2004.tb02728.x>.
- Theurer, F.D., Voos, K.A., and Miller, W.J., 1984, Instream water temperature model. Instream Flow Information Paper 16: U.S. Fish and Wildlife Service, Office of Biological Services Report FSW/OBS 84/15, 347 p.
- USDA Forest Service, 2011, Administrative forest boundaries: USDA Forest Service, updated September 2011, <https://data.fs.usda.gov/geodata/edw/datasets.php?xmlKeyword=Administrative+Forest+Boundaries>.
- U.S. Geological Survey, 2000, A simple device for measuring differences in hydraulic head between surface water and shallow ground water: U.S. Geological Survey Fact Sheet 077–00, 2 p., <https://doi.org/10.3133/fs07700>.
- U.S. Geological Survey, 2016, National hydrography dataset: U.S. Geological Survey, web page accessed January 18, 2016, at <https://www.usgs.gov/core-science-systems/national-geospatial-program/national-map>.
- Wehrly, K.E., Wang, L., and Mitro, M., 2007, Field-based estimates of thermal tolerance limits for trout: Incorporating exposure time and temperature fluctuation: Transactions of the American Fisheries Society, v. 136, p. 365–374.
- Westenbroek, S.M., Kelson, V.A., Dripps, W.R., Hunt, R.J., and Bradbury, K.R., 2010, SWB—A modified Thornthwaite-Mather soil-water-balance code for estimating groundwater recharge: U.S. Geological Survey Techniques and Methods 6–A31, 60 p., <https://pubs.usgs.gov/tm/tm6-a31/>.
- Westenbroek, S.M., Stewart, J.S., Buchwald, C.A., Mitro, M., Lyons, J.D., and Greb, S., 2010, A model for evaluating stream temperature response to climate change scenarios in Wisconsin, in Potter, K.W., Frevert, D.K., eds., Proceedings, Watershed Management 2010: Innovations in Watershed Management under Land Use and Climate Change, Madison, Wisc., August 23–27, 2010: Madison, Wisc., American Society of Civil Engineers, <https://doi.org/10.1061/9780784411438>.
- Western Regional Climate Center, 2018, Remote Automatic Weather Stations, Clam Lake, Wisconsin, Daily Summary: Western Regional Climate Center web page accessed October 2, 2018 at <https://wrcc.dri.edu/cgi-bin/rawMAIN.pl?sdWCLA>.
- Wheeler, M., and Bodette, C., 2011, Bad River Watershed Culvert Restoration Program, in Fitz, T., Mills, A., Wilson, K., Bodette, C., and Cramer, D., eds., Proceedings, Institute on Lake Superior Geology, 57th annual meeting, Ashland, Wisc., May 18–20, 2020, Field trip guidebook: Institute on Lake Superior Geology, v. 57, part 2, p. 85–96.
- Wiley, M.J., Kohler, S.L., and Seelbach, P.W., 1997, Reconciling landscape and local views of aquatic communities: lessons from Michigan trout streams: Freshwater Biology, v. 37, p. 133–148.
- Wisconsin Department of Natural Resources, 2011, Wetland mapping: Wisconsin Department of Natural Resources web page accessed 2011, at <https://dnr.wi.gov/topic/wetlands/inventory.html>.
- Wisconsin Initiative on Climate Change Impacts (WICCI), 2011, Wisconsin's changing climate: Impacts and adaptation: Madison, Nelson Institute for Environmental Studies, University of Wisconsin-Madison, and the Wisconsin Department of Natural Resources, 226 p., <https://wicci.wisc.edu/wp-content/uploads/2019/12/2011-wicci-report.pdf>.
- Wisconsin State Climatology Office, 2018, Northwest and north-central Wisconsin climate normals (1971–2000): Wisconsin State Climatology Office web page accessed January 24, 2018, at <http://www.aos.wisc.edu/~sco/clim-history/division>.



Marengo River at the North Country Trail crossing | Pete Chase



Published by and available from:

Wisconsin Geological and Natural History Survey

3817 Mineral Point Road ■ Madison, Wisconsin 53705-5100
608.263.7389 ■ www.WisconsinGeologicalSurvey.org
Kenneth R. Bradbury, Director and State Geologist



Wisconsin Geological
and Natural History Survey
DIVISION OF EXTENSION
UNIVERSITY OF WISCONSIN-MADISON

This report is an interpretation of the data available at the time of preparation. Every reasonable effort has been made to ensure that this interpretation conforms to sound scientific principles; however, the report should not be used to guide site-specific decisions without verification. Proper use of the report is the sole responsibility of the user.

The use of company names in this document does not imply endorsement by the Wisconsin Geological and Natural History Survey.

ISSN: 0375-8265
ISBN: 978-0-88169-975-3

University of Wisconsin–Madison Division of Extension, in cooperation with the U.S. Department of Agriculture and Wisconsin counties, publishes this information to further the purpose of the May 8 and June 30, 1914, Acts of Congress. An EEO/AA employer, the University of Wisconsin–Madison provides equal opportunities in employment and programming, including Title VI, Title IX, the Americans with Disabilities Act (ADA), and Section 504 of the Rehabilitation Act requirements. If you have a disability and require this information in an alternative format, contact the Wisconsin Geological and Natural History Survey at 608-262-1705 (711 for Wisconsin Relay).

Our Mission

The Survey conducts earth-science surveys, field studies, and research. We provide objective scientific information about the geology, mineral resources, water resources, soil, and biology of Wisconsin. We collect, interpret, disseminate, and archive natural resource information. We communicate the results of our activities through publications, technical talks, and responses to inquiries from the public. These activities support informed decision making by government, industry, business, and individual citizens of Wisconsin.